Biosynthesis of Heparosan, A Bioengineered Heparin Precursor in *Bacillus megaterium* – A Metabolic Engineering Approach

by

Ganesh N

A thesis submitted
in Partial Fulfillment of the Requirements
for the Degree of

DOCTOR OF PHILOSOPHY

Department of Biosciences and Bioengineering
Indian Institute of Technology Guwahati
Guwahati 781039, India.

March 2021

Biosynthesis of Heparosan, A Bioengineered Heparin Precursor in *Bacillus megaterium* – A Metabolic Engineering Approach

by

Ganesh N
Roll No. 146106009

A thesis submitted
in Partial Fulfillment of the Requirements
for the Degree of

DOCTOR OF PHILOSOPHY

Supervisor
Dr. Senthilkumar Sivaprakasam

Department of Biosciences and Bioengineering
Indian Institute of Technology Guwahati
Guwahati 781039, India.

March 2021

Dedicated to my Amma and Appa

CERTIFICATE

It is certified that the work contained in the thesis entitled "*Biosynthesis of Heparosan, A Bioengineered Heparin Precursor in Bacillus megaterium – A Metabolic Engineering Approach*" by Mr. Ganesh N, a student of the Department of Biosciences and Bioengineering, IIT Guwahati was carried out under my supervision and has not been submitted elsewhere for the award of any degree.

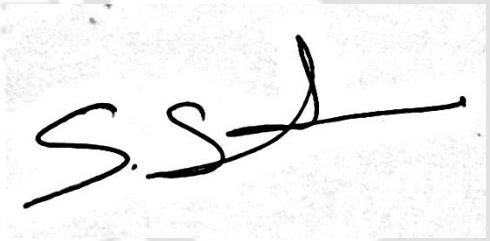

Dr. Senthilkumar Sivaprakasam,
Department of Biosciences and Bioengineering,
Indian Institute of Technology Guwahati,
Guwahati-781039, Assam, India.
DATE: .....

Six years are past. A lot of people crossed my way during this exciting time. I would like to say THANK YOU to all of you!

First, I'm deeply grateful to my supervisor Dr. Senthilkumar Sivaprakasam. Thanks for the help, guidance, and unremitting motivation. He has been very understanding and provided all the necessary facilities to carry out the present work. He was a source of strength through out my research endeavour.I am indebted to him for the moral support, generosity and encouraging me in difficult times. I am thankful to him for the discussions and valuable suggestions and helped me grow as an independent researcher.

I express my sincere thanks to my Doctoral committee members Dr. Anil Mukund Limaye, Dr. Sachin Kumar and Dr. Soumen Kumar Maiti. Through doctoral meetings and informal discussions, they helped to provide invaluable advice and guidance. My heartfelt gratitude to Dr. Sachin Kumar for helping me to get *E. coli* K5 strain; with out that this thesis wouldn't have been materialized. I would also like to thank all the faculty of our department for their support. My sincere thanks to Dr. Anil Mukund Limaye for providing the access to his lab facilities.

Now the lab people: First of all, I thank the entire BioPAT lab for the nice and friendly atmosphere. Srikanth, Naresh, Subbi, Kiran, Pavan, Nivedhitha, Siddharth, Payal, Sandhya, Rohit, Indhumathi, Manoj, Siva, Kota - thank you all for the discussions, helping out in the lab and of course, for all the wonderful tea breaks that we spend together.

My sincere gratitude goes to Subbi and Pavan, who have been a great source of strength, for their unconditional support in performing experiments and moral support during difficult times.

I thank my friends, Sajitha, Sheeba, Vimal, Rakesh, Sudhir, Barnali, Manisha, Kamal, Anjali, Mohan, Uttariya, Gaurav, Snigdha, Musfica, Sonya, Akshitha, Yoganand, Siddharth, Himanshu, Siranjeevi, Manasa, Arun, Payel, Bapi, Sunanda, Rohan, Sanjana, Anshuman, Vinay, Feba for the cordial support. Thank you all for making my stay at

IITG joyful and more memorable.

I am thankful to Ministry of Human Resource and Development for providing the fellowship and Department of Biosciences and Bioengineering and Central Instruments facility, IIT Guwahati for the infrastructure and lab facilities

I extend my thanks to all the supporting staff in the Department of BSBE, IIT Guwahati for their help. My special thanks to Mr. Nurul Islam, for allowing me to use B.Tech lab facilities whenever required.

My special thanks to Ma'am. Ambika for her concern, support and memorable lab gatherings.

Most importantly, None of this work would have been possible with out the love and support of my parents and sister, and for that I am forever indebted.

ABSTRACT

Heparosan is a commercially expensive glycosaminoglycan (GAG), composed of repeating disaccharide units of GlcA and GlcNAc linked by α (1→4) and β (1→4) glycosidic bonds. Heparosan is a highly anionic and hydrophilic polysaccharide, attributed to the carboxylate and hydroxyl groups. Traditionally, pharmaceutical grade heparin is extracted from animal tissues such as porcine intestine and bovine lung. In early 2008, Animal-derived heparin caused serious adverse reactions leading to hypotension and the death of nearly a hundred patients. Heparin contamination was identified to be caused by anaphylactic response due to the contaminant, over-sulfated chondroitin sulfate (OSCS) present in the raw heparin. The heparin contamination crisis prompted the FDA to devise strict regulations on the production and manufacturing of animal derived heparin. Chemoenzymatic synthesis emerged as an attractive alternative to the conventional animal derived heparin. Chemoenzymatic synthesis of heparin requires the linear, unsulfated heparan sulfate backbone as a starting molecule. The heparan sulfate backbone is also known as heparosan. This thesis deals with the biosynthesis of heparosan polysaccharide, which is the first step of chemoenzymatic heparin synthesis process.

Heparosan production through microbial fermentation is a promising method to prepare chemoenzymatic heparin. Until now, *E. coli* K5, *P. multocida* type D and genetically modified microorganisms have been used to produce heparosan. Biosynthesis of heparosan in *E. coli* K5 is catalyzed by four proteins, KfiA, KfiB, KfiC and KfiD, present in serotype specific region 2 of *kps* loci. Though the heparosan production is high, *E. coli* K5 causes urinary tract infections in humans. *E. coli* K5 uses the heparosan capsule to masquerade against the host immune system, thus causing the infections. Moreover, *E. coli* K5 produces exotoxins and endotoxins, which require extensive purification and subsequent increase in the processing cost. Above all, *E. coli* K5 genome encodes N-acetyl heparosan lyase which depolymerize the heparosan chain. Expression of the N-acetyl heparosan lyase throughout the fermentation could adversely affect the molecular weight and polydispersity of the heparosan. These limitations have prompted for the usage of

safe recombinant bacteria such as *E. coli*, *Bacillus subtilis* and *Bacillus megaterium* for the production of heparosan.

Bacillus megaterium, a safe gram-positive bacterium has been an important industrial host due to its superior characteristics such as the efficient expression of heterologous genes, stable plasmid maintenance, lack of alkaline protease activity and efficient secretion capability. It has been widely used for the recombinant production of various enzymes and vitamins. In addition, *B. megaterium* is free of endotoxins as opposed to *E. coli* K5.The present thesis aimed to address the gaps pertaining to the heparosan production in *B. megaterium*. The primary focus of the present thesis is (i) Metabolic engineering of *B. megaterium* for heparosan production (ii) Enhancing the heparosan production by molecular and bioprocessing strategies.

The first chapter of the thesis deals with engineering a functional heparosan synthesis pathway in *Bacillus megaterium* by the expression of *E. coli* K5 *kfiC* and *kfiA* glycosyltransferase genes. SDS-PAGE analysis confirmed the heterologous expression of KfiC and KfiA proteins of size 59 kDa and 27 kDa, respectively. Upregulation of individual UDP-sugar precursor pathway genes enhanced the heparosan production, indicating that UDP-precursor sugar concentrations were limiting the biosynthesis. The engineered *B. megaterium* yielded a maximum heparosan concentration of 394 mg/L in batch bioreactor. The heparosan titer was further increased to 1.32 g/L in fed-batch fermentation. Carbazole analysis revealed that heparosan was primarily accumulated in the cell pellet during the course of fermentation. Nuclear magnetic resonance analysis revealed that the chemical structure of *B. megaterium* derived heparosan was identical to *E. coli* K5 heparosan. The heparosan molecular weight varied from 31 to 60 kDa, indicating its potential as a precursor for chemoenzymatic heparin synthesis.

The second chapter of the thesis deals with the development of dual promoter expression system for heparosan production in *B. megaterium*. Heparosan production is facilitated by the formation of KfiC-KfiA enzyme complex and the concerted action of KfiC and KfiA glycosyltransferases. Hence, the comparable co-expression of KfiC and KfiA proteins are essential to increase the polymerization activity of KfiC-KfiA complex. In the previous chapter, *kfiC* and *kfiA* genes were expressed in polycistronic manner, resembling the *E. coli* K5 gene cluster. We observed an unbalanced expression of KfiC and KfiA proteins. Hence, dual promoter plasmid system was constructed to increase the expression levels of KfiC and KfiA proteins. Dual promoter plasmid system along with UDP-glucuronic acid pathway overexpression (CADuet-DB) increased the heparosan production to 203

mg/L in shake flask experiments. In addition, the process variables such as temperature, inducer concentration and OD prior to the induction was also optimized to improve the heparosan production. Batch and fed-batch fermentation of strain CADuet-DB under controlled conditions yielded a maximum heparosan concentration of 627 mg/L and 1.96 g/L, respectively.

The third chapter deals with the influence of sucrose and GlcNAc concentration on Biomass growth and heparosan production. The heparosan production significantly influenced by certain factors like substrate concentration and process conditions. Thus, determining the substrate concentration to identify the inhibition phenomenon on heparosan production and *B. megaterium* growth. To achieve this, the experiments were conducted at an initial sucrose concentration range of 10 to 50 g/L in the batch fermentation. Heparosan concentration was enhanced with increase in sucrose concentration and the yield was found to be inversely proportional to sucrose concentration. Increase in the sucrose concentration increased lag time and specific growth rate of the biomass. It indicates the inhibition effect of the sucrose at high concentration. Further, experimental data was modeled using modified logistic equation and the kinetic parameters were determined. we studied the effect of precursors (N-acteylglucosamine and glucuronic acid) concentration on heparosan production. Batch fermentation with sucrose and N-acteylglucosamine resulted in the highest heparosan concentration of 911 mg/L in batch fermentation under optimal conditions. We found the simultaneous consumption of sucrose and N-acetylglucosamine, hence interactive multi substrate kinetic model was used to describe the biomass growth and heparosan production. Overall, this thesis addressed a safe approach to synthesize heparosan from *B. megaterium*, which have potential applications as a heparin precursor and in drug delivery applications.

TABLE OF CONTENTS

List of Figures

List of Tables

CHAPTER 1

INTRODUCTION

1.1 Glycosaminoglycans

Glycosaminoglycans (GAGs) are negatively charged polysaccharide molecules, composed of repetitive disaccharide units linked by glycosidic bonds. The repetitive disaccharide units consist of an uronic acid and an amino sugar moieties (Figure 1.1). GAGs are primarily classified into four different groups based on the repeating disaccharide units, which include (i) heparin/heparan sulfate, (ii) keratan sulfate, (iii) chondroitin sulate/dermatan sulfate and (iv) hyaluronic acid. They are covalently attached to the proteins of extracellular matrix (ECM) as proteoglycans except hyaluronic acid, which

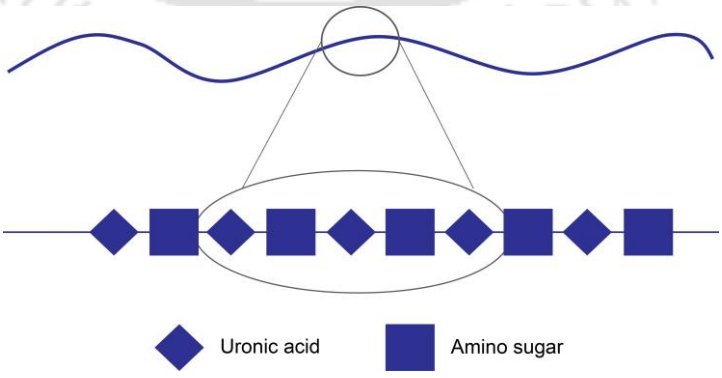

Figure 1.1: Schematic representation of glycosaminoglycan structure

Table 1.1: Structure and monosaccharide components of different GAGs

GAG type	Monosaccharide composition	Molecular structure
heparin / heparan sulfate	D-glucuronic acid or L-iduronic acid and N-acetyl-D-glucosamine	→4) β-D-GlcA or α-L-IdoA (1→4) α-D-GlcNAc (1→, with sulfation
chondroitin sulfate / dermatan sulfate	D-glucuronic acid or L-iduronic acid and N-acetyl-D-galactosamine	→4) β-D-GlcA or α-L-IdoA (1→3) β-D-GalNAc (1→, with sulfation
Keratan sulfate	Galactose and N-acetyl-D-glucosamine	→3) β-D-Gal (1→4) β-D-GlcNAc (1→, with sulfation
Hyaluronic acid	D-glucuronic acid and N-acetyl-D-glucosamine	→4) β-D-GlcA (1→3) β-D-GlcNAc (1→, without sulfation

is present within the ECM. They are of critical importance in various functions of the cells including signal transduction, coagulation and complement cascade reactions, cell adhesion and pathogen recognition. The physiological significance of the GAGs within the body is determined by the molecular structure [20]. The structure, monosaccharide sugar composition and the glycosidic linkages of the GAGs are given in Table 1.1.

1.2 Heparin and heparan sulfate

Among the GAGs mentioned above, heparin/heparan sulfate is one of the naturally occurring, highly sulfated and the most complex GAGs. Heparin and heparan sulfate are synthesized in golgi apparatus of mammalian cells by the concerted action of different enzymes and its isoforms. Heparan sulfate is a major component of the ECM and the cell surfaces, generally found as proteoglycans. It is found to be involved in the regulation of a wide range of biological processes such as angiogenesis, cell signalling and tumor metastasis. On the other hand, heparin is present intracellularly in the granules of mast cells. It is mainly involved in the blood anticoagulation, wound healing, cellular communication, inflammation and pathogen recognition [62]. It is widely used as an anticoagulant agent for the prevention of blood coagulation during extracorporeal therapies.

1.2.1 Heparin production methods

Pharmaceutical grade heparin is traditionally extracted from animal sources such as porcine intestine and bovine lung. The preparation of pharmaceutical grade heparin from animal tissues comprises of the following steps. (i) collection and stabilization of the tissue, (ii) Digestion and release of heparin, (iii) recovery of raw heparin, (iv) purification of heparin and bleaching, (v) recovery of purified heparin. The process flow chart for extraction of heparin is presented in Figure 1.2. Briefly, heparin extraction process begins with soaking of the intestine in a salt solution and subsequent removal of intestinal mucosa. The resulting mucosa was preserved in sodium bisulphite, an oxygen scavenger, to limit microbial growth until further processing. The preparation of mucosa was carried out at pig slaughtering facility (not under current good manufacturing practices (cGMP) conditions) to reduce the environmental impact. The mucosa was further digested with proteolytic enzymes to release the heparin from the cells and proteoglycans. The raw heparin was purified by precipitation with quaternary ammonium salts, ion exchange resins, precipitation and bleaching. The purification of raw heparin was carried out in Food and Drug Administration (FDA) approved facilities under cGMP conditions to eliminate all potential contaminants such as other GAGs, residual proteins, endotoxins and viruses. The final yield of heparin was found to be approximately 300 mg per animal [113].

1.2.2 Heparin contamination crisis

In early 2008, the patients administered with heparin developed a serious adverse clinical reactions including angioedema, hypotension, swelling of the larynx and other severe symptoms. subsequently, these adverse symptoms resulted in the death of nearly hundred patients in the united states and turned this into a national health care crisis. As a result, the contaminated heparin lots were voluntarily recalled from the international market. The symptoms suggested an anaphylactoid response, however the exact etiology was not known [63]. The multiple orthogonal techniques such as multi-dimensional NMR was employed to identify the structure of the contaminated lots of heparin, which revealed the over-sulfated chondroitin sulfate (OSCS) as a potential contaminant, a highly sulfated "*heparin like*" polysaccharide [37]. Heparin contamination crisis prompted the FDA to devise strict regulations on the production and manufacturing of animal-derived heparin.

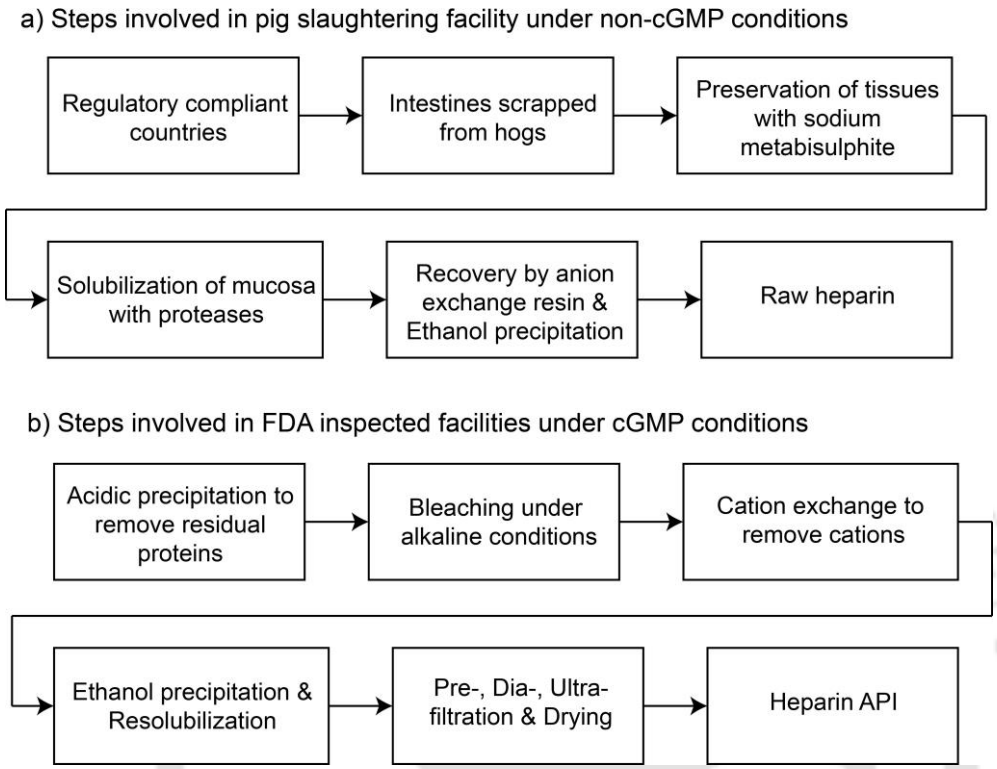

Figure 1.2: Process flow chart for the extraction of heparin from porcine intestinal tissues. GMP: Good Manufacturing Practices, FDA: Food and Drug Administration

1.2.3 Heparin production from non-animal sources

Currently, heparin extraction from animal sources fulfils the worldwide demands, however it is not a sustainable option due to safety, quality control issues and adverse environmental impact. These limitations triggered the scientific community to explore an alternative sources of heparin production. Chemical and chemoenzymatic synthesis emerged as an attractive alternative to the conventional animal-derived heparin. Fondaparinux, a heparin anti-thrombin binding domain based drug was synthesized using chemical methods, which showed a safer and superior characteristics than animal-derived heparin. Chemical synthesis of fondaparinux was achieved in approximately 55 steps, which corresponds to its very low yield and extremely high cost [16]. Consequently, animal-derived heparin is preferred over fondaparinux due to its lower price.

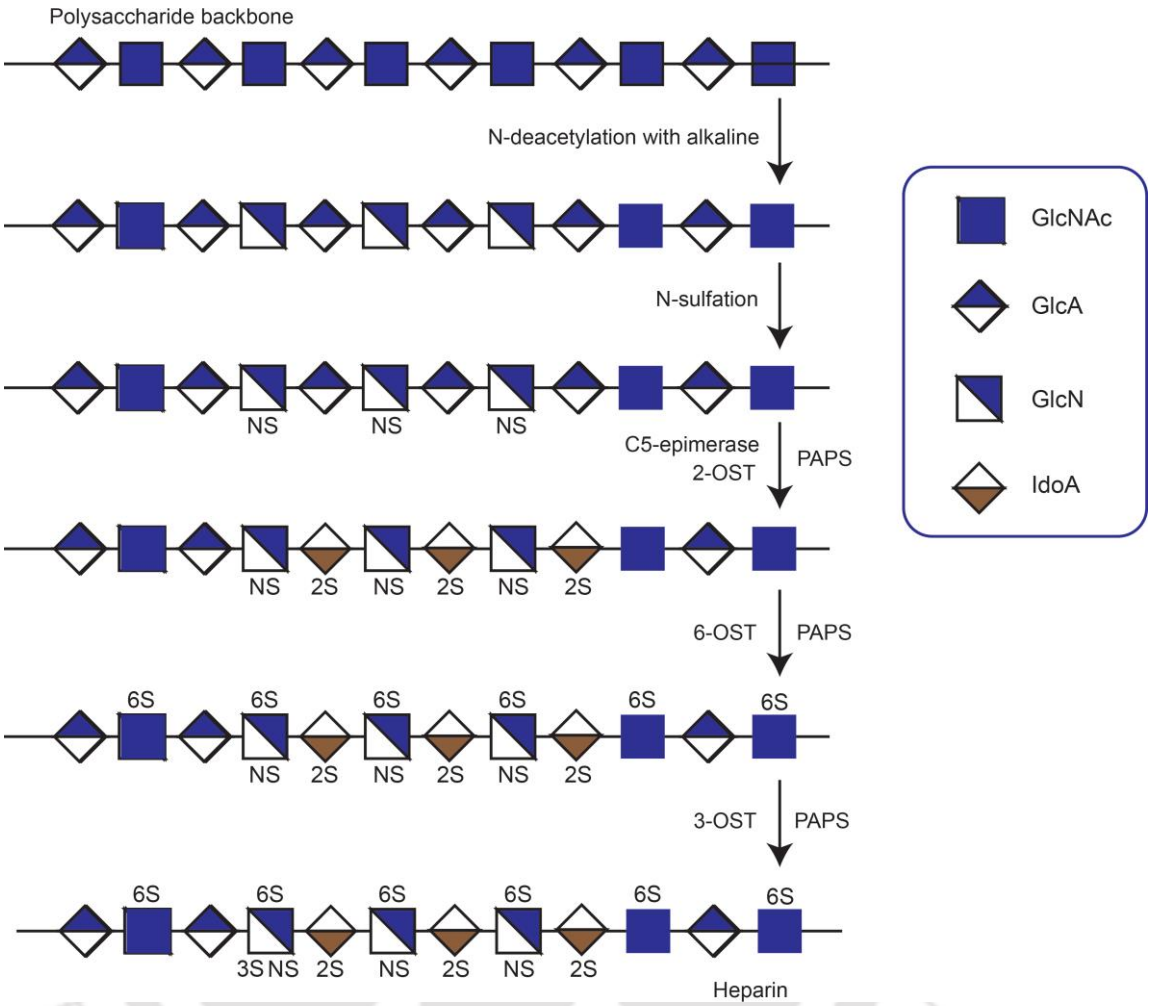

Figure 1.3: Chemoenzymatic synthesis of heparin. PAPS, 3-phosphoadenosine-5-phosphosulfate; OST, O-sulfotransferase

Chemoenzymatic synthesis of heparin offers several advantages over chemical synthesis such as scalability, cost-effective, lesser steps and generation of longer chain polysaccharides [130]. Chemoenzymatic synthesis employs heparan sulfate biosynthetic enzymes to synthesize the disaccharide backbone consisted of D-glucuronic acid (GlcA) and N-acetylglucosamine (GlcNAc). Further modification of the backbone relies on recombinantly expressed enzymes including N-deacetylase/ N-sulfotransferase, C5-epimerase, 2-O-sulfotransferase, 6-O-sulfotransferase, and 3-O-sulfotransferase. Chemoenzymatic synthesis of an ultra low molecular weight heparin with an excellent anticoagulant properties was achieved in 10 steps with an overall yield of 45% from simple disaccharide backbone. The synthesized heparin exhibited excellent anticoagulant and pharmacokinetic properties comparable to fondaparinux [130]. In another study, heparan sulfate

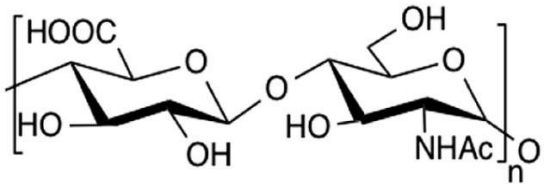

Figure 1.4: Chemical structure of heparosan. It is composed of repeating disaccharide units of GlcA and GlcNAc linked by β (1→4) and α (1→4) glycosidic bonds

pentasaccharide with antithrombin III-binding domain was enzymatically synthesized in 6 steps with two-fold higher yield compared to chemical synthesis [55]. chemoenzymatic synthesis offers an efficient method to prepare heparin with an excellent anticoagulant activity. Chemoenzymatic process of heparin synthesis is illustrated in Figure 1.3.
However, chemoenzymatic synthesis of heparin requires the linear, unsulfated heparan sulfate backbone as a starting molecule. The heparan sulfate backbone is also known as heparosan. The chain length and monosaccharide composition of the heparosan determines the molecular weight and size distribution of heparin, which in turn affect the biological activity. This dissertation deals with the biosynthesis of heparosan polysaccharide, which is the first step of chemoenzymatic heparin synthesis process [20].

1.3 Heparosan

Heparosan is a commercially expensive GAG, composed of repeating disaccharide units of GlcA and GlcNAc linked by β (1→4) and α (1→4) glycosidic bonds (Figure 1.4). Heparosan is a highly anionic and hydrophilic polysaccharide, attributed to the carboxylate and hydroxyl groups. Heparosan is an endogenous precursor in the biosynthesis of heparin and heparan sulfate in humans, thus does not elicit any immune response. Unlike heparin and heparan sulfate, heparosan is devoid of any biological activity with respect to coagulation, inflammation and others due to the lack of GlcA epimerization and sulfation. In addition, Heparosan is biodegradable through lysozyme mediated heparin/heparan sulfate degradation pathway in humans. Owing to these characteristics, heparosan has wide utility in biomaterials and drug delivery applications [26].

1.3.1 Applications of heparosan

The superior characteristics of heparosan has a potential to replace polyethylene glycol (PEG) as a conjugating vehicle in drug delivery applications [48, 58]. Heparosan based nano-drug carrier was developed for intracellular drug delivery [21]. The novel drug delivery platform, HEPtune, was developed based on heparosan to enhance the therapeutic potential by increasing the plasma half life and the lack of immunogenicity [26]. Recently, heparosan was proven to be a potential alternative to hyaluronic acid, a well known polysaccharide/biopolymer, as a nano-carrier for anticancer therapy [95]. In addition to drug delivery applications, heparosan is also used in biomaterials, gel and scaffolds for tissue engineering due to biocompatibility and water retention properties.

1.3.2 Sources of heparosan

1.3.2.1 Production of heparosan from microorganisms

Certain pathogenic microorganisms produce glycosaminoglycans as a capsule, which mimic the host polysaccharides, to evade host immune system during infection. So far, heparosan has been found to be synthesized by some pathogenic bacteria including *Escherichia coli* K5 [114], *Pasteurella multocida* Type D [85, 94] and *Avibacterium paragallinarum* [129]. However, *E. coli* K5 has been extensively studied for heparosan production by fermentation. The *E. coli* fermentation offers cost-effective and high production of heparosan.

1.3.2.2 Production of heparosan using glycosyltransferases

The natural heparosan producing microorganisms and mammalian cells possess glycosyltransferases, which catalyse the synthesis of heparosan polysaccharide chain. Harnessing the glycosyltransferases facilitate the synthesis of heparosan *in-vitro* and in other heterologous hosts. The mammalian glycosyltransferases, EXT1 and EXT2 have shown to form an active hetero-oligomeric complex, when co-expressed in yeast and mammalian cells. These cells were able to synthesize heparan sulfate chains [104]. In Drosophila, TTV, SOTV and BOTV enzymes, which are homologous to the mammalian EXT1, EXT2 and EXTL3 enzymes, were involved in the formation of heparan sulfate chains [44]. Similarly, heparosan biosynthesis in *E. coli* K5 is regulated by the stable association of KfiC and KfiA enzymes that possess glucuronyltransferase and glucosaminyltrans-

ferase activities, respectively [42, 108]. Unlike *E. coli* K5, *P. multocida* Type D possesses PmHS1, a bifunctional glycosyltransferase that has both glucuronyltransferase and glucosaminyltransferase activities [27]. PmHS2, a cryptic homolog to PmHS1 was identified and shown to produce heparosan when expressed in recombinant *E. coli* cells [28].

1.4 Definition of the problem

Heparosan can be efficiently produced by microbial fermentation and substantial reports are available on heparosan production by *E. coli* K5 fermentation [64, 123, 124]. Though enhanced heparosan production was reported, there are serious limitations associated with *E. coli* K5. All the natural producers are highly pathogenic and especially, *E. coli* K5 causes urinary tract infections in humans [114]. *E. coli* K5 uses the heparosan capsule to masquerade against the host immune system, thus causing the infections [24]. Moreover, *E. coli* K5 produces exotoxins and endotoxins, which require extensive purification and subsequent increase in the processing cost. Moreover, *E. coli* K5 genome encodes N-acetyl heparosan lyase which depolymerize the heparosan chain. Expression of the N-acetyl heparosan lyase throughout the fermentation could adversely affect the molecular weight and polydispersity of the heparosan [59]. These limitations have prompted for the usage of safe recombinant bacteria such as *E. coli*, *Bacillus subtilis* and *Bacillus megaterium* for the production of heparosan.

Bacillus megaterium, a safe gram-positive bacterium has been an important industrial host due to its superior characteristics such as the efficient expression of heterologous genes, stable plasmid maintenance, lack of alkaline protease activity and efficient secretion capability. It has been widely used for the recombinant production of various enzymes and vitamins [13, 68]. In addition, *B. megaterium* is free of endotoxins as opposed to *E. coli* K5. The genome sequences of *B. megaterium* expression strains DSM319 and QM B1551 are available in NCBI database (CP001982 and CP001983 respectively). A well characterized versatile expression systems allow efficient genetic manipulation in *B. megaterium* [12, 32, 101]. Whole genome sequence analysis revealed the presence of all homologous genes involved in the heparosan synthesis pathway except glycosyltransferase genes. In addition, *B. megaterium* genome does not encode any enzyme that depolymerize the heparosan. These characteristics endorse *B. megaterium* as an efficient heparosan production system in the present work.

1.5 Objectives of the present work

Natural producers of heparosan are highly pathogenic to humans. In addition, they are associated with the secretion of endotoxins and expression of heparosan lyase, which would adversely depolymerize the heparosan. To overcome the bottlenecks in heparosan production using natural producers, recombinant safe production of heparosan was attempted in *B. megaterium* expression system using metabolic engineering approaches. Accordingly, the following objectives were formulated in this thesis work:

1. Metabolic engineering of *B. megaterium* for heparosan biosynthesis using *E. coli* K5 glycosyltransferases
2. Application of Dual promoter expression system for the enhanced heparosan production in *B. megaterium*
3. Influence of sucrose concentration and N-acetylglucosamine supplementation on heparosan biosynthesis in *B. megaterium*

CHAPTER 2

REVIEW OF LITERATURE

Heparosan production through microbial fermentation is a promising method to prepare chemoenzymatic heparin. Until now, *E. coli* K5, *P. multocida* type D and genetically modified microorganisms have been used to produce heparosan. A clear understanding of the heparosan metabolic pathway is critical in devising any strategies to tackle the challenges in heparosan production. Briefly, heparosan biosynthesis in producing microorganisms consisted of three steps. (i) UDP-precursor sugar biosynthesis, (ii) polymerization by glycosyltransferases and (iii) heparosan transportation to the cell surface [6]. The following section explains the metabolic pathways involved in heparosan biosynthesis in *E. coli* K5 and *P. multocida*.

2.1 Heparosan biosynthesis in *E. coli* K5

2.1.1 Genetic organization of *E. coli* K5 heparosan biosynthesis gene cluster

E. coli K5 belongs to the family of group 2 capsule producers. The biosynthesis of group 2 capsules is facilitated by proteins encoded by *kps* loci in the genome. Group 2 *kps* loci is divided into three regions (Figure 2.1). Region 2 genes encode for glycosyltransferases and rate-limiting UDP-nucleotide sugar synthetases involved in capsular polysaccharide biosynthesis. Region 2 genes are serotype specific and varies according to the structure

Figure 2.1: Genetic organization of *E. coli* K5 *kps* loci. Region 2 consists of serotype specific glycosyltransferases (*kfiA,B,C,D*) which involve in the biosynthesis of heparosan. Region 1 (*kpsF,E,D,U,C,S*) and 3 (*kpsM,T*) are conserved among different serotypes and involve in the export of heparosan to the cell surface

and repeating disaccharide units of the capsule [87]. Region 1 and 3 genes are highly conserved among different serotypes and work independently of the capsular polysaccharide synthesis. Region 1 and 3 genes are involved in the export and the assembly of capsular polysaccharide on the cell surface [4, 36, 93].

The schematic representation of heparosan production and export is given in Figure 2.2. Biosynthesis of heparosan in *E. coli* K5 is catalyzed by four proteins, KfiA, KfiB, KfiC and KfiD, present in serotype specific region 2 of *kps* loci. These proteins forms a hetero-oligomeric complex on the inner face of the cytoplasmic membrane [87]. KfiC and KfiA encode for β-glucuronyltransferase and α-glucosaminyltransferase, respectively. Heparosan biosynthesis involves the formation of glycosidic bonds by the addition of monosaccharide sugars from UDP-precursor sugars. The glycosyltransferase reaction occurs either by inversion mechanism in which β-GlcA is formed from α-linked UDP-precursor sugar or by retaining mechanism in which α-GlcNAc is formed from α-linked UDP-precursor sugar. Both glycosyltransferases add the monosaccharide moiety to the non-reducing end of heparosan chain [42, 108]. The role of KfiB remains elusive. However, the structural analysis of KfiB predicted the formation of coiled-coil structure, which suggested that the probable role of KfiB in the formation and stabilization of the KfiC-KfiA enzyme complex [36]. *kfiD* encodes for UDP-glucose dehydrogenase, which oxidizes the UDP-glucose to UDP-GlcA, one of the precursors in heparosan biosynthesis [105].

KpsU encodes for CMP-Kdo synthetase, which catalyzes the formation of CMP-Kdo (3-deoxy-d-manno-2-octulosonic acid). Kdo binds to the acceptor molecule α-glycerophosphate to form phosphatidyl-Kdo [99]. KpsC and KpsS proteins attach the phosphatidyl-Kdo moiety to the reducing end of the heparosan polysaccharide chain, which then entered into the export pathway [128]. ABC (ATP-binding cassette) transporter system drives the translocation of heparosan across cell membrane at the expense of ATP hydrolysis. ABC transporters are characterized by the presence of two domains, a transmembrane domain

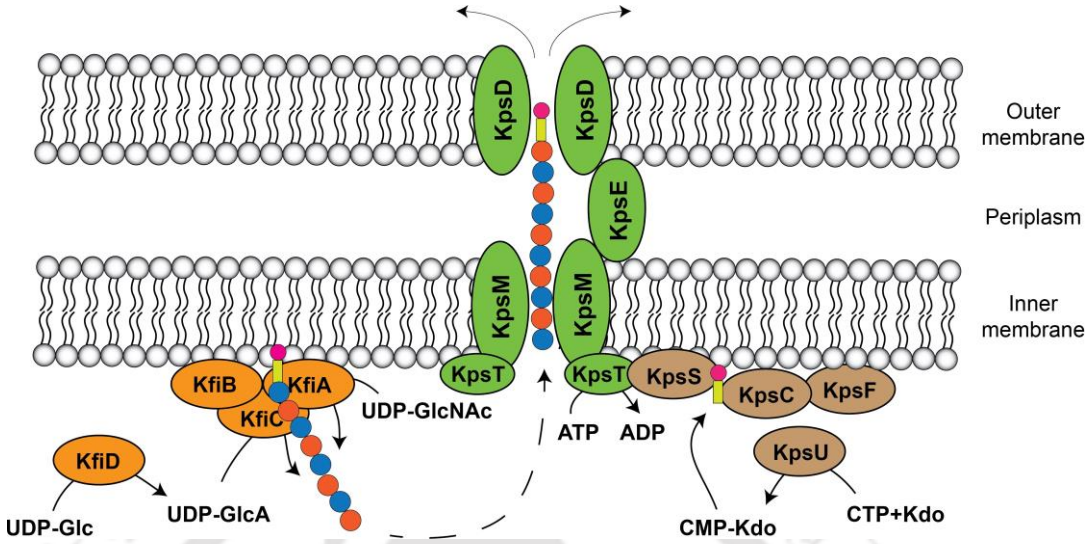

Figure 2.2: Schematic represenation of *E. coli* K5 heparosan capsule assembly complex

and a nucleotide binding domain. The proteins encoded by region 3 genes, kpsM and kpsT constitute the ABC transporter system in *E. coli* K5. KpsM is the integral transmembrane subunit with six transmembrane helices present in the inner membrane whereas KpsT is a cytoplasmic ATPase. ATP hydrolysis leads to the conformational change of KpsT and interacts with KpsM, thereby facilitating the export of heparosan across inner membrane [36]. KpsD and KpsE proteins mediate the subsequent translocation of heparosan to the cell surface [4, 98].

2.1.2 Biochemistry of heparosan metabolic pathway in *E. coli* K5

E. coli K5 uses simple carbon sources such as glucose to produce heparosan. Figure 2.3 depicts the heparosan biosynthesis pathway from glucose in *E. coli* K5. Glucose is metabolized via glycolysis to glucose-6-phosphate (G-6-P) and fructose-6-phosphate (F-6-P). Two parallel metabolic branches emerge from G-6-P and F-6-P, which result in the synthesis of UDP-GlcA and UDP-GlcNAc through multiple sugar intermediates. G-6-P is converted to glucose-1-phosphate (G-1-P) by α-phosphoglucomutase. The subsequent conversion of G-1-P to UDP-glucose by UDP-glucose pyrophosphorylase. G-1-P is also used as a precursor for cell wall synthesis (teichoic acid and other cell wall components). UDP-glucose is oxidized to UDP-GlcA by UDP-glucose dehydrogenase (*kfiD*) with a concomitant re-

duction of two NAD^+ molecules. The second branch point emerges from F-6-P, which leads to the formation of UDP-GlcNAc. Glutamine–fructose-6-phophate transaminase catalyzed the formation of glucosamine-6-phosphate (GlcN-6-P) from F-6-P by transferring the amino group from glutamine. GlcN-6-P is converted to glucosamine-1-phosphate (GlcN-1-P) by Phosphoglucosamine mutase. Glucosamine-1-phosphate acetyltransferase / N-acetylglucosamine-1-phosphate uridylyltransferase, a bifunctional enzyme is responsible for the acetylation of GlcN-1-P to N-acetylglucosamine-1-phosphate (GlcNAc-1-P) followed by synthesis of UDP-GlcNAc. The latter is also an essential precursor for peptidoglycan biosynthesis involved in the cell wall formation. The glycosyltransferases (*kfiC* and *kfiA*) transfer GlcA and GlcNAc from the UDP-precursors to elongate the heparosan chain.

Microbial heparosan synthesis is a carbon and energy intensive process. One mole of heparosan disaccharide production requires 2 moles of glucose, 2 moles of ATP, 2 moles of UTP, one mole of acetyl-CoA. Excess amount of heparosan synthesis causes substantial metabolic burden on the microbial cell. Moreover, precursors of heparosan biosynthesis are also required for cell wall synthesis, glycolysis and pentose phosphate pathway (Figure 2.3). In order to synthesize large quantities of heparosan, all the precursor metabolites must be maintained at sufficient levels to sustain proper cell growth and heparosan production.

UDP-glucose dehydrogenase catalyzes the oxidation of UDP-Glucose to UDP-GlcA, which determined to be a rate limiting step in mammalian glycosaminoglycan biosynthesis [107, 125]. However, the over-expression of UDP-glucose dehydrogenase in *E. coli* K5 led to the decreased production of heparosan, which suggested that the heparosan biosynthesis is strictly regulated in *E. coli* K5 [97]. In addition, over-expression of UDP-glucose dehydrogenase increases the G-6-P flux towards UDP-GlcA synthesis, thus reducing the synthesis of F-6-P, a precursor of UDP-GlcNAc. Hence, the efficient synthesis of heparosan requires the balanced proportions of UDP-GlcA and UDP-GlcNAc precursors [124].

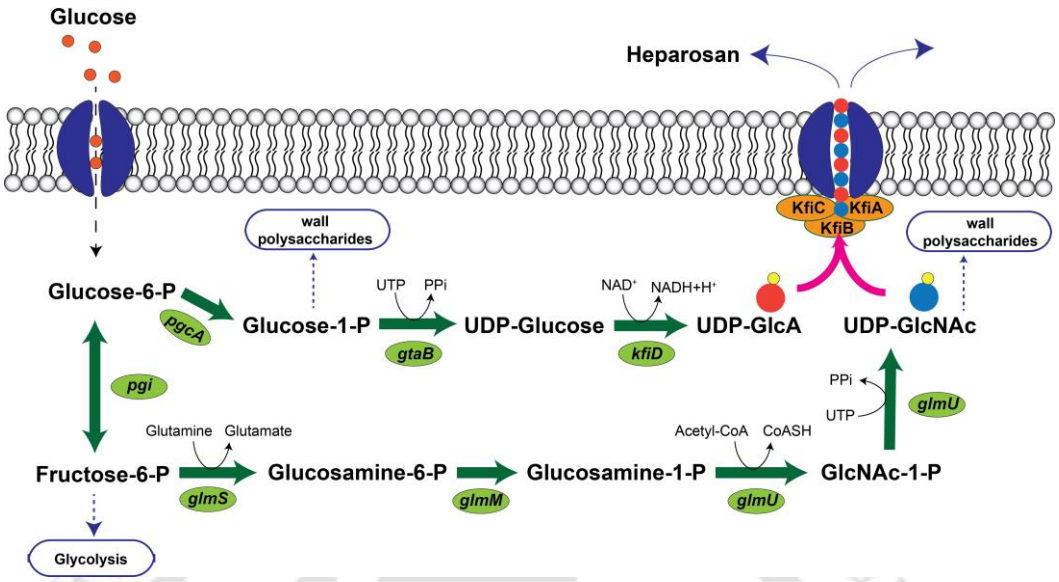

Figure 2.3: Metabolic pathway for heparosan production in *E. coli* K5

2.1.3 Regulation of heparosan molecular weight in *E. coli* K5

The anticoagulant activity of heparin is influenced by its molecular weight. The heparin molecular weight obtained through chemoenzymatic synthesis is entirely depends on the molecular weight of heparosan. Hence, heparosan molecular weight is an important attribute to be considered for the chemoenzymatic synthesis of heparin. However, the molecular weight control or chain termination mechanism is not known. The heparosan chain elongation was facilitated by the relative proportions of UDP-GlcA and UDP-GlcNAc precursors. The imbalanced supply of any of the UDP-precursors would lead to the termination of heparosan chains [61, 97].

elmA gene encodes for K5 lyase in *E. coli* K5 genome, which depolymerize the heparosan through β-elimination mechanism [59]. Expression of K5 lyase aids in improving the heparosan productivity by shedding the heparosan from cell surface to fermentation medium. The deletion of *elmA* from *E. coli* K5 genome caused a significant decrease in the amount of heparosan in the supernatant and also influences cell associated heparosan. This study indicated that *elmA* involves in the shedding of heparosan into the medium [41]. Another protein, WaaR was involved in the biosynthesis of lipo-polysaccharide outer core in *E. coli* K5. Mutation in the *waaR* gene decreased the retention of heparosan on to the *E. coli* K5 cell surface [111]. In another study, deletion of *waaR* in *E. coli* K5 resulted in the synthesis of low molecular weight heparosan [43].

E. coli K5 lyase could be an ideal molecular tool to depolymerize or regulate the molecular weight of heparosan. High constitutive expression of K5 lyase could adversely affect the heparosan molecular weight. The regulation of K5 lyase expression is not known. Previous studies have shown that growth and culture conditions influence the *E. coli* K5 lyase activity [69, 70]. The regulatable K5 lyase expression system using inducible promoter might offer the synthesis of heparosan with distinct molecular weight [124].

2.1.4 Fermentative production of heparosan using *E. coli* K5

Fermentative production of heparosan was carried out using *E. coli* K5 on various growth media such as LB medium, M9 medium, glucose defined medium and glycerol defined medium. Heparosan obtained from glucose and glycerol defined medium showed higher purity levels than complex LB medium as determined by nuclear magnetic resonance (NMR) analysis. Since, heparosan production in *E. coli* shown to be growth-associated, fed-batch fermentation with exponential glucose feeding was carried out to enhance the *E. coli* K5 growth. A high heparosan yield of 15 g/L was achieved with the weight-average molecular weight of 84 kDa [123].

In another study, glycerol was employed as an alternative carbon source for the heparosan production. Glycerol defined medium yielded higher heparosan titer and volumetric productivity compared to glucose defined medium. Among different glycerol feeding strategies used, DO-stat fed-batch cultivation yielded the highest heparosan concentration of 8.63 g/L [64].

2.2 Heparosan biosynthesis in *Pasteurella multocida* Type D

Pasteurella multocida Type D produces extracellular polysaccharide capsule, which serves as a virulence factor that causes atrophic rhinitis in swine and pasteurellosis in other domestic animals. The extracellular capsule aids the bacteria to evade host defence mechanism. The capsule structure resembles unsulfated and unepimerized heparin backbone and sensitive to depolymerization by heparin lyase III. Heparosan synthase (PmHS1) was identified from the genome of *P. multocida* type D. The sequence encoding PmHS1 was cloned and expressed in recombinant *E. coli*, which catalyzes the formation of heparosan by polymerizing the monosaccharide UDP-precursor sugars, UDP-GlcA

and UDP-GlcNAc. Addition of exogenous polymer acceptor stimulated the heparosan synthase activity by 7 to 25-fold. PmHS1 is the dual action glycosyltransferase, which possesses both GlcA-transferase and GlcNAc-transferase activities [27]. In contrast, *E. coli* K5 employs two separate proteins, KfiC and KfiA to catalyze the polymerization of UDP-GlcA and UDP-GlcNAc precursors. Although, *P. multocida* is not yet utilized for microbial production, *P. multocida* derived heparosan synthase PmHS1 was extensively used for the recombinant and in-vitro synthesis of heparosan. The genes encoding heparosan synthase, UDP-precursor sugar forming proteins and transport proteins are found in operon architecture designated as capsule biosynthesis gene locus.

Later, another gene product which is 73 % similar to the heparosan synthase was identified outside of the capsule biosynthesis gene locus. This cryptic homolog of heparosan synthase was determined to be functional and designated as PmHS2. Unlike PmHS1, addition of exogenous polymer acceptor did not greatly increase the PmHS2 activity and produced smaller molecular weight heparosan [28]. PmHS2 also can able to incorporate many unnatural UDP-precursor sugar analogues into heparosan chain in-vitro [106]. In addition to *P. multocida* Type D, the gene sequence encoding PmHS2 is also present across *P. multocida* Type A and Type F strains [28].

To date, PmHS2 has been widely used as a catalyst to polymerize UDP-precursor sugar analogues to produce heparosan in-vitro [18, 19, 78]. PmHS2 was efficiently purified and incubated in the presence of 5 mM of each UDP-GlcA and UDP-GlcNAc to produce the average heparosan molecular weight of 102 kDa. The heparosan molecular weight distribution was modulated by changing the initial UDP-precursor sugar concentration. Low UDP-precursor sugar concentration resulted in the formation of high molecular weight of heparosan with low polydispersity index [18]. The removal of N-terminal 80-aminoacids in PmHS2 greatly improved the protein expression level and stability while maintaining the substrate promiscuity. The reverse glycosylation of PmHS2 led to the size controlled synthesis of heparosan decasaccharide [78].

2.3 Heparosan biosynthesis in recombinant microorganisms

E. coli K5 derived heparosan has emerged as a promising precursor for chemoenzymatic heparin synthesis. However, pathogenicity and potential to secrete endotoxins would

hamper the application of *E. coli* K5 derived heparosan in pharmaceutical and biomedical applications. The recombinant production of heparosan using safe microorganisms would eliminate the aforementioned limitations. The production of heparosan in heterologous hosts requires the expression of *E. coli* K5 glycosyltransferase or *P. multocida* heparosan synthase genes. The expression of glycosyltransferase genes has been found to produce negligible amounts of heparosan [133]. Though the genes responsible for the UDP-precursor sugar synthesis are present in heterologous hosts, the expression was found to be limiting for other capsular polysaccharide synthesis [88, 133]. Hence, co-expression of glycosyltransferase genes and UDP-precursor synthesis pathway genes would yield a high amounts of heparosan. so far, *E. coli*, *Bacillus subtilis*, *Bacillus megaterium* and cyanobacteria were engineered to produce heparosan.

2.3.1 Heparosan biosynthesis in non-pathogenic *E. coli*

Heterologous expression of region 2 genes of K5 gene cluster in non-pathogenic *E. coli* K12 resulted in the intracellular accumulation of heparosan, which could be due to the lack of region 1 and 3 genes. Subsequently, intracellular expression of K5 lyase resulted in the partial degradation of heparosan to produce degree of polymerization (DP) 2-10 oligosaccharides [8].

The region 2 of K5 gene cluster were heterologously expressed in *E. coli* BL21 (DE3) to synthesize heparosan. Four recombinant clones were constructed containing sAC, sABC, sACD and sABCD gene combinations. The clones sACD and sABCD produced comparable heparosan yield, which implies that UDP-GlcA concentration was limiting the heparosan production in *E. coli* BL21. Interestingly, the heparosan was transported into the fermentation medium even the region 1 and 3 genes of K5 gene cluster were not expressed. This result suggests that *E. coli* BL21 transport machinery is efficient enough to translocate the heparosan outside the cell. Polydispersity index of heparosan recovered from *E. coli* BL21 was less than that of *E. coli* K5 [133].

E. coli trigger factor (TF) was fused with KfiC to stabilize KfiCA complex in the absence of the stabilisator KfiB. Heparosan was accumulated intracellularly in the early stages of the culture and made available extracellular at the end of fermentation due to passive diffusion or partial cell disruption [60].

Various non-pathogenic *E. coli* strains were developed by expressing the region 2 of K5 gene cluster. Heparosan molecular weight ranging from 5 kDa to >150 kDa was produced

by modulating the culture conditions and media composition. In addition, controllable expression of K5 lyase using different inducible promoter led to the synthesis of size-specific heparosan (DP4, DP6, DP8 and DP10) oligosaccharides [100].

2.3.2 Heparosan biosynthesis in *Bacillus* strains

Bacillus sp. was found to be an efficient expression system for the synthesis of capsular polysaccharides such as hyaluronic acid, heparosan and chondroitin due to the well established plasmid systems for heterologous protein expression and an efficient secretion pathway for proteins and polysaccharides [22, 47, 126, 127].
kfiC and *kfiA* glycosyltransferase genes were integrated into the genome of *B. subtilis* to facilitate the synthesis of heparosan. Homologous over-expression of UDP-glucose dehydrogenase encoded by *tuaD* enhanced the heparosan production to 5.82 g/L in fed-batch fermentation. The molecular weight and polydispersity index obtained from recombinant *B. subtilis* closely resemble the *E. coli* K5 derived heparosan [47].
In another study, *B. subtilis* was engineered with *P. multocida* heparosan synthase PmHS1 to synthesize heparosan. Xylose inducible promoter was used to express the *pmHS1* gene whereas the UDP-precursor pathway genes (*tuaD*, *gtaB* and *gcaD*) were expressed under IPTG inducible promoter. By optimizing the induction time of heparosan synthase module and UDP-precursor module, different molecular weight range of heparosan was obtained. Hence, heparosan molecular weight was proved to be modulated by the amount of heparosan synthase and UDP-precursors [22].
In another study, cryptic heparosan synthase PmHS2 was expressed in *B. megaterium* using T7 RNA polymerase dependent expression system. The obtained heparosan was polydisperse in nature predominantly consisted of high molecular weight and less abundent low molecular weight [127].

2.3.3 Heparosan biosynthesis in cyanobacteria

Cyanobacteria was engineered using *P. multocida* PmHS2 for the photosynthetic production of heparosan. *Synechococcus elongatus* PCC 7942 was chosen as an expression host for heparosan production due to generally regarded as safe (GRAS) status, fast photoautotropic growth and enhanced sugar phosphate pathway flux to synthesize UDP-precursor sugar. The expression of PmHS2 enabled the heparosan synthesis pathway in *S. elongatus*. To further increase UDP-GlcA nucleotide pool, UDP-glucose pyrophospho-

rylase (*galU*) was expressed along with PmHS2. The recombinant *S. elongatus* produced the maximum heparosan of 2.8 μg/L under high CO_2 and light conditions [103]. This study presented a proof of concept for *S. elongatus* as a production host for complex polysaccharide synthesis.

2.4 *Bacillus megaterium*

2.4.1 General characteristics

Bacillus megaterium is a gram positive soil bacterium, first described by De Bary more than 100 years ago [25]. It was named "megat(h)erium" (Greek for big animal) after the size of 1.5 x 4 μm and volume of 100 times bigger than *E. coli*. Owing to its large size of vegetative cells, it has been extensively exploited for the studies on cell structure, sporulation, protein localization and morphological analysis long before *B. subtilis* was introduced as a gram positive model organism [30]. Phylogenetic and 16S rRNA sequence analysis revealed that *B. megaterium* lies within the same group as *B. subtilis*, but closely related to *B. licheniformis*, *B. cereus*, *B. anthracis* and *B. pumulis* than *B. subtilis* [5]. Though *B. megaterium* is a soil bacterium, it has been found in the diverse ecological habitats such as rice paddies, sediments, honey, fish, and dried foods. Moreover, it is capable of utilizing the wide variety of carbon sources, including sugars and tricarboxylic acid cycle intermediates such as citrate, formate and acetate. In addition, it does not produce endotoxins in contrast to gram negative *E. coli*. It also does not possess any alkaline proteases which could degrade the recombinant proteins. These characteristics make *B. megaterium* an ideal industrial workhorse for the production of commercially relevant proteins including penicillin G acylase [71], amylases [75, 110], glucose dehydrogenase [79]. Furthermore, it is also used to produce vitamin B_{12}, oxetanocin, antimicrobial agents and P450 cytochrome monooxygenases [39, 77, 92].

2.4.2 *B. megaterium* as an expression host

Beyond traditional applications, *B. megaterium* has emerged as an ideal expression host for the production of novel recombinant proteins. Whole genome sequence of *B. megaterium* DSM319 is available in NCBI database under the accession number CP001982, thus broadening the scope of engineering of *B. megaterium* [30]. In contrast to *B. sub-*

Table 2.1: Portfolio of proteins and industrial products of *B. megaterium* and their applications

Product/protein	Industrial applications	Reference
α-amylases	alternative to pullulanases	[110]
β-amylases	Bread industry	[75]
Chitosanases	Fungal and yeast cell wall lysis	[86]
Glucose dehydrogenase	NADH/NADPH regeneration, blood glucose test and biosensors	[79]
Neutral protease	Leather industry	[57, 74]
Oxetanocin	Inhibits HIV, hepatitis B virus, cytomegalovirus, herpes virus	[77, 112]
Penicillin amidase	development of synthetic penicillins	[71, 132]
Antibody fragments	Therapeutic applications	[49, 50]
Clostridium difficile toxin A and B	clinical diagnosis development	[131]
Vitamin B_{12}	Aerobic vitamin B_{12} producer	[13, 92]
Polyhydroxybutyrate (PHB)	Polypropylene alternative, biodegradable plastic material	[51, 56]
Functionalized PHB beads	Vaccines, diagnostics and enzyme immobilization	[35]
Keratinase	Poultry and leather industry	[89, 90]

tilis, it does not posses any alkaline proteases which enhances the stability of secreted proteins. It has excellent structural and segregational stability of multiple plasmids i.e. stable plasmid replication system even in the absence any selection pressure [73, 118]. Other interesting characteristics such as high biosynthetic and secretion capacity of recombinant proteins and absence of endotoxins make this bacterium an attractive alternative to conventional *E. coli* protein expression system [116]. Unlike *B. subtilis*, the mechanism of natural transformation of exogenous DNA is not known. However, *B. megaterium* can be efficiently transformed using polyethylene glycol (PEG)-mediated protoplast transformation [72, 117]. Genetic manipulation of *B. megaterium* is facilitated

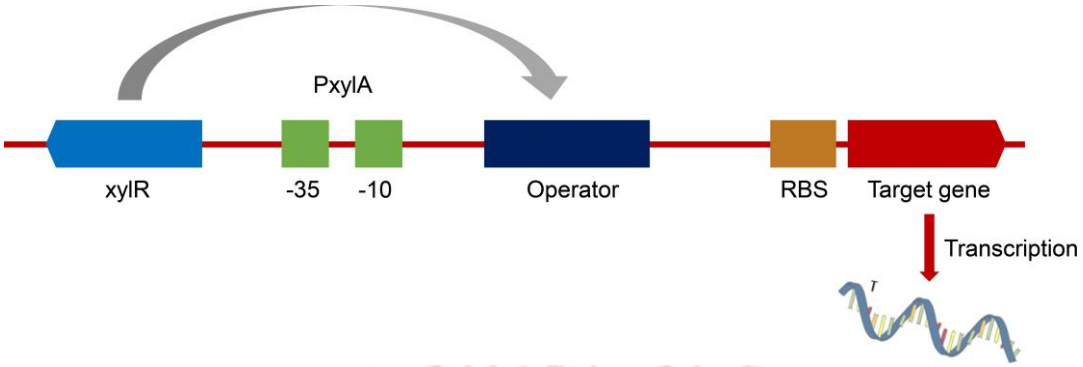

Figure 2.4: Genetic organization of xylose utilization operon in *B. megaterium*

by the wide varieties of expression systems. Constitutive and inducible expression systems were developed for the heterologous expression of foreign genes [73, 101, 102]

2.4.3 Constitutive expression system

The construction of constitutive expression plasmid was based on the control sequences of glucose dehydrogenase (*gdh*) gene in *B. megaterium*. Using *gdh* promoter, homologous glucose dehydrogenase (*gdh*)and heterologous chloramphenicol acetyltransferase (*cat*) were expressed efficiently in *B. megaterium* [73].

2.4.4 xylose-inducible expression system

Controllable production of biomolecules can be achieved by the inducible promoter. Recombinant gene expression can be modulated by the amount of inducer added to the medium. Rygus et al. observed that several-fold enhancement of the xylose utilization genes when xylose was added into the culture medium [102]. Genome mining of *B. megaterium* revealed the presence of xylose inducible promoter sequence P_{xylA} along with the gene for regulatory repressor protein XylR. P_{xylA} transcribes xylose isomerase XylA, xylulokinase XylB and xylose permease XylT, which constitutes the xylose operon found in *B. megaterium* genome. Xylose repressor protein, XylR located upstream of the P_{xylA} regulates the transcription of *xyl*-operon. The genetic architecture of xylose utilization operon is depicted in Figure 2.4. In the absence of xylose, XylR binds to the operator sequence and inhibits the transcription of *xyl*-operon. Presence of xylose changes the

confirmation of XylR, which results in the release of XylR from operator sequence. RNA polymerase binds to P_{xylA} and enhanced the expression of *xyl*-operon to approximately 350-fold [102]. In addition, glucose-mediated repression of P_{xylA} activity is regulated by catabolite response element (cre) sequence present in the *xylA* open reading frame and catabolite regulatory protein (CcpA) [38].

Based on P_{xylA}, Rygus and Hillen developed a plasmid-borne xylose-inducible expression system for the overproduction of recombinant proteins in *B. megaterium* [101]. The plasmid consists of P_{xylA} sequence, *xylR* sequence and multiple cloning site. Inhibition of recombinant gene expression by glucose through carbon catabolite repression was eliminated by the removal of cre sequence. The production of glucose dehydrogenase, β-galactosidase, mutarotase and urokinase like plasminogen activator proteins in *B. megaterium* using xylose inducible plasmid system was successfully demonstrated [101]. Later, this plasmid provided the basis for efficient and commercialized xylose-inducible expression system for *B. megaterium* (MoBiTec, Göttingen, Germany). Several heterologous proteins including Dextransucrase, levansucrase, antibody fragments and Clostridium difficile toxin A were successfully produced using xylose-inducible plasmid system [15, 49, 50, 54, 68].

2.4.5 Sucrose-inducible expression system

Sucrose-inducible promoter is a viable alternative to xylose-inducible promoter for the production of recombinant proteins. Secretome analysis suggested that *B. megaterium* strongly secreted a 52 kDa protein in the presence of sucrose in LB medium, which was not present in the absence of sucrose. The secreted protein was determined to be levansucrase, SacB by MALDI-TOF/MS analysis. The promoter sequence, P_{sacB} was identified and cloned in the replicating plasmid to develop sucrose-inducible expression system. Homologous levansucrase and heterologous green fluorescent protein were successfully produced using sucrose-inducible plasmid system [12].

2.4.6 T7 RNA polymerase dependent expression system

Bacteriophage originated DNA-dependent RNA polymerases were proven to be efficient in transcribing the gene of interest in other gram positive and gram negative microorganisms [23, 109]. Gamer et al. constructed a T7 RNA polymerase dependent plasmid system for the intracellular and extracellular expression of recombinant proteins in *B.*

megaterium [32]. A two-plasmid expression system was developed with compatible origin of replications of *B. megaterium* (pBM100 and pBC16 replicons). One plasmid carrying T7 RNAP gene under the control of xylose-inducible promoter and the other carrying the gene of interest under T7 RNAP-dependent promoter. The cytosolic production of green fluorescent protein and the extracellular secretion of levansucrase were demonstrated as model proteins. Compared with xylose-inducible expression system, T7 RNAP dependent plasmid system showed a 7-fold improvement in recombinant GFP production [32].

2.5 Kinetic modeling

Kinetic modeling refers to a set of mathematical expressions, which describe the relationship between cell growth, substrate consumption and product formation [2, 83]. It is employed in several industries owing to its advantages in saving time, labour and cost associated with the experimental work. Estimation of kinetic parameters such as specific growth rate, yield coefficients in batch fermentation would provide the information about the optimal feed rate or dilution rate needed to be maintained in the and fed-batch and chemostat fermentation systems. Inhibition coefficients aid in determining the maximum substrate concentration can be used in fed-batch fermentation and in redesigning of fermentation medium. Kinetic models used in bioprocess were classified into four categories [82].

(i) Structured model: cells as a multi component system, which consider cell structure, metabolic pathways and intracellular biochemical reactions

(ii) Unstructured model: cells as a black box entity, which does not account the physiological characterization of cells and consider only the biochemical reactions at extracellular conditions

(iii) Segregated model: take account of the heterogeneity between cells and considers cells as a multi component system

(iv) non-segregated model: consider cells a uniform entity with average cellular properties

Based on the type of kinetic model and the complexity, the biological system is classified into structured and segregated, unstructured and non-segregated, structured and non-segregated, unstructured and segregated. A structured and segregated model is often best describes the microbial production of biological molecules [31]. However, Unstructured and non-segregated models are extensively used in modeling the bacterial growth and biopolymer or polysaccharide production due to its low level of complexity

[29, 96, 120, 122]. They assume a homogeneous reactor environment where the average cell behavior can be used to predict the kinetics of the system. The simplest unstructured kinetic models are described by Eq. 2.1 to Eq. 2.3, where the substrate consumed by microorganisms is channeled into cell growth and product formation. The rate of cell growth (r_X), substrate consumption (r_S) and product formation (r_P) are given as a linear function of specific growth rate (μ).

The rate of cell growth is represented in Eq. 2.1

$$r_X = \frac{dX}{dt} = \mu X \tag{2.1}$$

The rate of product formation is represented as Luedeking-Piret equation in Eq. 2.2

$$r_P = \frac{dP}{dt} = \alpha\frac{dX}{dt} + \beta X = (\alpha\mu + \beta)X \tag{2.2}$$

where, α and β are Luedeking-Piret constants [66], which denotes growth associated ($\alpha \neq 0$, $\beta = 0$) and non-growth associated ($\alpha = 0$, $\beta \neq 0$) and mixed-growth associated ($\alpha \neq 0$, $\beta \neq 0$) product formation.

The rate of substrate consumption is represented in Eq. 2.3

$$r_S = -\frac{dS}{dt} = \frac{1}{Y_{X/S}}\frac{dX}{dt} + m_S X + \frac{1}{Y_{P/S}}\frac{dP}{dt} \tag{2.3}$$

2.5.1 Substrate independent kinetic models

Kinetic modeling of the cell growth aids to establish a relationship between the parameters such as specific growth rate (μ_m) and lag phase of growth (λ_X) to understand the cell growth behavior on various culture conditions and different growth media. Substrate independent models such as Logistic and Gompertz explain the cell growth kinetics based on the sigmoidal nature independent of substrate concentration. The logistic equation (Eq. 2.4) relates the rate of cell growth to specific growth rate and unused carrying capacity. It presents the macroscopical description of cell growth and widely used to describe cell growth kinetics

$$r_X = \frac{dX}{dt} = \mu_m X\left(\frac{X_m - X}{X_m}\right) \tag{2.4}$$

where, X_m is the maximum cell concentration (g/L) and μ_m is the maximum specific growth rate (h^{-1}).
The logistic equation (Eq. 2.4) of modified to obtain different forms of integrated expression for X as a function of t based on the behavior of cell growth with certain assumptions [17, 34, 52, 65, 96, 119, 121].
The modified logistic equation [9] as described by Benkortbi et al. is given by Eq. 2.5

$$X = \frac{X_o\, e^{\mu_m t}}{[1 - \frac{X_o}{X_m}(1 - e^{\mu_m t})]} \tag{2.5}$$

Vázquez and Murado [119] proposed a modified logistic equation (Eq. 2.6) by incorporating the lag time of growth (λ_X) and cell growth rate (v_X)

$$X = \frac{X_m}{1 + \frac{4v_X(\lambda_X}{X_m}} \tag{2.6}$$

where, X is the cell concentration (g/L), X_m is the maximum cell concentration obtained (g/L), v_X is the maximum cell growth rate (g/L. h), and λ_X is the lag phase of cell growth.

2.5.2 Substrate dependent kinetic models

The substrate dependent kinetic models are classified into (i) substrate limiting and (ii) substrate inhibition models. Monod model (Eq. 2.7) is widely used to describe the relationship between the specific growth rate (μ) and substrate concentration (S). Monod model is valid only when the substrate is in a limiting concentration.

$$\mu = \frac{\mu_m S}{K_S + S} \tag{2.7}$$

where, K_S is saturation constant (g/L) and μ_m is the maximum specific growth rate
Several substrate inhibition models are derived by incorporating the inhibition coefficient in Monod's equation. Andrew [3] and Aiba [1] models are widely used to obtain the kinetic parameters when the substrate is used in inhibitory concentration.
Andrew model is given in Eq. 2.8

$$\mu = \frac{\mu_m S}{(Ks + S + \frac{S^2}{K_I})} \tag{2.8}$$

Aiba model is given in Eq. 2.9

$$\mu = \frac{\mu_m S}{Ks + S} exp^{(\frac{S}{K_I}} \tag{2.9}$$

2.5.3 Multi-substrate kinetic models

Multi substrate kinetic modeling determines the contribution of individual substrate to biomass growth, product formation and cellular maintenance [7]. Substrate consumption pattern is classified into (i) Additive type model (Eq. 2.11), where sequential consumption of the substrates due to catabolite repression (ii) interactive or multiplicative type model (Eq. 2.10), where simultaneous consumption of the substrates (iii) Non-interactive type model (Eq. 2.12) [11].

Interactive and multiplicative type:

$$\mu = \mu_{max} * \mu(S_1) * \mu(S_2) * .... * \mu(S_n) \tag{2.10}$$

Additive type:

$$\mu = \mu_{max} * \frac{\mu(S_1) + \mu(S_2) + ... + \mu(S_n)}{n} \tag{2.11}$$

Non-interactive type:

$$\mu = \mu_{max} * \mu(S_1) or \mu(S_2) or .... or \mu(S_n) \tag{2.12}$$

Multi substrate kinetic models were used to describe the glucose and GlcNAc kinetics of *Streptococcus zooepidemicus* for hyaluronic acid production and glucose and ammonium sulfate kinetics for rifamycin B synthesis [7, 76].

CHAPTER 3

METABOLIC ENGINEERING OF *Bacillus megaterium* FOR HEPAROSAN BIOSYNTHESIS USING *E. coli* K5 GLYCOSYLTRANSFERASES

Summary

Heparosan is an un-sulfated polysaccharide primarily used as a precursor for heparin synthesis that has recently been used in drug delivery applications. Heparosan synthesis from recombinant bacterial systems provides a safer alternative to naturally producing pathogenic bacterial systems. In this chapter, *B. megaterium* was explored as a safe expression host for the production of heparosan. The functional heparosan synthesis pathway was established in *B. megaterium* by the heterologous expression of *E. coli* K5 *kfiC* and *kfiA* glycosyltransferase genes. Upregulation of UDP-GlcA (*tuaD* and *gtaB*) and UDP-GlcNAc (*gcaD* and *glmM*) pathway genes enhanced the heparosan production, indicating that UDP-GlcA and UDP-GlcNAc concentrations were limiting the heparosan biosynthesis. *B. megaterium* over-expressed with UDP-GlcA pathway genes yielded a maximum heparosan concentration of 394 mg/L in batch fermentation. Heparosan titer was further increased to 1.32 g/L in fed-batch fermentation. Nuclear magnetic resonance

An article based on this chapter is published as follows: Nehru, G., Tadi, S. R. R., Limaye, A. M., & Sivaprakasam, S. (2020). Production and characterization of low molecular weight heparosan in *Bacillus megaterium* using *Escherichia coli* K5 glycosyltransferases. *International Journal of Biological Macromolecules*, **160**, 69-76. ©Elsevier

(NMR) analysis revealed that the chemical structure of *B. megaterium* derived heparosan was identical to *E. coli* K5 heparosan. The heparosan molecular weight varied from 31 to 60 kDa, indicating its potential as a precursor for chemoenzymatic heparin biosynthesis. This chapter provides an efficient process to produce heparosan in non-pathogenic *B. megaterium* using *E. coli* K5 glycosyltransferases.

3.1 Introduction

Heparosan is a linear un-sulfated polysaccharide, with repeating disaccharide units of D-glucuronic acid (GlcA) and N-acetyl-D-glucosamine (GlcNAc) linked through α-1,4 and β-1,4 glycosidic bonds [20]. In addition to heparin synthesis, heparosan has wide utility as a drug delivery vehicle due to its non-immunogenic nature and biocompatibility [58]. Recently, heparosan was proven to be a potential alternative to hyaluronic acid, a carbohydrate polymer extensively utilized for the design of drug carriers for anticancer therapy [95]. Certain pathogenic microorganisms such as *Escherichia coli* K5 and *Pasteurella multocida* type D produce heparosan as a capsular material to evade the host immune system [24]. Hence, microbial-derived heparosan could serve as the precursor for chemoenzymatic heparin synthesis.

To date, heparosan production has been exclusively focused on *E. coli* K5 as a potential host strain [64, 67, 123]. Heparosan biosynthesis operon in *E. coli* K5 consists of four genes, *kfiA*, *kfiB*, *kfiC*, and *kfiD*. *kfiC* and *kfiA* encode for D-glucuronyltransferase and N-acetylglucosaminyltransferase, respectively. The KfiC-KfiA enzyme complex is involved in the polymerization of GlcA and GlcNAc to synthesize heparosan [42]. *kfiD* encodes for UDP-glucose dehydrogenase and the role of the protein encoded by *kfiB* remains elusive. Heparosan synthesis in *P. multocida* is regulated by PmHS1 and PmHS2, which are dual-action glycosyltransferases exhibiting both D-glucuronyltransferase and N-acetylglucosaminyltransferase activities. But, the high risk of pathogenicity, presence of endotoxins and exotoxins limits the utility of *E. coli* K5 and *P. multocida* derived heparosan in biomedical applications. Hence, the development of a safe and alternative heparosan production system through the engineering of safe microorganisms are gaining attention. Consequently, heterologous expression of *E. coli* K5 or *P. multocida* type D glycosyltransferase genes were attempted in other microorganisms considered safe [8, 22, 47, 60, 127, 133].

B. megaterium, a safe gram-positive bacterium has been an important industrial host

due to its superior characteristics such as the efficient expression of heterologous genes, stable plasmid maintenance, lack of alkaline protease activity and efficient secretion capability. In addition to aforementioned characteristics, *B. megaterium* does not produce endotoxins in contrast to the *E. coli* K5, which facilitates the use of value-added products expressed by *B. megaterium* in clinical and food applications. Moreover, the absence of endotoxins also reduces the number of steps involved in the downstream processing. Hence, it has been widely used for the recombinant production of various therapeutic enzymes and vitamins [13, 50, 68, 84]. Recently, it has proven to be an ideal host in the production of capsular polysaccharides and biopolymers such as hyaluronic acid and polyhydroxybutyrate [35]. Besides, it possesses all the essential enzymes for the production of heparosan except heparosan synthase. The whole genome sequence of *B. megaterium* does not encode any enzymes, which depolymerize heparosan. The aforementioned characteristics endorse the selection of *B. megaterium* as an efficient expression system for the production of heparosan.

Heparosan molecular weight is an important quality attribute to be considered for bioengineered heparin synthesis. The molecular weight of microbial-derived heparosan depends on the source of heparosan synthase genes. High molecular weight heparosan of 100-800 kDa suitable for biomaterial production is derived from *P. multocida* heparosan synthase [106]. Conversely, lower molecular weight heparosan of 50-80 kDa could serve as a precursor for bioengineered heparin synthesis is obtained from *E. coli* K5 [123]. For this reason, *E. coli* K5 was chosen to obtain *kfiC* and *kfiA* glycosyltransferase genes for heparosan synthesis.

In this chapter, the safe production of heparosan was demonstrated in *B. megaterium* by the heterologous expression of *E. coli* K5 *kfiC* and *kfiA* glycosyltransferase genes. In addition, the synthetic operons of UDP-GlcA and UDP-GlcNAc pathway genes were constructed to identify the rate limiting heparosan synthesis pathway enzymes. The performance of recombinant strains was evaluated in 3-L bioreactor experiments. The structural and molecular weight characterization of *B. megaterium* derived heparosan was elucidated. This chapter demonstrated a safe alternative approach to produce heparosan for bioengineered heparin synthesis.

3.2 Materials and methods

3.2.1 Media

Luria-Bertani (LB) broth (5 g/L yeast extract, 10 g/L tryptone and 5 g/L NaCl) was used for the propagation of *E. coli* and *B. megaterium* strains. The modified fermentation medium comprising 10 g/L sucrose, 10 g/L yeast extract powder, 2 g/L tryptone, 7.8 g/L sodium dihydrogen phosphate dihydrate, 3.9 g/L potassium sulfate and 1.2 g/L magnesium sulfate heptahydrate was used for batch and fed-batch fermentation experiments. The pH of the medium was adjusted to 7.0 using 2 M NaOH. The fermentation medium was filter-sterilized using 0.22 μm PVDF membrane filter (Pall Corporation). Antibiotics (Ampicillin 100 μg/mL, Tetracycline 10 μg/mL, Chloramphenicol 34 μg/mL for *E. coli* and 4.5 μg/mL for *B. megaterium*) were supplemented in the fermentation medium for the selection of recombinant strains. All the chemicals and media components were purchased from HiMedia Laboratories, Mumbai, India unless mentioned.

3.2.2 Genomic DNA isolation

The fresh overnight culture of *B. megaterium* was inoculated in 10 mL of LB broth and incubated at 37 °C. The cells were harvested at OD_{600} of 0.8 to 1.0 by centrifugation (10 min, 5000 rpm). The cells were resuspended in 400 μL G-1 buffer (10 mM Tris-Cl pH 8, 10 mM EDTA, 150 mM NaCl). 20 μL lysozyme was added to the solution and incubated for 20 min at 37 °C. 2 μL RNase A was added and incubated for 3 min at 65 °C. 40 μL SDS, 10 μL proteinase K and 550 μL G-2 buffer (10 mM Tris-Cl pH 8, 1 mM EDTA, 50 mM NaCl) were added to the cell lysate and incubated for 2 h at 65 °C. The genomic DNA was extracted twice with 900 μL TE buffer equilibrated phenol pH 7.5-8.0. DNA extraction was repeated twice with 24:1 chloroform and isoamyl alcohol. The aqueous phase was transferred into 2 mL of ice-cold ethanol and incubated for 1 h at -20 °C. The precipitated DNA was recovered by centrifugation and residual ethanol was dried for 20 min. The genomic DNA was dissolved in 100 μL of G-2 buffer and stored at -20 °C.
E. coli K5 genomic DNA was isolated based on the protocol by Sambrook and Russell's Molecular Cloning: A Laboratory Manual.

3.2.3 Recombinant plasmids construction

The recombinant plasmids and bacterial strains used in this chapter are given in Table 3.1 and 3.2. The genes, *kfiC*, and *kfiA* were PCR amplified from the *E. coli* K5 genome using Q5 high fidelity DNA polymerase. The primers used for the amplification of gene fragments are listed in Table 3.3. The amplified gene fragments were cloned into pRBBm34 digested with BsrGI and EagI using isothermal assembly [33]. *E. coli* TOP10 strain was used as a cloning host for the construction of recombinant plasmids expressing *kfiC* and *kfiA* genes. The resulting recombinant plasmid, pMM-kfiCA was transformed into *B. megaterium* DSM319 and the positive transformants were selected on the tetracycline resistance plate. In order to construct UDP-precursor pathway operons, the analogous genes *tuaD*, *gtaB*, *gcaD*, and *glmM* were amplified from *B. megaterium* DSM319 genome. The recombinant plasmids, pMGB-tuaD, pMGB-tuaDgtaB, pMGB-gcaD, pMGB-gcaDglmM were constructed by cloning gene fragments into pSP6-RNAP digested with BamHI and SpeI. The cloning of UDP-precursor pathway genes was performed in *E. coli* TOP10 harboring pBAD33-xylR. The plasmid pBAD33-xylR encodes xylose repressor protein from *B. megaterium* to prevent the xylose promoter activity during cloning in *E. coli* [50]. The *xylR* gene of *B. megaterium* was amplified and cloned into pCyPet-His digested with SacI and SphI to generate the plasmid, pBAD33-xylR. 0.2 % (w/v) of L-arabinose was added to induce the expression of *xylR* during the cloning of UDP-precursor pathway genes in *E. coli*.

3.2.4 Isothermal assembly

Linearized plasmid DNA and PCR amplified gene fragments were assembled using isothermal assembly [33]. The gene fragments to be assembled have 25-30 bp terminal sequence overlaps. This method uses T5 exonuclease to generate complementary sticky ends, which then annealed and repaired by Taq DNA ligase and DNA polymerase, respectively. An assembly master mixture was prepared by mixing 32 μL of 5x ISO reaction buffer (2 M Tris-HCl pH 7.5, 1.5 mL; 2 M $MgCl_2$, 150 μL; Each 100 mM dNTPs, 60 μL; 1 M DTT, 300 μL; PEG8000, 1.5 g; 100 mM NAD^+, 300 μL and sterile water upto 6 mL), 0.64 μL of 0.1 U/mL T5 exonuclease (NEB), 1.2 μL of 2 U/mL Phusion DNA polymerase (NEB), 1.6 μL of 4 U/mL Taq DNA ligase (NEB), and water up to a final volume of 120 μL. 15 μL of the master mixture aliquoted and stored at -20°C. Equimolar concentrations of each DNA fragments were used in assembly reactions. 5 μL of DNA

Table 3.1: List and description of the strains

Strain	Description/characteristic	Reference
E. coli TOP10	Cloning host, F'(lacIq Tn10 (Tet^R)) mcrA Δ(mrr-hsdRMS-mcrBC) Φ80lacZΔM15 ΔlacX74 recA1 araD139 Δ(ara-leu)7697 galU galK rpsL endA1 nupG	Invitrogen
E. coli K5	Serotype O10:K5:H4	BEI Resources, NIAID, NIH
E. coli TOP10-*xylR*	*E. coli* TOP10 harboring pBAD33-xylR	Present study
B. megaterium DSM319	Wildtype, Expression host	DSMZ, Braunschweig, Germany
B. megaterium CA	*B. megaterium* DSM319 harboring pMM-kfiCA	Present study
B. megaterium CA-D	*B. megaterium* CA harboring pMGB-tuaD	Present study
B. megaterium CA-DB	*B. megaterium* CA harboring pMGB-tuaDgtaB	Present study
B. megaterium CA-U	*B. megaterium* CA harboring pMGB-gcaD	Present study
B. megaterium CA-UM	*B. megaterium* CA harboring pMGB-gcaDglmM	Present study

need to be assembled was added to 15 μL of assembly master mixture. The reaction mixture was incubated at 50°C for 60 min and transformed into *E. coli*.

3.2.5 *B. megaterium* transformation

The constructed plasmids were introduced into *B. megaterium* by modified polyethylene glycol (PEG)-mediated protoplast transformation method [72]. Briefly, *B. megaterium* culture grown overnight was inoculated into 20 mL of transformation medium. Transformation medium consisted of 1 g/L NH_4Cl, 12 g/L tris-base, 35 mg/L KCl, 58 mg/L NaCl, 300 mg/L $Na_2SO_4{\cdot}10H_2O$, 140 mg/L KH_2PO_4, 4.26 g/L $MgCl_2{\cdot}6H_2O$, 5 g/L yeast

Table 3.2: List and description of the plasmids

Plasmid	Description/characteristic	Reference
pCyPet-His	*E. coli* expression vector, pBAD-MCS, Cm^R	Addgene plasmid # 14030
pRBBm34	*E. coli* – *B. megaterium* shuttle vector, P_x*yl*-MCS, Amp^R, Tet^R	Addgene plasmid # 48114
pSP6-RNAP	*E. coli* – *B. megaterium* shuttle vector, P_x*yl*-MCS, Amp^R, Cm^R	Addgene plasmid # 48143
pBAD33-xylR	pCyPet-His derivative, CyPet replaced with *xylR* of *B. megaterium*, PBAD-xylR	Present study
pMM-kfiCA	pRBBm34 derivative, GFP replaced with *kfiC-kfiA* of *E. coli* K5, Pxyl-kfiCA	Present study
pMGB-tuaD	pSP6-RNAP derivative, RNAP replaced with *tuaD* of *B. megaterium*, Pxyl-tuaD	Present study
pMGB-tuaDgtaB	pSP6-RNAP derivative, RNAP replaced with *tuaD-gtaB* of textitB. megaterium, Pxyl-tuaDgtaB	Present study
pMGB-gcaD	pSP6-RNAP derivative, RNAP replaced with *gcaD* of *B. megaterium*, Pxyl-gcaD	Present study
pMGB-gcaDglmM	pSP6-RNAP derivative, RNAP replaced with *gcaD-glmM* of textitB. megaterium, Pxyl-gcaDglmM	Present study

Table 3.3: List and sequences of the primers

Primer	Sequence (5' → 3')
kfiC-F	GTTCACTTAAATCAAAGGGGGAAATGTACAATGAACGCAGAA TATATAAATTTAGTTGAACGT
kfiC-R	CTATTGTTCAATTATTCCTGATACATCTTTAAACAAAC
kfiA-F	GATGTATCAGGAATAATTGAACAATAGTAAAAAGGGGGAAAT GTACAATGATTGTTGCAAATATGTCATCATACCC
kfiA-R	TTAGCGAGGTGCCGCCGGCATGCGGCCGTTACCCTTCCACAT TATACACTAATTCGA
tuaD-F	TCAAAGGGGGAAATGACAAATGGTCCAAACTAGTACTAATAT CACAGTAGCGGGTACTG
tuaD-R	AGTTGAATATAAATGACTCTAGAGGATCCTTATCAGACATTA GCTTTAATTTTAGCTTTGTATCC
tuaD-R2	TCAGACATTAGCTTTAATTTTAGCTTTGTATCC
gtaB-F	AAGCTAAAATTAAAGCTAATGTCTGATAAAAAGGGGGAAATG ACAAATGACGATAAAAAAGGCAGTTATTCCAG
gtaB-R	CAGTTGAATATAAATGACTCTAGAGGATCCTTAGCTGAAGTT GTTTGCTCGTTC
gcaD-F	AAAGGGGGAAATGACAAATGGTCCAAACTAGTTCAAAAAGAT ATGCAGTCATATTGGCAG
gcaD-R	CAGTTGAATATAAATGACTCTAGAGGATCCTTATCAGGATTT TTTATTAATATCAAGCTTTTCAGCA
gcaD-R2	TCAGGATTTTTTATTAATATCAAGCTTTTCAGCA
glmM-F	AGCTTGATATTAATAAAAAATCCTGATAAAAAGGGGGAAATG ACAAATGGGTAAGTATTTTGGAACAGACG
glmM-R	ACAGTTGAATATAAATGACTCTAGAGGATCCTTACTCTAAGC CCATTTCTTCTTTTACTACT

extract, 5 g/L tryptone, 68.46 g/L sucrose and 2 g/L glucose. The pH was adjusted to 7.5 with HCl before the addition of $MgCl_2 \cdot 6H_2O$. Glucose was added to the media after sterilization. The actively growing cells (OD_{600} of 0.5 to 0.8) were centrifuged at 8000 rpm and suspended in 2 mL of transformation medium. Subsequently, 600 μg/mL of lysozyme was added and the mixture incubated at 37°C for 20 min to generate the protoplasts. The protoplasts were harvested by centrifugation at 2000 rpm, washed gently with 2 mL of transformation medium, then centrifuged again, and resuspended in 1 mL of transformation medium. 250 μL of protoplasts were taken for each transformation. 4 μg of plasmids (dissolved in nuclease-free water) and 250 μL of 35 % PEG 8000 (prepared in transformation medium) were added to the protoplast suspension, swirled gently, and incubated for 2 min at room temperature. The suspension was diluted immediately with 5 mL of transformation medium, centrifuged at 2000 rpm for 5 min. The pellet was resuspended in 1 mL of transformation medium and incubated at 37°C for 90 min to allow expression of the antibiotic resistance gene. 250 μL of protoplasts were plated on transformation agar medium containing either 5 μg/mL of tetracycline or 1.5 μg/mL of chloramphenicol or both and incubated at 37°C for overnight. The colonies obtained were cultured in LB media containing either 10 μg/mL of tetracycline or 4.5 μg/mL of chloramphenicol or both.

3.2.6 Bioreactor fermentation experiments

The recombinant *B. megaterium* cells were cultivated in LB broth for 14 h and served as seed cultures for batch and fed-batch fermentation experiments. Batch fermentation of recombinant clones was carried out in a 3 L bioreactor (Biojenik engineering, India) containing 1.7 L of fermentation medium and inoculated using 5 % (v/v) of seed culture. The temperature and pH were maintained at 30°C and 7, respectively. D-xylose was added at a final concentration of 0.5 % (w/v) to actively growing cells (OD_{600} of 0.3 to 0.4) to induce the expression of recombinant genes. The aeration rate and agitation speed were maintained at 1 vvm and 600 rpm, respectively. Fed-batch fermentation was carried out in a 3 L bioreactor containing 1.7 L of fermentation medium with 10 g/L sucrose. 0.5 % (w/v) of D-xylose was induced at 6 h and sucrose was fed at 10 h and maintained the concentration of about 2 g/L to 5 g/L. Dissolved oxygen concentration was maintained above 20 % throughout the fermentation by controlling the agitator speed range from 400 rpm to 800 rpm with an aeration rate of 1 vvm. Periodic samples were drawn and

subjected to biomass, substrate, and product analysis. UV spectrophotometer (Infinite M200 PRO, Tecan, Männedorf, Switzerland) was used to measure the optical density (OD_{600}) of the samples. 1 OD_{600} corresponds to 1.059 g/L dry cell weight (DCW). Total sugar concentration was estimated by anthrone method. The xylose and organic acids were quantified by HPLC (Shimadzu, Kyoto, Japan) equipped with a refractive index (RI) detector and Rezex RHM-monosaccharide H column (Phenomenex Inc., Torrance, CA). The mobile phase was 5 mM H_2SO_4 at a flow rate of 0.5 mL/min.

3.2.7 Heparosan purification

Acidic protein precipitation and anion exchange chromatography methods were employed to purify heparosan from fermentation broth [123, 133]. The fermentation broth was centrifuged to remove the supernatant and the pellet was washed twice with distilled water. The cell pellet was suspended in lysis buffer (1 g/L Lysozyme, 0.5 mM EDTA and Tris-HCl pH 7.5) and incubated for 2 h. The cell lysate was further subjected to autoclaving at 121°C for 20 min for the complete disruption of the cells. The resulting cell lysate was centrifuged and the supernatant containing heparosan was collected. The supernatant pH was adjusted to 4 using glacial acetic acid to precipitate the protein and subsequently filtered through Buchner funnel with the fritted disc (40-60 μm). Diethylaminoethyl (DEAE) sepharose fast flow resin (Sigma Aldrich, MO, USA) was packed into the column and equilibrated with buffer A (50 mM sodium chloride, 20 mM sodium acetate, pH 4). The supernatant was passed through the column, and the column was washed with 5 column volumes of buffer A. The heparosan was eluted with buffer B (1 M sodium chloride, 20 mM sodium acetate, pH 4). Eluted samples were dialyzed overnight (10 kDa membrane cut off) against deionized water and lyophilized.

3.2.8 Nuclear magnetic resonance (NMR) spectroscopy analysis

The purified heparosan was analyzed by both one dimensional ^{1}H-NMR and ^{13}C-NMR. The experiments were performed using Bruker Ascend 600 MHz NMR spectrometer (Bruker, MA, USA) with TOPSPIN data acquisition software (Bruker). The sample was dissolved in 0.4 mL of D_2O (Sigma Aldrich, MO, USA) and lyophilized twice to facilitate hydrogen-deuterium exchange. The sample was again dissolved in 0.6 mL of D_2O and transferred to a 5 mm standard NMR tubes. ^{1}H spectrum was acquired in water suppression mode for 160 scans. ^{13}C spectrum was acquired for 8000 scans at 298 K.

3.2.9 Heparosan concentration determination

The modified carbazole assay was carried out to measure heparosan concentration [14]. 200 μL of appropriately diluted cell lysate supernatant was layered on to 1 mL of sulphuric acid reagent (25 mM sodium tetraborate in 98 % H_2SO_4) in precooled glass test tubes. The test tubes were shaken vigorously and incubated at a boiling water bath for 15 min. After cooling the tubes to room temperature, 40 μL of carbazole reagent (0.125 % w/v of carbazole in absolute ethanol) was added, shaken again and incubated for 15 min at boiling water bath. The absorbance of samples was recorded at 530 nm. D-glucuronic acid was used as a standard for the quantification of heparosan. *B. megaterium* DSM319 strain was used as a control to remove the background values under the same conditions.

3.2.10 Heparosan molecular weight determination

High performance size exclusion chromatography (HPSEC) equipped with a RI detector (Shimadzu, Kyoto, Japan) was used to determine the molecular weight distribution of heparosan. LabSolutions software (Shimadzu, Kyoto, Japan) was used to acquire and process the chromatogram data. The purified heparosan sample was filtered through a 0.45 μm filter and then loaded on to a polysep-GFC-P-6000 (Phenomenex Inc., Torrance, CA). 100 mM $NaNO_3$ was used as a mobile phase at a flow rate of 0.5 mL/min at 40°C. Dextran standards of different molecular weights viz. 10 kDa, 20 kDa, 40 kDa, 70 kDa, 100 kDa and 200 kDa (Sigma Aldrich, MO, USA) were used to obtain a calibration plot.

3.3 Results and discussion

3.3.1 Cloning and expression of *E. coli* K5 heparosan biosynthesis genes in *B. megaterium*

The construction of recombinant *B. megaterium* heparosan biosynthesis pathway was based on the mechanism of heparosan biosynthesis in *E. coli* K5 (Figure 3.1). Heparosan production in *E. coli* K5 is facilitated by the concerted action of KfiC and KfiA proteins and the formation of the KfiC-KfiA enzyme complex [42, 108]. Whole genome sequence analysis suggested that *B. megaterium* is devoid of *kfiC* and *kfiA* genes encoding glycosyltransferases. However, it encodes all genes for the synthesis of UDP-GlcA and UDP-GlcNAc precursors. Hence, the expression of *kfiC* and *kfiA* is indispensable to

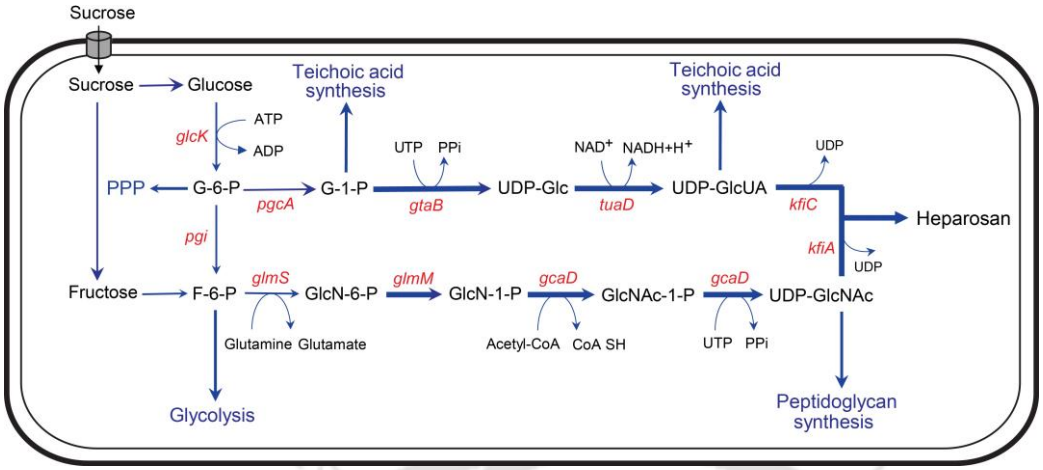

Figure 3.1: Heparosan biosynthetic pathway in engineered *B. megaterium* expressing *E. coli* K5 glycosyltransferases. Schematic representation of heparosan production in engineered *B. megaterium*. The heterologous genes, *kfiC*, and *kfiA* are derived from *E. coli* K5. The thick arrow represents the gene overexpression targets. G-6-P, Glucose-6-phosphate; F-6-P, Fructose-6-phosphate; G-1-P, Glucose-1-phosphate; UDP-Glc, UDP-Glucose; UDP-GlcA, UDP-glucuronic acid; GlcN-6-P, Glucosamine-6-phosphate; GlcN-1-P, Glucosamine-1-phosphate; GlcNAc-1-P, N-acetylglucosamine-1-phosphate; UDP-GlcNAc, UDP-N-acetyl glucosamine; *glcK*, glucokinase; *pgi*, phosphoglucoisomerase; *pgcA*, phosphoglucomutase; *gtaB*, UTP-glucose-1-phosphate uridylyltransferase; *tuaD*, UDP-glucose dehydrogenase; *glmS*, Glucosamine-fructose-6-phosphate aminotransferase; *glmM*, phosphoglucosamine mutase; *gcaD*, bifunctional N-acetyl glucosamine- 1-phosphate uridyltransferase/glucosamine-1-phosphate acetyltransferase; *kfiC*, glucuronyltransferase; *kfiA*, N-acetylglucosaminyltransferase

establish heparosan synthesis pathway in *B. megaterium*. The genomic DNA of *E. coli* K5 and *B. megaterium* was isolated (Figure 3.2a). The *E. coli* K5 glycosyltransferase genes, *kfiC*, and *kfiA* were PCR amplified from *E. coli* K5 and cloned into the *E. coli-B. megaterium* shuttle plasmid pRBBm34 under xylose-inducible promoter to generate plasmid pMM-kfiCA (Figure 3.2c). A consensus ribosomal binding site (RBS) of *B. megaterium* (AAGGGGG) was introduced for translation initiation of *kfiA*. Lysate PCR and DNA sequencing analysis were performed to validate the successful recombinant plasmid construction (Figure 3.2d). The resulting plasmid was transformed into *B. megaterium* to generate the strain CA. Further, SDS-PAGE analysis confirmed the heterologous expression of KfiC and KfiA proteins of size 59 kDa and 27 kDa, respectively (Figure 3.2e). The absence of protein expression in uninduced samples indicates tight regulation of the xylose-inducible promoter system.

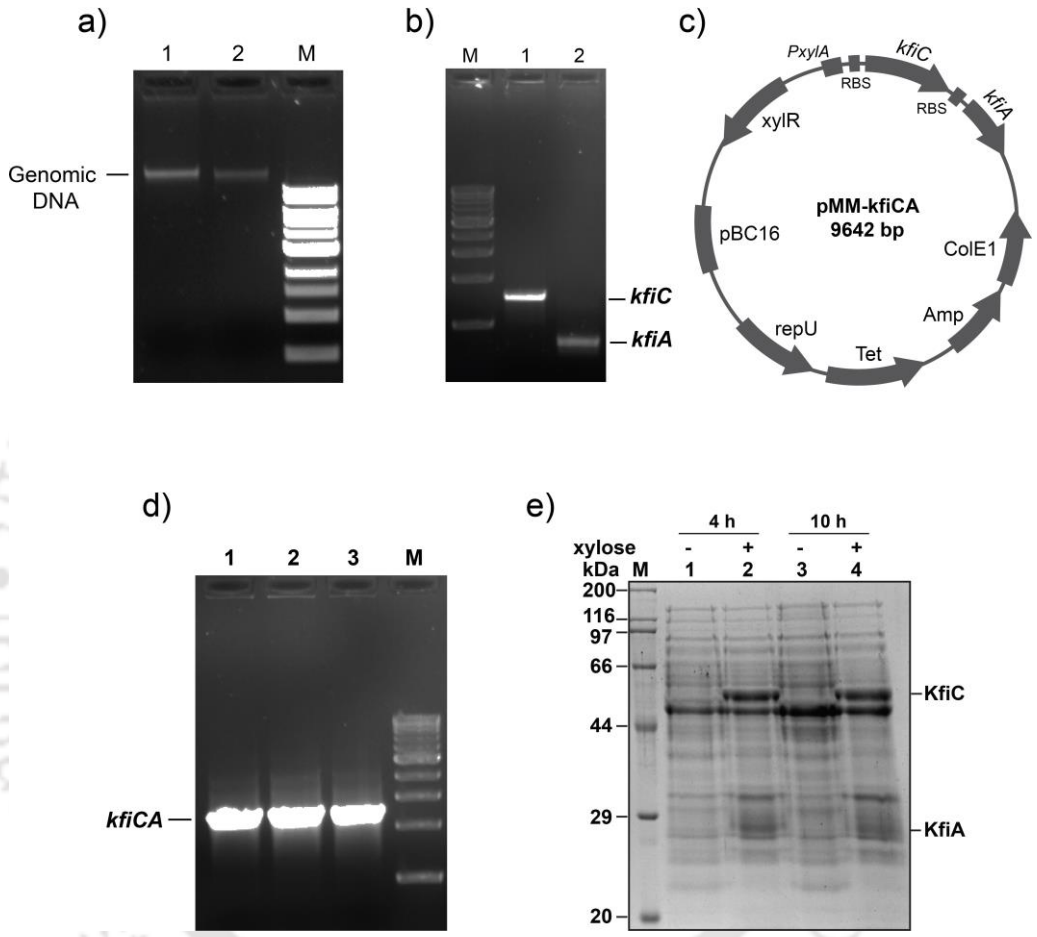

Figure 3.2: Cloning and expression of *E. coli kfiC* and *kfiA* genes in *B. megaterium* **a)** Genomic DNA isolation of *B. megaterium* (lane 1)and *E. coli* K5 (lane 2) **b)** PCR amplification of *kfiC* (lane 1) and *kfiA* (lane 2) genes from *E. coli* K5 genomic DNA **c)** Schematic diagram of the pMM-kfiCA expressing *kfiC* and *kfiA* genes **d)** Lysate PCR confirmation of positive clones **e)** Expression of KfiC and KfiA proteins at 4 h and 10 h by SDS-PAGE analysis. Lane 1 and 3, lysate of the uninduced culture at 4 h and 10 h; Lane 2 and 4, lysate of the culture induced with 0.5 % (w/v) of D-xylose. Production of 59 kDa and 27 kDa proteins corresponding to KfiC and KfiA after the addition of 0.5 % D-xylose as evident from Lane 2 and 4

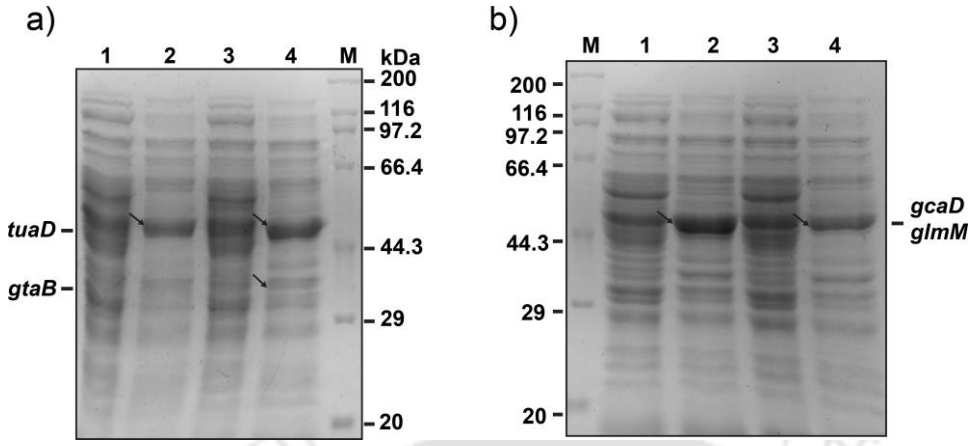

Figure 3.3: a) Expression analysis of UDP-GlcA synthesis pathway proteins (tuaD and gtaB) by SDS-PAGE. Lane 1, lysate of the uninduced strain CA-D; Lane 2, lysate of strain CA-D induced with 0.5 % (w/v) of D-xylose; Lane 3, lysate of the uninduced strain CA-DB; Lane 4, lysate of strain CA-DB induced with 0.5 % (w/v) of D-xylose; Lane 5, protein marker. **b)** Expression analysis of UDP-GlcNAc synthesis pathway proteins (gcaD and glmM) by SDS-PAGE. Lane 1, protein marker; Lane 2, lysate of the uninduced strain CA-UM; Lane 3, lysate of strain CA-UM induced with 0.5 % (w/v) of D-xylose; Lane 4, lysate of the uninduced strain CA-U; Lane 5, lysate of strain CA-U induced with 0.5 % (w/v) of D-xylose

3.3.2 Homologous expression of UDP-precursor pathway genes

In addition to KfiC and KfiA, heparosan synthesis in *B. megaterium* involves other homologous enzymes to produce precursors, UDP-GlcA and UDP-GlcNAc. Literature reports suggested that expression of glycosyltransferases alone was not sufficient to produce high amounts of capsular polysaccharides in heterologous production hosts [88, 133]. The expression of UDP-precursor sugar pathway genes and the UDP-precursor sugar concentration may also influence the heparosan production. Hence, the homologous gene clusters, *tuaD*, *tuaD-gtaB*, *gcaD*, and *gcaD-glmM* were systematically assembled in pSP6-RNAP under xylose-inducible promoter to construct the plasmids pMGB-tuaD, pMGB-tuaDgtaB, pMGB-gcaD and pMGB-gcaDglmM, respectively. The resulting plasmids were transformed into strain CA to generate strains, CA-D, CA-DB, CA-U, and CA-UM, respectively. A consensus RBS of *B. megaterium* (AAGGGGG) was introduced for translation initiation in operon constructions. The expression of UDP-precursor synthesis pathway proteins were confirmed by SDS-PAGE analysis (Figure 3.3).

During the cloning of UDP-precursor sugar synthesis genes, the growth of *E. coli* was severely compromised due to toxicity and intracellular acidification. The toxicity

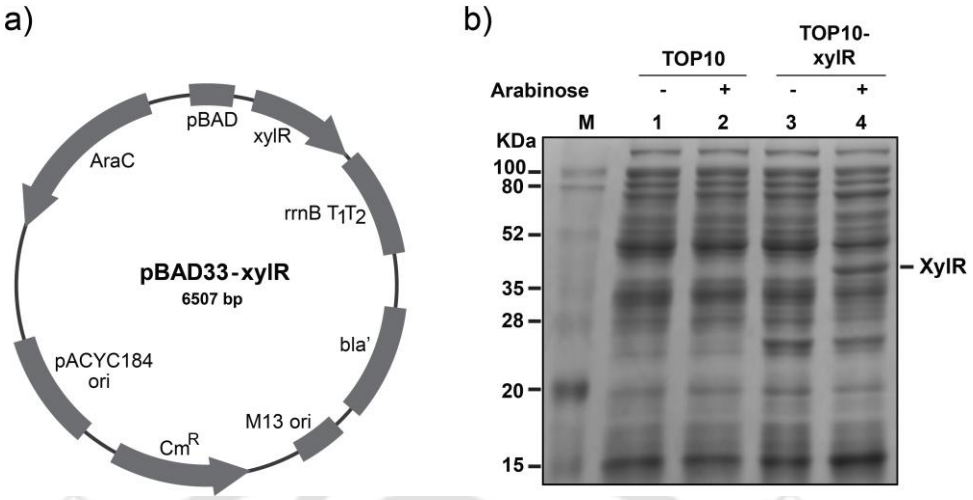

Figure 3.4: a) Schematic diagram of the pBAD33-xylR expressing *xylR* gene from *B. megaterium* under arabinose inducible promoter **b)** Expression analysis of XylR protein by SDS-PAGE. Lane 1, lysate of uninduced TOP10 culture; Lane 2, lysate of TOP10 culture induced with 0.2 % (w/v) L-arabinose; Lane 3, lysate of uninduced TOP10-xylR culture; Lane 4, lysate of TOP10-xylR culture induced with 0.2 % (w/v) L-arabinose

was due to the leaky expression of xylose inducible promoter system in *E. coli* [50]. To alleviate this, *B. megaterium xylR* encoding xylose repressor protein was overexpressed, which binds to the xylose operator, thus preventing the leaky expression driven by P_{xylA} promoter during cloning in *E. coli* TOP10. The *xylR* was cloned under arabinose-inducible promoter, P_{BAD} to generate the plasmid pBAD33-xylR (Figure 3.4a). The resulting plasmid was transformed into *E. coli* TOP10. *E. coli* TOP10 cells harboring the plasmid pBAD33-xylR was designated as TOP10-xylR. The TOP10-xylR cells were made competent and used to clone UDP-sugar precursor pathway genes. XylR expression was induced by the addition of 0.2 % (w/v) L-arabinose (Figure 3.4b).

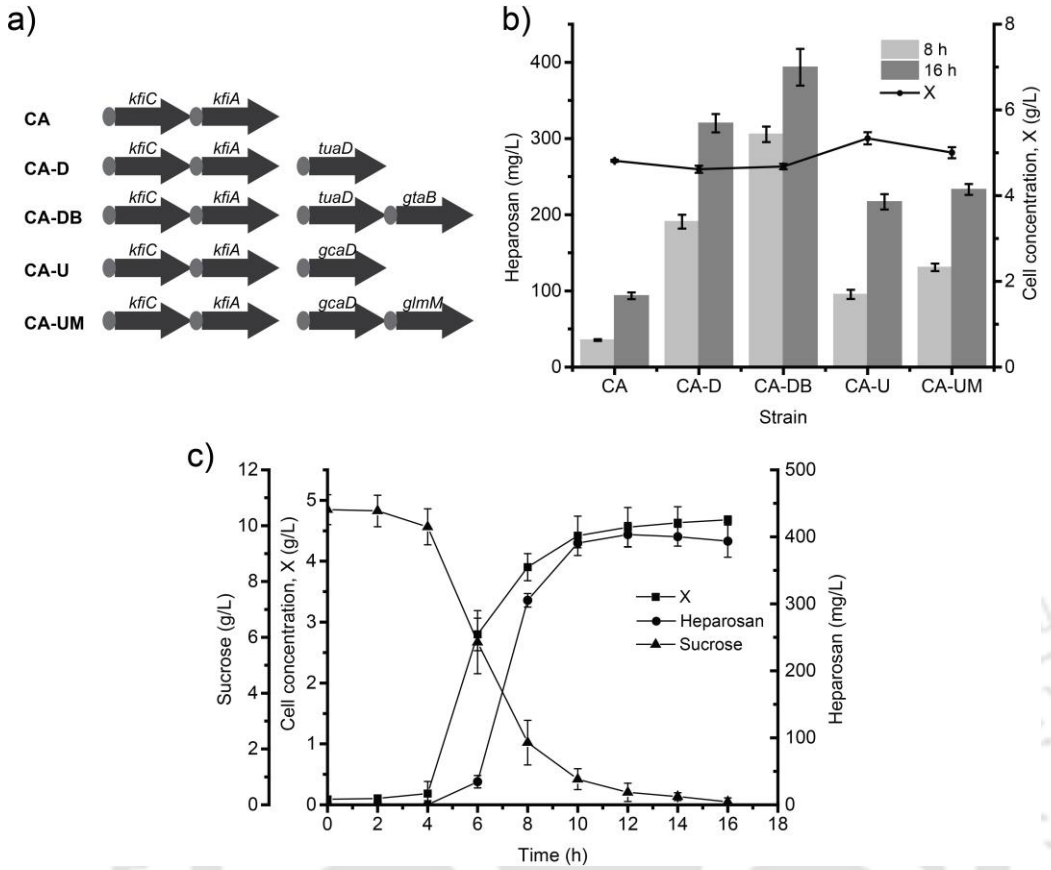

Figure 3.5: a) Genetic organization of artificial operons to increase the UDP-precursor sugar levels in different recombinant strains **b)** Heparosan titer and cell concentration of different recombinant strains at 8 h and 16 h in batch bioreactor **c)** Time course of heparosan production and cell growth of strain CA-DB. The culture was induced at 4 h when the OD_{600} reached 0.3 to 0.5

3.3.3 Performance evaluation of recombinant *B. megaterium* strains in batch bioreactor

Batch fermentation was performed to evaluate the heparosan production capability of different recombinant strains. Figure 3.5b illustrates the coexpression of *kfiC* and *kfiA* genes in *B. megaterium* (strain CA) yielded 36 mg/L and 94 mg/L of heparosan in 8 h and 16 h, respectively. Previous studies shown that only KfiC and KfiA proteins were involved in the heparosan biosynthesis in *E. coli* K5 and this result was consistent in *B. megaterium* [42, 108]. In order to determine the influence of UDP-precursor sugar pathway genes overexpression, the strains CA-D, CA-DB, CA-U, and CA-UM were cultivated under identical conditions and compared with strain CA. The UDP-GlcA

synthesis pathway overexpressed strains, CA-D and CA-DB significantly enhanced the heparosan production to 320 mg/L and 394 mg/L at 16 h. This significant improvement of heparosan titer exemplifies that UDP-glucose dehydrogenase encoded by *tuaD* and UTP-glucose-1-phosphate uridylyltransferase encoded by *gtaB* are rate limiting enzymes for heparosan production in *B. megaterium*. The UDP-GlcA pathway intermediates, glucose- 1-phosphate, and UDP-glucose are consumed for cell wall polysaccharide synthesis in addition to heparosan synthesis during cell growth (Figure 3.1). Diversion of these intermediates to UDP-GlcA synthesis could lead to enhanced heparosan production. This result corresponds to the previous reports that found an increase in the hyaluronic acid titer in *B. subtilis* and *Lactococcus lactis*, when overexpressed with UDP-GlcA synthesis pathway genes [46, 88]. Conversely, the upregulation of UDP-glucose dehydrogenase in *E. coli* K5 decreased the heparosan production [97], which indicated that UDP-GlcA concentration differently regulates the heparosan biosynthesis in *E. coli* K5 and heterologous producers. Similarly, UDP-GlcNAc pathway genes, *gcaD*, and *glmM* were overexpressed to improve the UDP-GlcNAc levels. The upregulation of *gcaD* increased heparosan production to 217 mg/L at 16 h. However, coexpression of *gcaD* and *glmM* showed only marginal increase (233 mg/L) on heparosan biosynthesis. The introduction of plasmids did not affect the growth of recombinant *B. megaterium* strains (Figure 3.5b), and also the heparosan production was in concurrence with cell growth (Figure 3.5c). After the depletion of sucrose to a low level at about 10 h, cell growth ceased and subsequently heparosan production was stopped. Heparosan was accumulated primarily in cell pellet during the course of fermentation. Heparosan was not detected in the supernatant of all the recombinant strains. The absence of heparosan in the supernatant indicated that *B. megaterium* does not possess cell wall mediated export mechanism.

3.3.4 Fed-batch fermentation of heparosan in 3-L bioreactor

Batch fermentation results illustrated that the insufficient sucrose concentration was limiting heparosan production (Figure 3.5c). Hence, fed-batch fermentation was performed to sustain cell growth and heparosan production. The dynamic profiles of biomass growth, sucrose consumption, and heparosan production by strain CA-DB are depicted in Figure 3.6. In order to minimize the acetate accumulation due to carbon overflow metabolism, residual sucrose concentration in the fermentation medium was maintained at less than 5 g/L. Similar to batch fermentation, the accumulation of heparosan was

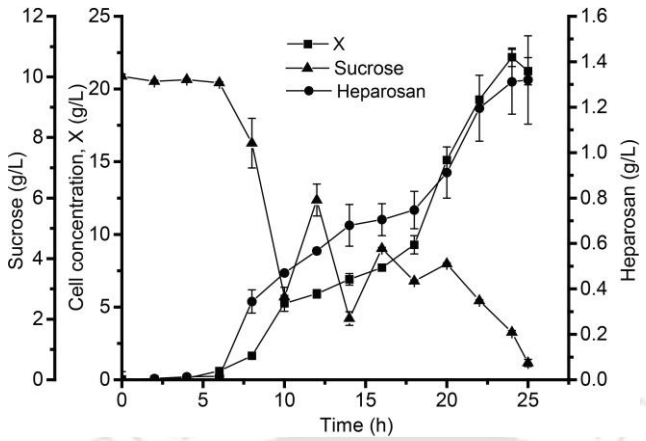

Figure 3.6: Fed-batch fermentation of strain CA-DB in 3-L bioreactor. Kinetics of cell growth, heparosan production, and sucrose consumption are shown. The culture was induced when the OD_{600} reached 0.3 to 0.5

coupled with cell growth and mainly occurred during growth phase. The heparosan concentration was significantly increased to 1.32 g/L at 25 h, which was 3.4 times that of batch fermentation. This result suggested that devising effective strategies for high cell density cultivation of recombinant *B. megaterium* would further enhance the heparosan production [134].

3.3.5 Structural characterization of recombinant *B. megaterium* derived heparosan

One dimensional ^{1}H-NMR and ^{13}C-NMR analyses were performed to determine the structure of *B. megaterium* derived heparosan. Heparosan obtained from the strain CA-DB was characterized by ^{1}H-NMR and ^{13}C-NMR (Figure 3.7). The proton and carbon chemical shifts are presented in Table 3.4 and were well corroborated with the previously published spectra of heparosan [22, 127, 133]. In addition, wild-type *B. megaterium* DSM319 did not show any anomeric proton signals for GlcA and N-acetyl group signal for GlcNAc, indicating the inability to produce heparosan. NMR analysis indicated that heparosan from *B. megaterium* has identical disaccharide repeating units with a structure of [(→4)-*β*-D-GlcA (1→4)-*α*-D-GlcNAc (1→)].

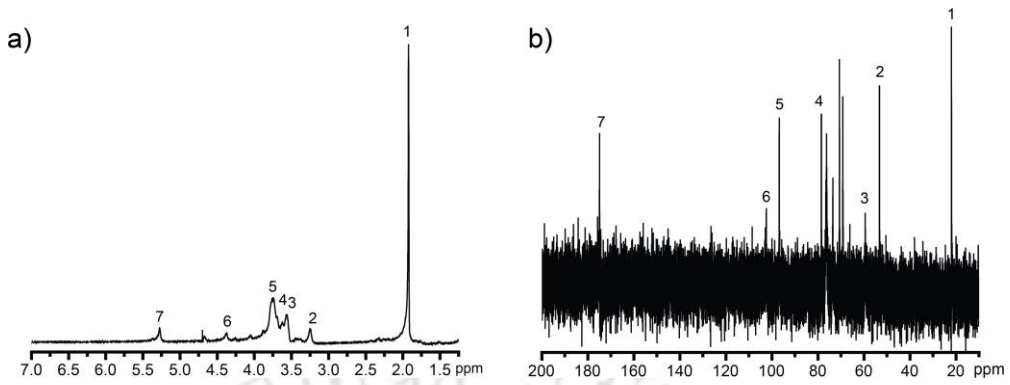

Figure 3.7: a) ^{1}H-NMR and b) ^{13}C-NMR spectra of *B. megaterium* derived heparosan. Chemical shifts assigned to the proton and carbon atoms of heparosan are mentioned in Table 3.4

Table 3.4: Chemical shift assignments of *B. megaterium* derived heparosan. Chemical shifts are represented in ppm

No.	Proton/carbon	Chemical shifts (ppm)
^{1}H-NMR		
1	Methyl H of GlcNAc	1.92
2	H-2 of GlcA	3.25
3	H-3, H-4 of GlcA and H-4 of GlcNAc	3.57
4	H-5 of GlcA	3.62
5	H-2, H-3, H-5 and H-6 of GlcNAc	3.74
6	H-1 of GlcA	4.38
7	H-1 of GlcNAc	5.27
^{13}C-NMR		
1	Methyl C of GlcNAc	21.98
2	C-2 of GlcNAc	53.29
3	C-6 of GlcNAc	59.50
4	C-4 of GlcNAc	78.51
5	α-anomeric C-1 of GlcNAc	96.42
6	β-anomeric C-1 of GlcA	102.02
7	Carboxyl C of GlcA	174.91

Table 3.5: Analyses of molecular weight distribution of heparosan obtained from different B. megaterium strains

Strain	M_w (kDa)
CA	31.35 ± 0.21
CA-D	59.17 ± 0.66
CA-DB	53.57 ± 0.59
CA-U	38.53 ± 0.11
CA-UM	55.78 ± 0.22
CA-DB (Fed-batch)	40.86 ± 2.93

3.3.6 Characterization of molecular weight of heparosan

Heparosan molecular weight is a critical parameter to be considered as a precursor for heparin synthesis. The molecular weight distribution of the heparosan obtained from different recombinant strains is given in Table 3.5. Single distribution of heparosan molecular weight was observed by HPSEC. The strain CA produced heparosan molecular weight of 31.35 kDa. Overexpression of *tuaD* and *tuaD-gtaB* genes increased the heparosan molecular weight to 59.17 kDa and 53.57 kDa, respectively. The UDP-GlcA pathway overexpressed strains favor the synthesis of longer heparosan polysaccharide chain. Similar results have been reported for heparosan production by *E. coli* and *B. subtilis* [22, 133]. The upregulation of *gcaD-glmM* also had positive effect on the molecular weight of heparosan. Fed-batch fermentation of the strain CA-DB decreased the molecular weight to 40.86 kDa. Heparosan can be obtained from different heparosan synthases, which determines the molecular weight. *E. coli* K5 typically produces heparosan molecular weight in the range of 20 to 80 kDa and used for chemoenzymatic heparin synthesis [130]. *P. multocida* heparosan synthases produces higher molecular weight of 100-800 kDa suitable for biomaterial applications [106]. *B. megaterium* engineered with *E. coli* K5 glycosyltransferases resulted in the molecular weight range of 31 kDa to 60 kDa, enumerates its potential as a precursor for heparin synthesis. Batch productivity (24.66 mg/L/h) of low molecular weight heparosan by *B. megaterium* was found to be significantly higher than the metabolically engineered *B. subtilis* (9.91 mg/L/h) reported in literature [22]. Also, the low molecular weight heparosan productivity by *B. mega-*

terium for batch and fed-batch (53 mg/L/h) compares favourably with the metabolically engineered *E. coli* (batch (21.73 mg/L/h) and fed-batch (53.7 mg/L/h)) as reported in literature [133]. Though the *B. megaterium* heparosan titer is lower compared to the pathogenic *E. coli* K5 at present, recombinant *B. megaterium* offers safe alternative for the production of heparosan with desirable molecular weight properties.

3.4 Conclusion

This chapter successfully addressed a safe and alternative approach to produce heparosan in *B. megaterium* utilizing *E. coli* K5 glycosyltransferase genes. The UDP-precursor sugar pathway enzymes were found to be rate limiting for efficient heparosan synthesis in *B. megaterium*. A maximum heparosan titer was achieved (394 mg/L) in batch fermentation and was further enhanced to 1.32 g/L in fed-batch fermentation. Concerted endeavors for optimizing the expression level of KfiC and KfiA proteins, balancing the carbon flux of the UDP-precursor sugar pathway and optimizing the medium and fermentation strategies would further enhance the heparosan production. The molecular weight range (31-60 kDa) of heparosan obtained could be a possible precursor material for chemoenzymatic heparin synthesis.

CHAPTER 4

DEVELOPMENT OF DUAL PROMOTER EXPRESSION SYSTEM FOR THE ENHANCED HEPAROSAN PRODUCTION IN *Bacillus megaterium*

Summary

Heparosan production in *B. megaterium* is catalyzed by the formation of KfiC-KfiA complex and the subsequent action of KfiC and KfiA proteins. Polycistronic expression of *kfiC* and *kfiA* in *B. megaterium* yielded an unbalanced expression of KfiC and KfiA proteins resulted in decreased heparosan production. In this chapter, a dual promoter plasmid system was constructed to enhance the expression levels of KfiC and KfiA proteins. Dual promoter plasmid system along with UDP-GlcA pathway overexpression (CADuet-DB) increased the heparosan production to 203 mg/L in shake flask experiments. Batch fermentation of strain CADuet-DB under controlled conditions yielded a maximum heparosan concentration of 627 mg/L, which is 59 % higher than strain CA-DB. A modified logistic model is applied to describe the kinetics of heparosan production and cell growth. Fed batch fermentation resulted in 3-fold enhancement in heparosan concentration (1.96 g/L), compared to batch fermentation. NMR analysis revealed that heparosan from strain CADuet-DB was similar to *E. coli* K5 heparosan. These results suggested that dual promoter expression system is a promising alternative to polycistronic expression

An article based on this chapter is published as follows: Nehru, G., Tadi, S. R. R., & Sivaprakasam, S. (2021). Application of Dual Promoter Expression System for the Enhanced Heparosan Production in *Bacillus megaterium*. *Applied Biochemistry and Biotechnology*, 1-14. ©Springer US

system to produce heparosan in *B. megaterium*.

4.1 Introduction

E. coli K5 heparosan biosynthesis is regulated by four genes, *kfiC*, *kfiA*, *kfiB* and *kfiD*, present in the serotype specific region 2 of *E. coli* K5 gene cluster. *kfiC* encodes D-glucuronyltransferase, *kfiA* encodes N-acetyl glucosaminyltransferase and *kfiD* encodes UDP-glucose dehydrogenase, which converts UDP-glucose to UDP-GlcA [87]. The role of *kfiB* in heparosan biosynthesis is still unclear. Heparosan production is facilitated by the formation of KfiC-KfiA enzyme complex and the concerted action of KfiC and KfiA glycosyltransferases [42]. Literature reports suggested that KfiC alone does not exhibit GlcA transferase activity, but in the presence of KfiA, KfiC exhibits GlcA activity and polymerization activity [108]. Hence, the comparable co-expression of KfiC and KfiA proteins are essential to increase the polymerization activity of KfiC-KfiA complex.

In previous chapter, *B. megaterium* was engineered with *E. coli* K5 *kfiC* and *kfiA* glycosyltransferases to produce heparosan. *kfiC* and *kfiA* genes were expressed in polycistronic manner, resembling the *E. coli* K5 heparosan synthesis gene cluster. SDS-PAGE analysis showed an unbalanced expression of KfiC and KfiA proteins [80]. Literature report also proved that optimizing the expression of chondroitin pathway genes using pseudo-operon structure is beneficial than the operon structure in order to improve the chondroitin production in *E. coli* [40]. To be specific, dual promoter expression system was found to be efficient for the co-expression of proteins or the production of protein complexes [53]. pETDuet plasmid system is widely used for the co-expression of proteins in *E. coli* and also, it is commercially available.

In this chapter, a dual promoter plasmid system was constructed for the co-expression of *kfiC* and *kfiA* genes in *B. megaterium* to improve the heparosan production. The process variables influencing the heparosan production were optimized. The heparosan production ability of recombinant *B. megaterium* was evaluated in 3-L bioreactor both in batch and fed batch fermentation conditions. In addition, structural characterization of heparosan was determined by NMR analysis. Overall, this present chapter addresses the significance of dual promoter expression system for heparosan production in *B. megaterium*.

Table 4.1: List and description of the strains

Strain	Description/characteristic	Reference
E. coli TOP10	Cloning host, F'(lacIq Tn10 (Tet^R)) mcrA Δ(mrr-hsdRMS-mcrBC) Φ80lacZΔM15 ΔlacX74 recA1 araD139 Δ(ara-leu)7697 galU galK rpsL endA1 nupG	Invitrogen
E. coli K5	Serotype O10:K5:H4	BEI Resources, NIAID, NIH
B. megaterium DSM319	Wildtype, Expression host	DSMZ, Braunschweig, Germany
B. megaterium CA	*B. megaterium* DSM319 harboring pMM-kfiCA	[80]
B. megaterium CA-DB	*B. megaterium* CA harboring pMGB-tuaDgtaB	[80]
B. megaterium CADuet	*B. megaterium* DSM319 harboring pMMDuet-kfiCA	Present study
B. megaterium CADuet-DB	*B. megaterium* CADuet harboring pMGB-tuaDgtaB	Present study

4.2 Materials and methods

4.2.1 Bacterial strains, plasmids and media

The bacterial strains and plasmids used in this study are presented in Table 4.1 and 4.2. *E. coli* and *B. megaterium* strains were cultivated and maintained in Luria-Bertani (LB) broth and LB agar (LB broth containing 1.5 % agar). The fermentation medium used for shake flask and bioreactor experiments consisted of 10 g/L sucrose, 10 g/L yeast extract powder, 2 g/L tryptone, 7.8 g/L sodium dihydrogen phosphate dihydrate, 3.9 g/L potassium sulfate and 1.2 g/L magnesium sulfate heptahydrate. The final pH of medium was adjusted to 7.0 by 2 M NaOH [80]. Sterile filtration of the fermentation medium was done using 0.22 μm PVDF membrane filter. 100 μg/mL of ampicillin for *E. coli* and 10 μg/mL of tetracycline and 4.5 μg/mL of chloramphenicol for *B. megaterium* were supplemented in the medium for the stable replication of recombinant plasmids. The

Table 4.2: List and description of the plasmids

Plasmid	Description/characteristic	Reference
pRBBm34	*E. coli* – *B. megaterium* shuttle vector, Pxyl-MCS, Amp^R, Tet^R	Addgene plasmid # 48114
pHBintN	*E. coli* – *B. megaterium* shuttle vector, Source of Pxyl-MCS sequence	Addgene plasmid # 48135
pMM-kfiCA	Pxyl-kfiCA, Polycistronic expression of *kfiC* and *kfiA* genes	[80]
pMGB-tuaDgtaB	Pxyl-tuaDgtaB, Expression of GlcA pathway genes, *tuaD* and *gtaB*	[80]
pMMDuet	Pxyl-MCS-Pxyl-MCS, Dual promoter expression system	Present study
pMMDuet-kfiC	pMMDuet derivative, Pxyl-*kfiC*-Pxyl-MCS	Present study
pMMDuet-kfiCA	pMMDuet derivative, Pxyl-*kfiC*-Pxyl-*kfiA*	Present study

media components and chemicals were procured from HiMedia Laboratories, Mumbai, India.

4.2.2 Construction of expression systems

The parent plasmid, pRBBm34 [12] was digested with SphI. The primers used in this study are presented in Table 4.3. The xylose promoter with multiple cloning site was PCR amplified from pHBintN [13] using the primers, Dual-F and Dual-R and subsequently cloned into SphI site of pRBBm34 to generate dual promoter plasmid system, pMMDuet. The glycosyltransferase genes, *kfiC* and *kfiA* were amplified from *E. coli* K5 genomic DNA. *kfiC* gene was cloned under the first promoter of pMMDuet restricted with BsrGI and EagI to yield the plasmid pMMDuet-kfiC. Similarly, *kfiA* gene was cloned under the second promoter of pMMDuet-kfiC digested with SpeI and KpnI to generate pMMDuet-kfiCA. *E. coli* TOP10 was used as a cloning host to construct recombinant plasmids. The resulting plasmid was transformed into *B. megaterium* by PEG-mediated protoplast

Table 4.3: List and sequence of the primers

Primer	Sequence (5' → 3')
Dual-F	CAAATAATGAATTCGCGGCCGCATGTTGAATTAGATATTTAA AAGTATCATATCTAATATTATAACTAAATTTTC
Dual-R	GAATCCGTTAGCGAGGTGCCGCCGGGGCCGGTACCGGAT
Dual-kfiC-F	GTTCACTTAAATCAAAGGGGGAAATGTACAATGAACGCAGAA TATATAAATTTAGTTGAACGT
Dual-kfiC-R	TAAATATCTAATTCAACATGCGGCCGTTACTATTGTTCAATT ATTCCTGATACATCTTTAAACAAAC
Dual-kfiA-F	AGGGGGAAATGACAAATGGTCCAAACTAGTATGATTGTTGCA AATATGTCATCATACCC
Dual-kfiA-R	CGTTAGCGAGGTGCCGCCGGGGCCGGTACCTTACCCTTCCAC ATTATACACTAATTCGAG

transformation [72]. The transformants obtained on antibiotic resistance plate were taken for protein expression analysis.

4.2.3 Expression analysis of KfiC and KfiA proteins

The overnight recombinant *B. megaterium* culture was inoculated in LB broth containing appropriate antibiotics. When the OD_{600} reached 0.3-0.4, the culture was induced with 0.5 % of D-xylose. The culture was incubated at 30 °C for 6 h. The cells were harvested by centrifugation and washed twice with deionized water. The cells were resuspended in 100 μl of lysis buffer and incubated at 37 °C for 45 min. The lysis buffer consisted of 100 mM Na_3PO_4 pH 6.5, 5 mg/mL of lysozyme, 5 mM $MgSO_4$ and 2 μl of benzonase. The cell lysate was centrifuged at 4 °C for 30 min to remove soluble proteins. The remaining pellet was resuspended in 50 μl of 8 M urea to dissolve the insoluble proteins. Bradford assay was performed to estimate the concentration of total proteins. 20 μg of proteins were separated by 10 % SDS-PAGE analysis.

4.2.4 Shake flask and bioreactor experiments

The seed culture for shake flask and bioreactor experiments were grown in LB broth at 30 °C for 14 h. For shake flask cultivations, the preculture was inoculated into 250 ml

baffled flask containing 25 ml of fermentation medium to the optical density of 0.05 and incubated at 30 °C with shaking at 200 rpm. When the OD_{600} reached 0.5, recombinant gene expression was induced by the addition of 0.5 % (w/v) D-xylose. After 24 h induction, cells were harvested by centrifugation and stored at -20 °C for growth and product analysis.

Batch and fed batch fermentation of the recombinant strain was performed in a 3 L fermenter (Biojenik engineering, Chennai, India) with a 1.7 L fermentation medium. 5 % (v/v) of preculture was used to inoculate the fermentation medium. When the OD_{600} reached 0.5, the culture was induced with 1.5 % (w/v) D-xylose for the recombinant gene expression. The temperature was maintained at 37 °C. The pH was controlled at 7.0 using 3 M NaOH. During batch phase of fermentation, the agitation speed and aeration rate were set at 600 rpm and 1 vvm, respectively. After the depletion of sucrose in the fermentation medium, 50 % (w/v) of sucrose feeding solution was supplemented in order to sustain the growth of recombinant culture. Dissolved oxygen concentration was maintained above 20 % by regulating the agitator speed with an aeration rate of 1 vvm. Samples were collected in regular intervals for determining biomass, product and substrate concentration. Optical density (OD_{600}) of these samples were measured using UV spectrophotometer (Infinite M200 PRO, Tecan, Männedorf, Switzerland). Total sugar concentration was determined by Anthrone method. Concentrations of xylose and acetate in fermentation broth were determined using HPLC (Shimadzu, Kyoto, Japan) equipped with refractive index detector and Rezex RHM-monosaccharide H column (Phenomenex Inc., Torrance, CA). The mobile phase was 5 mM H_2SO_4 at a flow rate of 0.5 ml/min.

4.2.5 Kinetic modelling of *B. megaterium* growth and heparosan production

The logistic models are unstructured models that describe the kinetics of microbial growth and product formation. Logistic model uses sigmoidal profiles, which is independent of substrate concentration to estimate the kinetic parameters. Logistic equation (Eq. 4.1) was used to describe the sigmoidal growth profile of *B. megaterium* and heparosan production with certain assumptions. The assumptions are (i) Sucrose is the only limiting factor, (ii) the rate of cell growth is directly proportional to the cell concentration, (iii) cell growth is dependent on the amount of sucrose in the medium and (iv) heparosan

production is associated with cell growth.

$$r_p = \frac{dP}{dt} = \mu_m.P.(\frac{P_m - P}{P_m}) \tag{4.1}$$

where, P_m is the maximum cell or heparosan concentration (g/L or mg/L) and μ_m is the maximum specific growth or heparosan production rate (h^{-1}).
The Eq. 4.1 was modified by incorporating the parameters υ_P and λ_P to yield reparameterized Eq. 4.2

$$P = \frac{P_m}{1 + \frac{}{\frac{4\upsilon_P\ (\lambda_P}{P_m}}} \tag{4.2}$$

where, P is the product estimated (X or H), P_m is the maximum cell or heparosan concentration (g/L or mg/L), υ_P is the maximum growth or heparosan production rate (g/L.h or mg/L.h), and λ_P is the lag phase of cell growth or heparosan production (h).
In addition, other parameters such as μ_P, τ_P and t_{mP} were calculated according to the following equations. These parameters describe the characteristics of cell growth and heparosan production of recombinant *B. megaterium* in the media studied.

$$\mu_P = \frac{4\upsilon_P}{P_m} \tag{4.3}$$

$$\tau_P = \lambda_P + \frac{2}{\mu_P} \tag{4.4}$$

$$t_{mP} = \tau_P + \frac{P_m}{2\upsilon} \tag{4.5}$$

where, μ_P is the maximum specific growth or heparosan production rate (h^{-1}), τ_P is the time required to reach half of the maximum production or growth (h) and t_{mP} is the time required to achieve maximum production (h).

4.2.6 Kinetic parameters estimation and statistical analysis

The experimental data obtained from batch bioreactor experiment was used to estimate the kinetic parameters. Kinetic parameters were estimated by minimizing objective function (f) formulated between the model predicted and experimental data using non-linear least square method. All the kinetic parameters estimation and model fitting

procedures were carried out using Microsoft Excel solver tool [122]. Model regression analysis was performed using Microsoft Excel data analysis tool kit.

$$f = \sum_{i=1}^{N} (P_{sim} - P_{exp})^2 \tag{4.6}$$

where, P_{sim} is the simulated data and P_{exp} is the experimental data.

4.2.7 Analysis and characterization of heparosan

The cells were harvested from fermentation broth by centrifugation and washed twice with deionized water. Heparosan was extracted by suspending the cells in lysis buffer (2 g/L lysozyme, 2 μl benzonase, 20 mM $MgSO_4$ and Tris-Cl pH 7.5) and incubated for 1 h. Complete lysis of the cells was achieved by autoclaving the cell lysate at 121 ◦C for 20 min. The cell debris was removed by centrifugation and the supernatant was used for heparosan quantification. The modified carbazole assay was used to estimate heparosan concentration [14].

Heparosan was purified from the fermentation broth using Diethylaminoethyl-sepharose chromatography [133]. The purified heparosan was characterized by NMR analysis. Heparosan characterization was performed using Bruker Ascend 600 MHz NMR spectrometer (Bruker, MA, USA) with TOPSPIN data acquisition software. The freeze-dried heparosan was dissolved in 0.6 mL D_2O and transferred into standard NMR microtubes. ^{1}H-NMR spectrum was recorded for 160 scans at 298 K.

The average molecular weight distribution of heparosan was analyzed by high performance size exclusion chromatography-refractive index detector (HPSEC-RID) with polysep-GFC-P-6000 column (Phenomenex Inc, Torrance, CA). The mobile phase was 100 mM $NaNO_3$ with a flow rate of 0.5 ml/min. The column temperature was maintained at 40 ◦C. The average molecular weight of the samples was determined using the calibration plot obtained from dextran standards of different molecular weights [127].

4.3 Results and discussion

4.3.1 Construction of dual promoter plasmid system expressing *kfiC* and *kfiA* genes

Heparosan is synthesized in *B. megaterium* by the KfiC-KfiA enzyme complex and the sequential action of KfiC and KfiA glycosyltransferases (Figure 3.1) [42]. In the previous chapter, KfiC and KfiA proteins were expressed in a polycistronic plasmid system under a single promoter as mimicking the K5 operon structure. Expression of KfiA was observed to be less compared to the KfiC, which is adjacent to the promoter [80]. The efficient production of heparosan requires the comparable expression of KfiC and KfiA and the formation of KfiC-KfiA protein complex. To overcome this, dual promoter expression system was constructed where the promoter sequence was inserted before *kfiA* on a polycistronic expression system [53]. *kfiC* and *kfiA* were cloned under individual xylose-inducible promoter to generate dual promoter expression system, pMMDuet-kfiCA (Figure 4.2a). Restriction digestion analysis was performed to validate the successful recombinant plasmid construction (Figure 4.1). The resulting plasmid was transformed into *B. megaterium* to generate the strain CADuet. SDS-PAGE analysis revealed that the KfiA expression is enhanced in the dual promoter expression system compared to the polycistronic expression system (Figure 4.2b). Dual promoter expression system was previously applied to improve the co-expression of proteins and protein complexes [10, 53]. Shake flask cultivation of strains, CADuet and CA resulted in the heparosan production of 55 mg/L and 40.5 mg/L, respectively (Figure 4.2c). Literature reports indicated that UDP-GlcA concentration was limiting the heparosan production in heterologous hosts [22, 47, 133]. The plasmid pMGB-tuaDgtaB, expressing UDP-glucose dehydrogenase (*tuaD*) and UDP-glucose pyrophosphorylase (*gtaB*) was constructed in the previous chapter to enrich the UDP-GlcA synthesis pathway [80]. The plasmid pMGB-tuaDgtaB was transformed into CADuet to generate the strain CADuet-DB. Shake flask experiments of CADuet-DB and CA-DB produced the heparosan concentrations of 195.7 mg/L and 115 mg/L (Figure 4.2c). These results indicated that dual promoter plasmid system and UDP-GlcA concentration increased the heparosan production in *B. megaterium*.

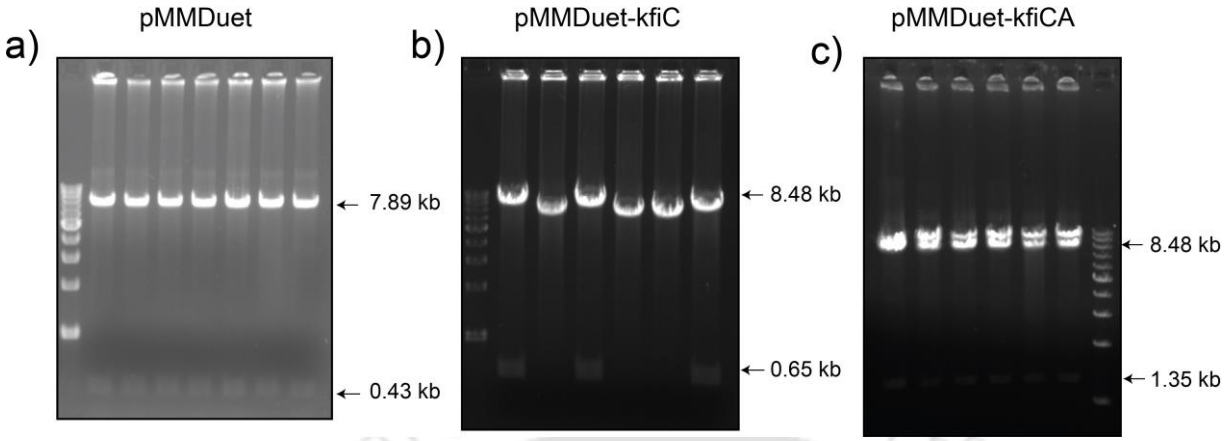

Figure 4.1: Development of dual promoter expression system expressing *kfiC* and *kfiA* genes. **a)** Construction of dual promoter plasmid, pMMDuet. Restriction digestion analysis with BamHI resulted in the expected size of 7.89 kb and 0.43 kb DNA fragments **b)** Construction of pMMDuet-kfiC. Plasmids were digested with BamHI to yield DNA fragments of 8.48 kb and 0.65 kb **c)** Construction of pMMDuet-kfiCA. Plasmids were digested with BamHI and KpnI to produce expected DNA fragments of 8.48 kb and 1.35 kb

4.3.2 Process optimization of heparosan production

Optimization of the process variables such as temperature, Inducer concentration and OD_{600} prior to induction was vital to improve the heparosan production and cell growth. To evaluate the influence of temperature on heparosan production, strain CADuet-DB was cultivated at four different temperatures (25 °C, 30 °C, 37 °C and 42 °C) for 24 h. The maximum heparosan concentration and cell concentration was observed to be 203 mg/L and 4.60 g/L at 37 °C, respectively (Figure 4.3a). At tested temperatures below 30 °C and above 37 °C, *B. megaterium* showed suboptimal growth and decreased heparosan production. D-xylose was used as an inducer to drive the expression of cloned genes under xylose inducible promoter. In addition, *B. megaterium* utilizes D-xylose along with sucrose during the course of fermentation. To determine the optimal xylose concentration, different xylose concentrations (0.5 %, 1 %, 1.5 % and 2 %, w/v) were used to induce strain CADuet-DB. No significant difference was observed in the cell growth among various inducer concentrations. The maximum heparosan production was observed at 1.5 % (w/v) of D-xylose (Figure 4.3b). In addition, the cell concentration has to reach certain threshold to resist the metabolic burden caused by higher xylose concentrations. In order to determine optimal OD_{600} prior to induction, the cultures were induced at different OD_{600} values of approximately 0.1, 0.4, 0.8 and 1.5. The highest heparosan concentration

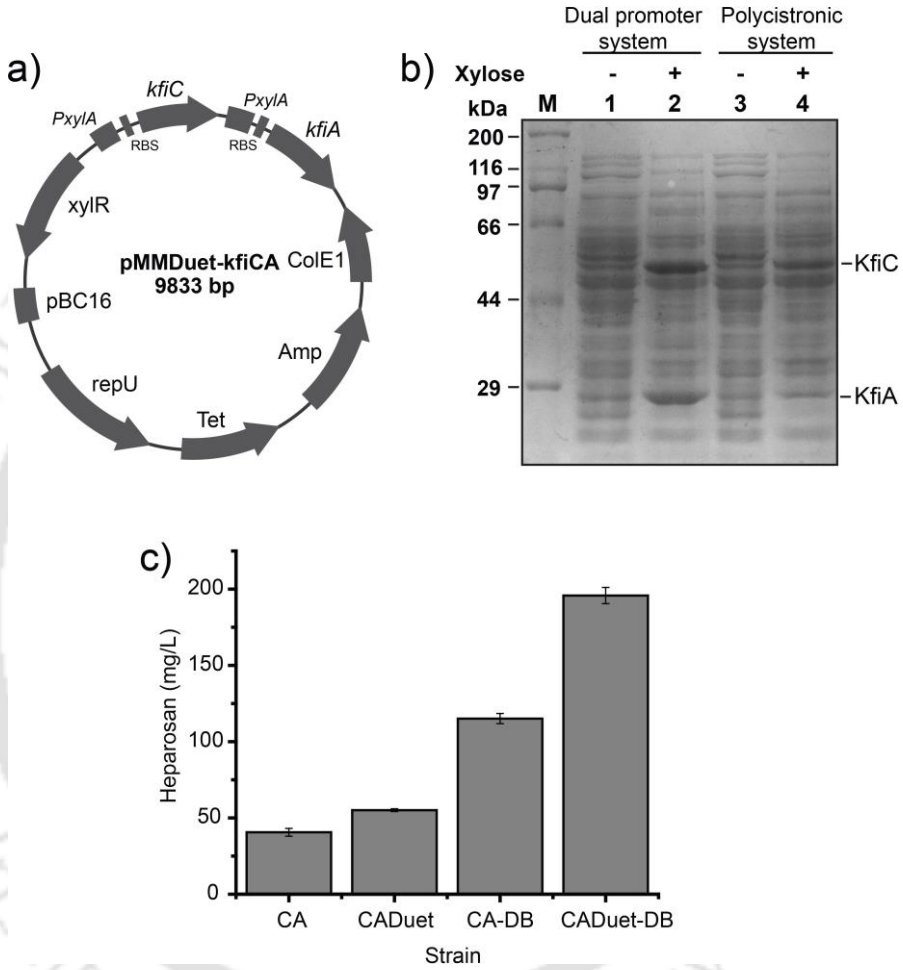

Figure 4.2: a) Schematic representation of dual promoter plasmid system, pMMDuet-kfiCA expressing *kfiC* and *kfiA* genes **b)** Expression analysis of KfiC and KfiA proteins by SDS-PAGE. Lane 1 and 2, lysate of strain CADuet uninduced and induced; Lane 3 and 4, lysate of strain CA uninduced and induced. The cultures were induced with 0.5 % (w/v) D-xylose. Production of KfiC and KfiA proteins at 59 kDa and 27 kDa, respectively after the addition of D-xylose as seen in lane 2 and 4 **c)** Heparosan titer comparison of different recombinant *B. megaterium* strains at shake flask culture level

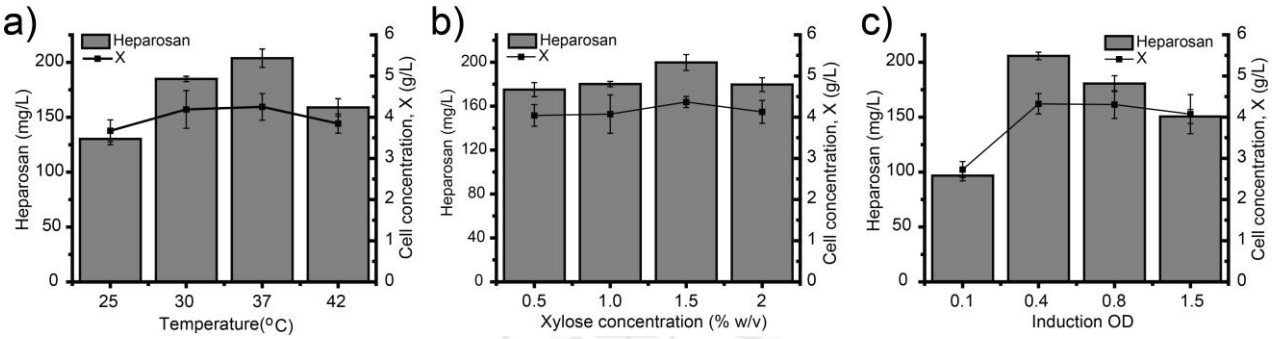

Figure 4.3: Effect of **a)** temperature **b)** inducer concentration and **c)** OD_{600} prior to induction on heparosan production and cell growth

was obtained when the gene expression was induced at OD_{600} of 0.4 (Figure 4.3c). The cell growth and heparosan production were severely affected when the cultures were induced at OD_{600} of 0.1. The late induction above the OD_{600} of 1.5 also decreased the heparosan yield as most of the cellular resources were diverted to cell growth instead of protein expression prior to the induction.

4.3.3 Batch fermentation and kinetic modelling of recombinant *B. megaterium* growth and heparosan production

Batch fermentation of strain CADuet-DB was carried out to scale-up the heparosan production in 3-L fermenter. The maximum cell concentration of 4.59 g/L was reached in the bioreactor at the end of 14 h. Heparosan concentration was increased to 627 mg/L at 14 h (Figure 4.4). Previously, batch fermentation of strain CA-DB resulted in the maximum heparosan production of 394 mg/L [80]. We observed a 59 % increase in the heparosan production in strain CADuet-DB than strain CA-DB. Carbazole analysis showed that the heparosan was retained in the cell pellet [80, 127].

Further, the estimation of growth and product related kinetic parameters aid in understanding the performance of recombinant strains and devising bioprocess strategies to improve the heparosan production. Modified logistic model was used to estimate the kinetic parameters by fitting the experimental data. Parameter estimations corresponding to the logistic equation were summarized in Table 4.4. The agreement between predicted and experimental data was satisfactory, with the correlation coefficient values above 0.99. The consistency of the model to describe the cell growth and heparosan production was also confirmed by statistical analysis using p-values from Fisher's F-test. High F-values

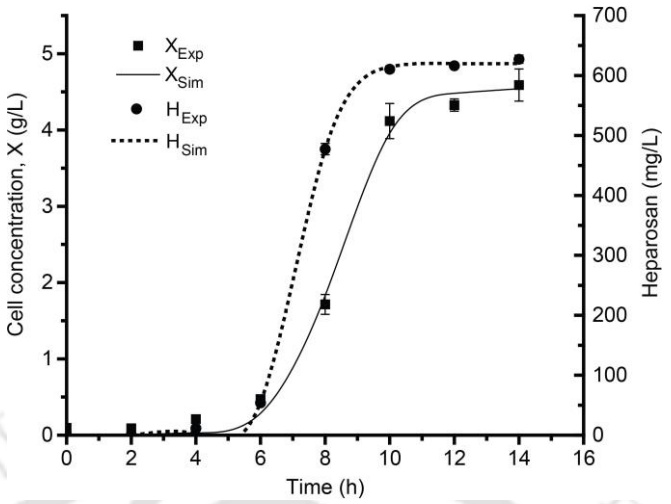

Figure 4.4: Batch fermentation of strain CADuet-DB in 3 L bioreactor. Experimental data of heparosan production and cell growth were fitted to the logistic model (Eq. 4.2) (continuous line). The corresponding parameter estimations were listed in Table 4.4. X_{exp}, experimental cell concentration; X_{sim}, model predicted cell concentration; H_{exp}, experimental heparosan; H_{sim}, model predicted heparosan

(1920.61 and 25599.42) and low p-values (<0.001) indicates the significance of the model. As illustrated in Figure 4.4, the strain CADuet-DB displayed a classic sigmoidal growth pattern. After a lag phase of 6.61 h, the cell concentration entered an exponential growth and reached a maximum of 4.59 g/L. Similarly, the heparosan production took place simultaneously with cell growth, following a similar sigmoidal profile.

4.3.4 High cell density cultivation of *B. megaterium* for heparosan production

The strain CADuet-DB was further cultivated in fed batch cultures to evaluate the heparosan production in 3-L fermenter. The time course of heparosan production, cell growth and sucrose consumption were represented in Figure 4.5. To prevent the acetate overproduction due to carbon overflow metabolism, sucrose was fed to maintain the concentration less than 10 g/L. The heparosan production is coupled to cell growth, similar to batch fermentation. The heparosan production was increased to 1.96 g/L at 25 h.

Table 4.4: Parametric estimations corresponding to the logistic model applied to batch cultures of strain CADuet-DB. The kinetic parameters were estimated using the Eq. 4.2 to Eq. 4.5

Kinetic parameters	Estimated values
Cell growth	
X_m (g/L)	4.55 ± 0.16
υ_X (g/L. h)	1.31 ± 0.06
λ_X (h)	6.61 ± 0.04
μ_X (h^{-1})	1.15 ± 0.02
τ_X (h)	8.34 ± 0.07
t_{mX} (h)	10.08 ± 0.09
R^2	0.99
MSE	0.02
F (α = 0.05)	1920.61
p	<0.001
Heparosan	
H_m (mg/L)	619.98 ± 5.22
υ_H (mg/L. h)	273.57 ± 0.73
λ_H (h)	6.19 ± 0.04
μ_H (h^{-1})	1.77 ± 0.01
τ_H (h)	7.32 ± 0.03
t_{mH} (h)	8.45 ± 0.03
R^2	0.99
MSE	25.71
F (α = 0.05)	25599.42
p	<0.001

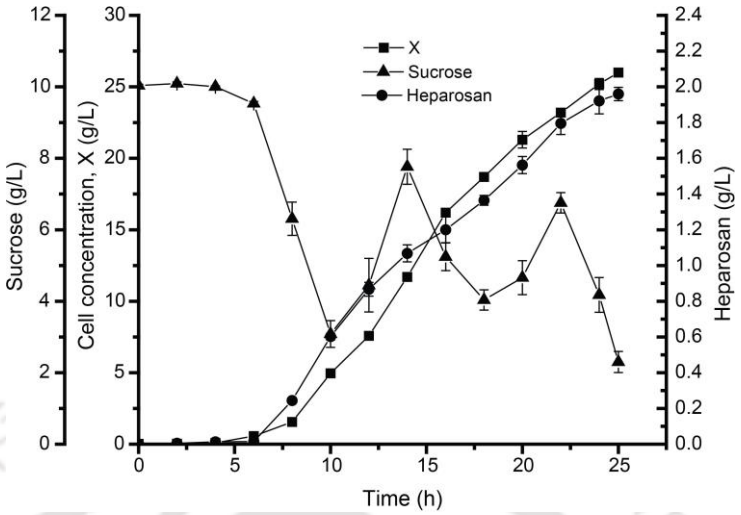

Figure 4.5: Fed batch fermentation of strain CADuet-DB in 3-L bioreactor. Time course of heparosan production, cell growth and sucrose consumption are shown

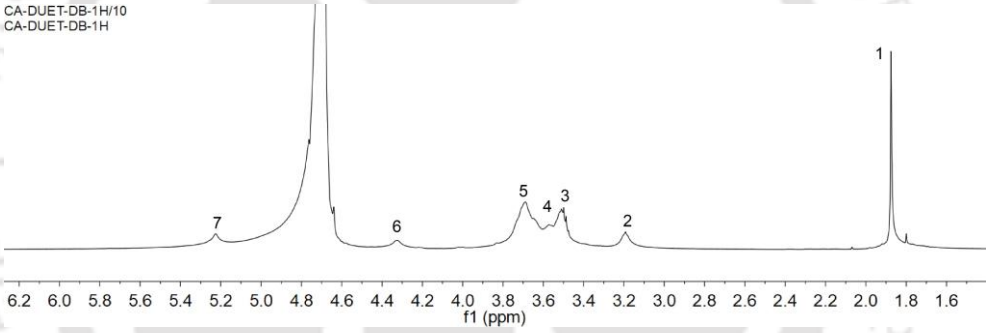

Figure 4.6: ^{1}H-NMR analysis of recombinant *B. megaterium* derived heparosan. The chemical shifts assigned to the protons are listed in Table 4.5

4.3.5 Structural and molecular weight characterization of heparosan

Heparosan was extracted from the cell pellet by acidic protein precipitation and anion exchange chromatography [60]. One dimensional ^{1}H-NMR was employed to determine the structural characteristics of heparosan produced by strain CADuet-DB. The chemical shifts obtained were similar to the previously published spectra of heparosan (Table 4.5) [22, 127, 133]. The peaks at 4.32 ppm and 3.19 ppm corresponds to the H-1 and H-2 of β-GlcA, respectively confirmed the presence of glucuronic acid residue. Similarly, the peak at 5.22 ppm represents the H-1 of GlcNAc along with the characteristic acetyl peak at 1.88 ppm confirmed the presence of N-acetylglucosamine residue of heparosan

Table 4.5: ^{1}H-NMR chemical shift assignments for heparosan derived from strain CADuet-DB

No.	Proton	Chemical shifts (ppm)
1	GlcNAc CH_3	1.88
2	GlcA H_2	3.19
3	GlcA H_3, H_4 and GlcNAc H_4	3.50
4	GlcA H_5	3.57
5	GlcNAc H_2, H_3, H_5, H_6	3.69
6	GlcA H_1	4.32
7	GlcNAc H_1	5.22

(Figure 4.6). The molecular weight distribution of heparosan was determined by HPSEC. The molecular weight of heparosan obtained with the strain CADuet-DB in batch and fed batch fermentation was 68.6 kDa and 41.9 kDa. The average molecular weight of heparosan obtained in this chapter is lower than *B. megaterium* derived heparosan engineered with *P. multocida* heparosan synthase [127]. This difference could be explained by the source of glycosyltransferases, gene expression levels and other growth conditions. Low molecular weight heparosan can be used as a precursor for chemoenzymatic heparin synthesis and drug conjugate vehicle for therapeutic applications.

4.4 Conclusion

This chapter shows that dual promoter plasmid system expressing KfiC and KfiA glycosyltransferases can efficiently produce heparosan compared to the polycistronic expression system. The over-expression of UDP-GlcA pathway genes enhances the heparosan production. The maximum volumetric production of heparosan reached 203 mg/L in shake flasks and 627 mg/L in batch bioreactor. Fed batch fermentation enhanced the heparosan concentration to 1.96 g/L paving the scope for its large-scale production. In addition, this chapter provides a safe approach to produce heparosan, which can be used as a precursor for heparin synthesis or a natural polymeric conjugative vehicle for drug delivery.

CHAPTER 5

INFLUENCE OF SUCROSE AND N-ACETYLGLUCOSAMINE SUPPLEMENTATION ON HEPAROSAN BIOSYNTHESIS IN *Bacillus megaterium*

Summary

An unstructured model of heparosan fermentation by recombinant *B. megaterium* considering the effect of different concentrations of sucrose was proposed. The modified logistic model characterized the *B. megaterium* growth, sucrose consumption and heparosan production. The model predicted that high initial sucrose concentration inhibited the biomass growth and substrate consumption. The addition of N-acetylglucosamine enhanced the heparosan concentration by 1.6-fold compared to control. The batch fermentation with dual substrates, sucrose and N-acetylglucosamine was modeled using double andrew's model. The maximum heparosan concentration of 0.91 g/L was obtained in batch fermentation. Sensitivity analysis of the predicted kinetic constants suggested that maximum specific growth rate and maximum heparosan production rate were found to be most sensitive parameters with respect to cell growth and heparosan concentration, respectively.

5.1 Introduction

Batch fermentation is a standard method for heparosan production, and studies have been carried out regarding the optimal culture conditions for heparosan production [133]. However, the principal disadvantages of batch heparosan fermentation is the inhibition of substrate and by-product concentration, a conventional property of batch fermentation. Don et al. reported that the metabolite production was limited due to the strong inhibition of substrates under high concentrations [29]. The high substrate or product concentrations and the presence of inhibitory substances in the medium inhibit growth [120].

Majority of models reported in the literature involved Monod-like relationships which considers the inhibition kinetics of many fermentation processes to describe the cell growth, substrate consumption and product formation [96, 122]. Subsequently, the Logistic model and Luedeking–Piret equations have been developed to explain the behavior of cell growth and product formation. The use of several models that involved more than one substrate state variable has also been reported on hyaluronan production by *S. zooepidemicus*.

It is well established that the fermentative pathway of *B. megaterium* channelizes the carbon substrate into biomass and heparosan synthesis and acetate production. Therefore, heparosan synthesis pathway competes for glycolytic intermediates and UDP-precursors with cell growth and peptidoglycan synthesis [80, 127]. Addition of GlcNAc found to increase carbon flux towards hyaluronic acid production in *S. zooepidemicus* and recombinant microorganisms [45, 76]. This chapter addresses a influence of initial substrate concentration and UDP-precursor supplementation on heparosan production in recombinant *B. megaterium*.

In this chapter, mathematical models that described growth, substrate utilization and inhibition, and heparosan production were proposed, considering the effect of the initial sucrose concentration on the kinetic parameters. To achieve this goal, experiments were performed at an initial sucrose concentration range of 10 to 50 g/L in the batch fermentation. Kinetic modeling analysis of GlcNAc supplementation in heparosan production dealt in the present chapter provides insight on the distribution of carbon towards cell growth, heparosan synthesis, and maintenance activities.

5.2 Materials and methods

5.2.1 Media

Luria-Bertani (LB) broth was used for the routine cultivation and maintenance of recombinant *B. megaterium* strain. The fermentation medium used for the heparosan production consisted of 10-50 g/L sucrose, 20 g/L yeast extract, 2 g/L tryptone, 50 mM potassium phosphate buffer pH 7.0 and 1.2 g/L magnesium sulfate heptahydrate. The medium was sterilized at 121 ◦C for 20 min. Precursor supplementation experiments were carried out in shake flasks by adding GlcA or GlcNAc to the fermentation medium.

5.2.2 Microorganism and inoculum preparation

Recombinant *B. megaterium* CADuet-DB was used to produce heparosan from the previous study [81]. Stock culture of recombinant *B. megaterium* was maintained at -80 ◦C in LB medium with 25 % (w/v) glycerol. Single colony was used to inoculate 5 mL of LB medium. 1 % (v/v) of pre-inoculum was used to prepare the seed culture. 10 % (v/v) of seed culture was used to inoculate the fermentation medium for shake flask and bioreactor experiments. The seed culture with an OD_{600} range from 0.8 to 1.2 was used to inoculate the fermentation medium. The cultute conditions for *B. megaterium* growth was maintained at 37 ◦C, 180 rpm for 12 h. 10 μg/mL of tetracycline and 4.5 μg/mL of chloramphenicol were supplemented in the fermentation medium for the stable maintenance of recombinant plasmids.

5.2.3 Shake flask and bioreactor experiments

The preculture for shake flask and bioreactor experiments were cultivated in LB medium at 37 ◦C for 12 h. Shake flask cultivations were performed by inoculating the preculture into 250 ml baffled Erlenmeyer flask containing 25 ml of fermentation medium to the initial OD_{600} of 0.05. The culture was induced with 1.5 % (w/v) of D-xylose for the recombinant gene expression when the OD_{600} range reached 0.4 to 0.6. Cells were centrifuged at 13000 rpm for 10 min and stored at -20 ◦C for cell and heparosan concentration estimation.

Recombinant *B. megaterium* was cultivated in a 3-L fermenter (Biojenik engineering, Chennai, India) containing 1.7-L working volume of fermentation medium at 37 ◦C.

The initial sucrose concentration in the fermentation medium was varied from 10 to 50 g/L. 10 % (v/v) of overnight grown seed culture was used to inoculate the fermentation medium. The pH was maintained at 7.0 using 5 M NaOH. Agitation and aeration were set at 500 rpm and 1 vvm, respectively. When the OD_{600} raised from 0.4 to 0.6, the culture was induced with 1.5 % (w/v) D-xylose for recombinant gene expression. Samples were drawn for the estimation of biomass, substrate and heparosan analysis.

5.2.4 Analytical methods

Cell concentration of the samples was determined by measuring the optical density at 600 nm using UV spectrophotometer (Infinite M200 PRO, Tecan, Männedorf, Switzerland). Sucrose and xylose concentration in the fermentation broth was determined using HPLC equipped with MetaCarb 67C column (300 × 6.5 mm, Agilent Technologies Inc, CA, USA) and refractive index detector. The deionized water at a flow rate of 0.5 mL/min was used as a mobile phase. The oven and column temperature were maintained at 85 °C and 40 °C, respectively.

5.2.5 Heparosan concentration determination

The cells were collected from fermentation broth by centrifugation and washed twice with deionized water to remove the media components. The cells were suspended in lysis buffer (2 g/L lysozyme, 2 μl benzonase, 20 mM $MgSO_4$ and Tris-Cl pH 7.5) and incubated at 37 °C for 1 h. Further, the cell lysate was autoclaved at 121 °C for 20 min to ensure the complete lysis of cells. The cell lysate was centrifuged and supernatant was used for heparosan estimation. Heparosan concentration was quantified using modified carbazole assay method [14].

5.2.6 Kinetic modelling of *B. megaterium* cultivation

The unstructured models such as logistic model or Monod model are commonly used to explain the kinetics of microbial growth. Logistic model is widely used to determine the kinetic parameters based on the sigmoidal profiles of the growth, which does not take account of substrate concentration.

5.2.6.1 Cell growth

Logistic equation was represented as a function of time with certain assumptions as follows: Sucrose is the only limiting factor; the rate of cell growth is directly proportional to the cell concentration; cell growth is dependent on the amount of sucrose in the medium and heparosan production is associated with cell growth.

$$r_X = \frac{dX}{dt} = \mu_m X\left(\frac{X_m - X}{X_m}\right) \tag{5.1}$$

where, X_m is the maximum cell concentration (g/L) and μ_m is the maximum specific growth rate (h^{-1}).Integrating Eq. 5.1

$$X = \frac{X_o X_m e^{\mu_m t}}{X_m - X_o + X_o e^{\mu_m t}} \tag{5.2}$$

To model the kinetics of *B. megaterium* cell growth (X), the above Eq. 5.2 was reparametrized by incorporating the maximum cell growth rate, υ_X (g/L. h) and lag time of the cell growth, λ_P (h) to yield Eq. 5.3

$$X = \frac{X_m}{1 + \frac{4\upsilon_X (\lambda_X}{X_m}} \tag{5.3}$$

where, X is the cell concentration (g/L), X_m is the maximum cell concentration obtained (g/L), υ_X is the maximum cell growth rate (g/L. h), and λ_X is the lag phase of cell growth.

5.2.6.2 Sucrose consumption

Sucrose consumption is a function of cell growth, product formation and maintenance energy in *B. megaterium*. The overall mass balance for sucrose consumption is given in Eq. 5.4

$$r_S = -\frac{dS}{dt} = \frac{1}{Y_{X/S}}\frac{dX}{dt} + m_S X + \frac{1}{Y_{P/S}}\frac{dP}{dt} \tag{5.4}$$

In Eq. 5.4, the substrate flux towards heparosan production is negligible. Hence, it is further reduce to Eq. 5.5.

$$r_S = -\frac{dS}{dt} = \frac{1}{Y_{X/S}}\frac{dX}{dt} + m_S X \tag{5.5}$$

Integrating the Eq. 5.5 and substituting for X from Eq. 5.3 results in an expression for sucrose consumption as a function of time, t (Eq. 5.6)

$$S = So - \frac{1}{Y_{X/S}}\left[\frac{X_m}{1 + exp\left[2 + \frac{4\upsilon_X}{X_m}(\lambda_X - t)\right]} - X_o\right] - \left(\frac{m_S X_m^2}{4\upsilon_X}\right)\ln\left[\frac{X_o\left(e^{\frac{4\upsilon_X t}{X_m}} - 1\right) + X_m}{X_m}\right] \tag{5.6}$$

Where, S is sucrose concentration (g/L), S_o is the initial concentration of substrate (g/L), $Y_{X/S}$ is the yield of cell concentration per sucrose consumed (g of cells produced/g of sucrose consumed), X_o is the initial cell concentration (g/L) and m_S is the maintenance coefficient (g of sucrose consumed/g of cells produced. h).

5.2.6.3 Heparosan production

Similar to the growth kinetics of *B. megaterium*, heparosan production kinetics was described using the logistic equation (Eq. 5.7)

$$H = \frac{H_m}{1 + \frac{4\upsilon_H}{H_m}(\lambda_H)} \tag{5.7}$$

Where, H is the heparosan produced (g/L), H_m is the maximum heparosan produced (g/L), υ_H is the maximum heparosan production rate (g/L. h) and λ_H is the lag phase of heparosan production.

5.2.7 Unstructured multi-substrate kinetic modelling

B. megaterium was cultivated in the fermentation medium containing two substrates, *viz.* sucrose and GlcNAc.

5.2.7.1 Cell growth

Rate of cell growth can be represented with the following Eq. 5.8

$$r_X = \frac{dX}{dt} = (\mu - K_d) * X \tag{5.8}$$

Death rate, K_d can be neglected considering the actively growing cells. Eq. 5.8 was further reduced to yield an Eq. 5.9

$$\frac{dX}{dt} = \mu X \tag{5.9}$$

Sucrose and GlcNAc are consumed simultaneously during the growth of *B. megaterium*. Hence, interactive or multiplicative multi substrate kinetic model was adopted to describe *B. megaterium* growth and heparosan production. In case of interactive multi substrate kinetics, specific growth rate (μ) on n number of substrates is given in Eq. 5.10

$$\mu = \mu_{max} * \mu(S_1) * \mu(S_2) * .... * \mu(S_n) \tag{5.10}$$

In dual substrate kinetics, resulting specific growth rate of *B. megaterium* on both substrates (sucrose- s_1 and GlcNAc-s_2) can be represented in Eq. 5.11

$$\mu(S_1, S_2) = \mu_{max} * \mu(S_1) * \mu(S_2) \tag{5.11}$$

Double Andrew's model presents an advantage for interactive dual substrates and inhibition term due to excess substrates. This model was chosen to get insight on the inhibitory effect of both substrate on cell growth. The final cell growth model is presented in Eq. 5.12

$$\frac{dX}{dt} = \mu_{max} * \left(\frac{S_1}{(K_{S_1} + S_1 + \frac{S_1^2}{K_{I_1}})}\right) * \left(\frac{S_2}{(K_{S_2} + S_2 + \frac{S_2^2}{K_{I_2}})}\right) * X \tag{5.12}$$

where, μ_{max} is the maximum specific growth rate (h^{-1}), S_1 is concentration of sucrose (g/L), K_{S_1} is sucrose saturation constant (g/L), K_{I_1} is sucrose inhibition constant (g/L), S_2 is concentration of GlcNAc (g/L), K_{S_2} is GlcNAc saturation constant (g/L) and K_{I_2} is GlcNAc inhibition constant (g/L)

5.2.7.2 Heparosan production

The rate of Heparosan production can be explained by the following Eq. 5.13

$$\frac{dH}{dt} = H_{max} * \left(\frac{S_1}{(K_{H_1} + S_1 + \frac{S_1^2}{K_{HI_1}})}\right) * \left(\frac{S_2}{(K_{H_2} + S_2 + \frac{S_2^2}{K_{HI_2}})}\right) * X \tag{5.13}$$

5.2.7.3 Substrate consumption

Substrate consumed are mainly used for cell growth, product formation and cell maintenance activities. the rate of sucrose consumption is given in Eq. 5.14

$$\frac{dS_1}{dt} = \left(\frac{1}{Y_{P/HS1}} * \frac{dP_H}{dt}\right) - \left(\frac{1}{Y_{X/S1}} * \frac{dX}{dt}\right) - m_{S1}X \tag{5.14}$$

where, $Y_{P/HS1}$ is heparosan yield coefficient on sucrose (g/g), $Y_{X/S1}$ is cell growth yield coefficient on sucrose (g/g) and m_{S1} is maintenance coefficient on sucrose (g/g. h) and X is cell concentration (g/L) The rate of N-acetylglucosamine consumption is given in Eq. 5.15

$$\frac{dS_2}{dt} = \left(\frac{1}{Y_{P/HS2}} * \frac{dp_H}{dt}\right) - \left(\frac{1}{Y_{X/S2}} * \frac{dX}{dt}\right) - m_{S2}X \tag{5.15}$$

where, $Y_{P/HS2}$ is heparosan yield coefficient on GlcNAc (g/g), $Y_{X/S2}$ is cell growth yield coefficient on GlcNAc (g/g) and m_{S2} is maintenance coefficient on GlcNAc (g/g. h) and X is cell concentration (g/L)

5.2.8 Parameter estimation and statistical analysis

The kinetic parameters were estimated using the experimental data obtained from a series of batch fermentations with different sucrose concentration. Kinetic parameters were estimated by minimizing the residual sum of square errors between experimental and model predicted data using non-linear least square method of Levenberg-Marquardt optimization (Eq. 5.16). All the fitting procedures and parameter estimations were performed using Microsoft Excel solver tool. Single substrate kinetic model regression analysis was carried out using Microsoft Excel data analysis tool kit.

$$f = \sum_{i=1}^{N} (P_{sim} - P_{exp})^2 \quad (5.16)$$

where, f is the objective function, P_{sim} is the simulated data and P_{exp} is the experimental data.

The kinetic parameter estimation for dual substrate kinetic modelling was performed using DYMOLA2019. The error function to be minimized was formulated using the calibration tool available in the design library of DYMOLA (Eq. 5.17). The bounds for parameters were chosen from the sensitivity analysis and genetic algorithm (GA) was used as the optimization technique to minimize the error with a tolerance of 0.001.

$$Error = \sum [(\cdot X_{exp} - X_{sim} \cdot) + (\cdot S_{1exp} - S_{1sim} \cdot) + (\cdot S_{2exp} - S_{2sim} \cdot) + (\cdot P_{exp} - P_{sim} \cdot)] \quad (5.17)$$

where, X, S_1, S_2, P represents the state variables and the subscripts *exp* and *sim* represent the respective experimental and simulated values.

5.2.9 Sensitivity analysis

The sensitivity analysis of the model parameters was performed by perturbing the parameters by ±10 % one at a time, while the other parameters were maintained at their nominal values. The sensitivity analysis was carried out to observe the effect of changes in the parameters on the state variables.

5.3 Results and discussion

5.3.1 Influence of initial substrate concentration on cell growth

In order to evaluate the influence of initial substrate concentration (S_o) on *B. megaterium* growth kinetics, the fermentation medium was supplemented with varying initial sucrose concentration ranging from 10 to 50 g/L in a batch bioreactor. A modified logistic expression (Eq. 5.3) was used to describe the *B. megaterium* growth kinetics. Figure 5.1 shows the experimental and simulated profiles of *B. megaterium* growth at different initial sucrose concentrations. Experimental cell growth data was modeled using logistic equation to determine the kinetic parameters (Table 5.1). The maximum cell

concentration (X_m) and specific growth rate (μ_m) were observed to be 5.30 g/L and 0.75 h^{-1}, respectively. A steady drop in the μ_m and X_m values at higher S_o indicated the onset of substrate inhibition on cell growth. The substrate inhibition phenomenon was further validated by gradual rise in the lag phase of growth (λ_X) from 0.80 h to 2.08 h with a concomitant increase in S_o from 10 to 50 g/L. Tadi et al. [91] reported a lag time of 2.2 h to 14.6 h for *B. megaterium* grown on different concentrations of millet bran and rapeseed meal hydrolysates for polyhydroxybutyrate (PHB) production. The decrease in lag phase in case of sucrose could be attributed to the simple nature of the substrate. Literature reports suggested that length of the lag phase is influenced by certain factors such as (i) media composition, (ii) inoculum age, (iii) inoculum size and (iv) physical parameters such as temperature and pH [29]. Since all the process parameters were maintained constant in all fermentation experiments, increase in the lag phase could be attributed to the increase in sucrose concentration. The model derived cell concentration values was in good agreement with experimental data ($R^2 > 0.95$). Hence, the modified logistic model was satisfactory enough to explain the sigmoidal growth pattern of *B. megaterium*. Similarly, logistic model was employed to describe the growth of *B. megaterium* and *Streptococcus zooepidemicus* for PHB and hyaluronic acid production, respectively [29, 91, 96].

5.3.2 Influence of initial substrate concentration on sucrose consumption

Sucrose was used as a primary carbon and energy substrate for *B. megaterium* growth, maintenance and heparosan production. Experimental substrate consumption data was fitted using simplified substrate consumption expression (Eq. 5.6). Figure 5.1 depicts the experimental and simulated profiles of sucrose consumption. The fitting results were found to be satisfactory ($R^2 > 0.90$) and the kinetic parameter values were estimated (Table 5.1). A proportional rise in the specific substrate uptake rate of sucrose (q_S) (0.18 g/g. h to 0.74 g/g. h) with corresponding increase in S_o from 10 to 50 g/L. However, a proportional decrease in growth yield coefficient on substrate ($Y_{X/S}$) from 0.46 to 0.11 g/g and an approximately 6-fold rise in cellular maintenance energy (m_S) from 0.11 g/g. h to 0.69 g/g. h. These results indicated that the substrate flux is predominantly diverted towards maintenance energy rather than cell growth when increasing the S_o from 10 to 50 g/L. Maintenance energy in microbial cell is attributed to the influx and

Table 5.1: Estimated kinetic parameter values for *B. megaterium* growth, sucrose consumption and heparosan production at different initial sucrose concentrations

Kinetic parameter	Initial sucrose concentration (g/L)				
	10	20	30	40	50
Biomass formation					
X_m (g/L)	4.32	5.30	4.55	4.55	3.93
υ_X (g/L. h)	0.59	0.74	0.87	1.10	1.21
μ (h^{-1})	0.66	0.75	0.56	0.44	0.41
λ_X (h)	0.88	1.00	1.48	2.00	2.08
R^2	0.97	0.96	0.96	0.99	0.99
RMSE	0.08	0.15	0.13	0.02	0.02
Sucrose consumption					
S_o (g/L)	10.07	20.24	30.91	40.14	50.57
$Y_{X/S}$ (g/g)	0.46	0.31	0.21	0.17	0.11
m_S (g/g. h)	0.11	0.17	0.20	0.33	0.69
R^2	0.96	0.99	0.98	0.97	0.94
RMSE	0.66	0.12	1.41	3.44	12.11
Heparosan production					
H_m (g/L)	0.51	0.56	0.70	0.74	0.82
υ_H (g/L. h)	0.09	0.08	0.13	0.29	0.22
λ_H (h)	1.19	1.76	1.97	3.26	2.43
R^2	0.98	0.96	0.99	0.99	0.99
RMSE	0.50	1.56	0.66	0.11	0.10

efflux of nutrients and extracellular products, for motility, to replenish the damaged cellular components and to adjust the osmolarity inside the cell [29]. In addition, a proportional increase in residual sucrose concentration at the end of fermentation with increasing S_o suggested that substantial inhibitory effect on the specific growth rate of *B. megaterium*. The inhibition could be due to osmotic stress at high sucrose concentrations. The change in osmotic pressure could lead to the water efflux from cells and decreased turgor pressure. *Corynebacterium glutamicum* increased the maintenance energy to 30-fold when the osmotic pressure was increased in the medium during lysine fermentation [115].

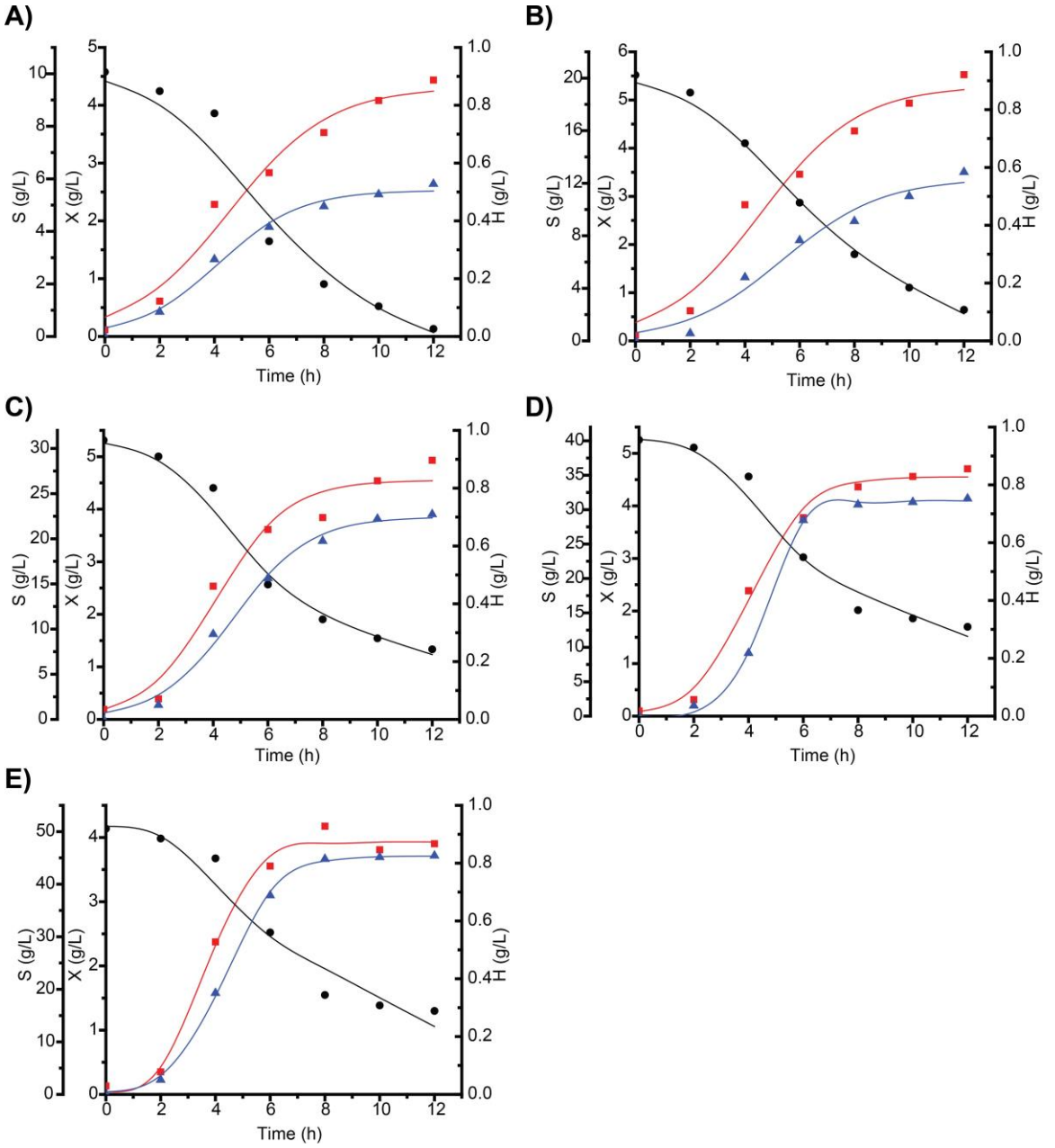

Figure 5.1: Profiles of cell growth (red square), sucrose utilization (black circle) and heparosan formation (Blue triangle) of experimental (points/symbols) and simulated (lines) data for batch fermentation experiments of *B. megaterium* under the influence of different initial sucrose concentrations. (A)10 g/L, (B) 20 g/L (C) 30 g/L (D) 40 g/L and (E) 50 g/L

5.3.3 Influence of initial substrate concentration on product formation

Heparosan production was observed only in the exponential phase Figure 5.1 of *B. megaterium* growth and minimal or no heparosan production was observed in the stationary phase [80, 81]. Heparosan production is growth associated in *B. megaterium*. Hence, the heparosan production kinetics was described using modified logistic equation (Eq. 5.7), similar to the growth kinetics. Experimental data was fitted to the model to determine the kinetic parameters. A proportional rise in the maximum heparosan production at the end of fermentation with respect to increase in S_o from 10 to 50 g/L was observed. The specific product formation rate (q_P) was increased from 0.01 to 0.02 g/g. h along with $Y_{P/X}$ from 0.12 to 0.21 g/g. However, residual sucrose concentration was increased with the change in S_o from 10 to 50 g/L. In addition, the lag time taken to produce heparosan was varied from 1.19 h to 3.26 h, which also substantiates the substrate inhibition on heparosan production. Considering the increase in the heparosan concentration, q_P, $Y_{P/X}$ and the substrate inhibition at higher sucrose concentration, S_o of 30 g/L was used for further experiments.

5.3.4 Effect of UDP-precursor sugar supplementation on heparosan production

Heparosan synthases catalyze the polymerization of UDP-GlcA and UDP-GlcNAc to synthesize heparosan in wild and recombinant strains [18, 20]. From the metabolic pathway perspective, heparosan synthesis pathway competes with glycolytic pathway and pentose phosphate pathway for the glycolytic intermediates. In addition, the intermediates such as glucose-1-phosphate and UDP-GlcNAc are also utilized for the cell wall and peptidoglycan biosynthesis. Diverting the carbon flux from competing metabolic pathways towards heparosan synthesis pathway would increase the heparosan production [124]. This can be achieved by the supplementation of UDP-GlcA and UDP-GlcNAc the fermentation medium. Supplementation of UDP-precursor sugars diminishes the metabolic burden towards central carbon metabolism. Varying levels of GlcA (0.1, 0.2, 0.4, 0.7 and 1.0 g/L) and GlcNAc (1, 2, 4, 7 and 10 g/L) were added to the medium in shake flasks at the time of inoculation (Figure 5.2). Different concentrations of GlcA supplementation did not improve the heparosan production significantly compared to

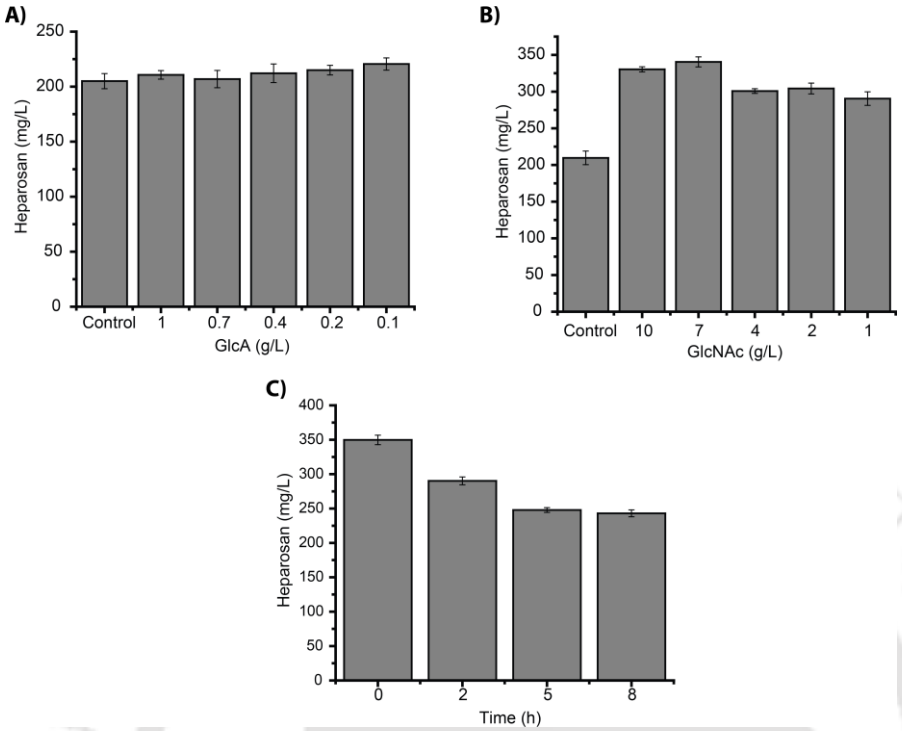

Figure 5.2: Optimization of (A) GlcA addition (B) GlcNAc addition and (C) time of GlcNAc addition in shake flask cultures of *B. megaterium*

control (Figure 5.2A). This could be due to the recombinant *B. megaterium* strain employed in this study is overexpressed with UDP-GlcA synthesis pathway enzymes [80]. These enzymes redirect the carbon flux from glycolytic pathway to UDP-GlcA synthesis pathway. Similarly, addition of 0.5 g/L GlcA did not increase the hyaluronic acid concentration in *Streptococcal* fermentation [45]. However, addition of 7 g/L GlcNAc resulted in the maximum concentration of 340.48 mg/L heparosan, which is 1.6-fold improvement compared to control (Figure 5.2B). GlcNAc concentration in fermentation broth was decreased over culture time, indicating that GlcNAc is metabolized by actively growing cells. Improvement in heparosan production could be attributed to the formation of UDP-GlcNAc through multitude of steps from GlcNAc. Further, GlcNAc was added to the medium at 0 h, 2 h, 5 h and 8 h to determine the optimal time of addition for enhanced heparosan production (Figure 5.2C). GlcNAc addition at 0 h gave the maximum heparosan concentration of 349.75 mg/L. This could be attributed to the adaptation of the strain to synthesize enzymes to metabolize GlcNAc from the inception of growth. GlcNAc addition during the growth of *B. megaterium* resulted in the gradual decrease of

heparosan production.

5.3.5 Dual substrate kinetic modelling

Based on previous optimization experiments, the optimal sucrose and GlcNAc concentration were determined to be 30 g/L and 7 g/L, respectively. Batch fermentation was performed to determine the influence of both substrates on cell growth and heparosan production. Figure 5.3 suggested that consumption of both sucrose and GlcNAc was in interactive manner, that is, both substrates were consumed simultaneously. In addition, cell growth was inhibited at high initial sucrose concentration (Figure 5.1). Hence, double Andrew's interactive multi substrate model was used to describe the kinetics of sucrose and GlcNAc for heparosan production. Previously, it was reported to describe multi substrate kinetics involving glucose and GlcNAc for hyaluronic acid production [76] and glucose and ammonium sulfate for rifamycin B synthesis [7]. Eq. 5.12 to Eq. 5.15 were adapted to express the cell growth, substrate consumption and heparosan production. Figure 5.3 depicts experimental and simulated profiles of cell growth, heparosan formation and substrate consumption. Estimated kinetic parameters were represented in Table 5.2. The maximum specific growth rate, μ_m was found to be 1.4 h^{-1} on dual substrates, which was relatively higher compared to the growth rate on single substrate. cell growth yield coefficient on GlcNAc (Y_{X/S_2} = 0.90) was approximately 2-fold higher than yield coefficient on sucrose (Y_{X/S_1} = 0.43). The increase in μ_m could be attributed to the growth support rendered by GlcNAc. Similarly, heparosan yield coefficient on GlcNAc (Y_{P/S_2} = 0.200) was approximately 2-fold higher than yield coefficient on sucrose (Y_{P/S_1} = 0.099), which indicated the primary contribution of GlcNAc in heparosan production and cell growth. Substrate affinity constant for sucrose (K_{S_1} = 2.65) and GlcNAc (K_{S_2} = 3.176) indicated the preferential utilization of sucrose compared to GlcNAc. The similar behavior can be observed from Figure 5.3. The inhibition constants were determined to be K_{I_1} = 47.29 g/L for sucrose and K_{I_2} = 91.58 g/L for GlcNAc. The maintenance coefficient on GlcNAc (m_{S2} = 0) was zero, which signified the diversion of GlcNAc flux towards cell growth and heparosan production. The maximum heparosan production rate was 0.44 h^{-1}. Good correlation between experimental and simulated data was evident from R^2 and RMSE values.

Table 5.2: Estimated kinetic parameter values for *B. megaterium* growth, sucrose and GlcNAc consumption and heparosan production under optimal conditions

Kinetic parameter	Predicted value
Biomass formation model	
μ_m (h^{-1})	1.425
K_{S_1} (g/L)	2.659
K_{I_1} (g/L)	47.295
K_{S_2} (g/L)	3.176
K_{I_2} (g/L)	91.585
SSE	7.848
RMSE	0.934
R^2	0.808
Sucrose consumption model	
Y_{X/S_1} (g/g)	0.429
Y_{P/S_1} (g/g)	0.099
m_{S1} (g/g. h)	0.003
SSE	7.510
RMSE	0.913
R^2	0.996
GlcNAc consumption model	
Y_{X/S_2} (g/g)	0.901
Y_{P/S_2} (g/g)	0.200
m_{S1} (g/g. h)	0.000
SSE	16.068
RMSE	1.284
R^2	0.945
Heparosan production model	
H_m (g/L)	0.443
K_{H_1} (g/L)	4.935
K_{HI_1} (g/L)	99.291
K_{H_2} (g/L)	7.382
K_{HI_2} (g/L)	41.202
SSE	0.247
RMSE	0.166
R^2	0.901

Table 5.3: Sensitivity ranking of the parameter for the different state variables of the developed model

Parameter	Reference value	Perturbation of parameters	Percentage of change in concentration				Rank of parameters based on sensitivity			
			Biomass	Sucrose	GlcNAc	Heparosan	Biomass	Sucrose	GlcNAc	Heparosan
μ_m	1.425	+10%	10.759	-3.415	-7.462	0.387	1	1	1	1
		-10%	-11.056	3.577	8.100	-0.667	1	1	1	1
K_{S^1}	2.659	+10%	-0.750	0.219	0.477	0.049	9	9	9	15
		-10%	0.759	-0.221	-0.483	-0.050	9	9	9	15
K_{I^1}	47.295	+10%	3.273	-1.113	-2.517	0.410	6	7	3	9
		-10%	-3.948	1.333	2.966	-0.453	6	7	3	10
K_{S^2}	3.176	-10%	-4.667	1.356	3.011	0.323	2	6	2	10
		+10%	5.020	-1.402	-3.026	-0.569	3	6	2	9
K_{I^2}	91.585	-10%	0.307	-0.118	-0.273	0.092	12	11	12	14
		+10%	-0.374	0.144	0.334	-0.113	12	11	11	14
Y_{X/S^1}	0.429	+10%	-0.287	2.665	0.099	0.131	13	2	14	12
		-10%	0.355	-3.276	-0.111	-0.176	13	2	14	12
Y_{P/S^1}	0.099	+10%	-0.278	2.366	0.103	0.117	14	4	13	13
		-10%	0.342	-2.882	-0.118	-0.155	14	3	13	13
m_{S^1}	0.003	-10%	0.001	-0.014	0.000	-0.001	16	15	16	16
		+10%	-0.001	0.014	0.000	0.001	16	16	16	16
Y_{X/S^2}	0.901	-10%	4.579	-2.523	1.751	4.391	3	3	5	3
		+10%	-5.100	2.775	-2.070	-4.752	2	4	4	3
Y_{P/S^2}	0.200	-10%	4.048	-2.261	1.662	4.002	4	5	6	4
		+10%	-4.625	2.536	-2.003	-4.383	4	5	5	4
m_{S^2}	-0.093	+10%	-1.700	0.882	-0.611	-1.418	8	8	8	6
		-10%	1.736	-0.903	0.608	1.453	8	8	8	6
H_m	0.443	-10%	-3.905	-0.201	-1.915	5.526	5	10	4	2
		+10%	4.150	0.217	1.953	-5.882	5	10	6	2
K_{H^1}	4.935	-10%	0.627	0.027	0.274	-0.865	10	14	11	7
		+10%	-0.643	-0.028	-0.288	0.890	11	14	12	8
K_{HI^1}	99.291	+10%	-0.578	-0.038	-0.311	0.849	11	13	10	8
		-10%	0.693	0.044	0.366	-1.012	10	13	10	7
K_{H^2}	7.382	-10%	2.644	0.111	1.148	-3.642	7	12	7	5
		+10%	-2.882	-0.123	-1.271	3.977	7	12	7	5
K_{HI^2}	41.2022	+10%	-0.001	-0.002	-0.001	0.221	15	16	15	11
		-10%	0.136	0.014	0.094	-0.219	15	15	15	11

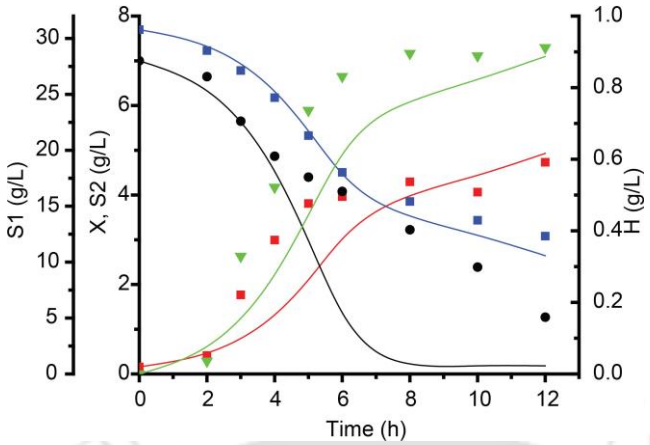

Figure 5.3: Profiles of cell growth (red square), sucrose (blue square) and GlcNAc (black circle) utilization and heparosan formation (green downward triangle) of experimental (points/symbols) and model predicted (lines) data for batch fermentation experiment of *B. megaterium* under the optimal conditions

Sensitivity analysis offers a systematic outline to study the accuracy and robustness of a mathematical model. The model predicted the experimental results within error value of 17.86 %, for the biomass, substrates and product. The sensitivity analysis revealed that the parameter μ_m showed the most sensitivity with respect to biomass and both substrates while the parameter H_m was found to be the most sensitive parameter with respect to the product concentration (Table 5.3). The knowledge from kinetic parameters would aid in developing optimal feeding strategy and also to develop soft sensor based monitoring and control of heparosan production.

5.4 Conclusion

The results clearly showed that the proposed unstructured mathematical model satisfactorily predicted the cell growth, substrate utilization, and heparosan production for the fermentation with an initial substrate concentration of 10–50 g/L. Supplementation of GlcNAc enhances the heparosan concentration by 1.6-fold. Double andrew's model was used to model the dual substrate system involving sucrose and GlcNAc and significance of the kinetic constants were explained. All the models tested not only adequately described the relationship between the principal state variables or quantitatively explained the behavior of a system, but could also be used for the design, optimal control of heparosan production process.

Table 5.4: Comparison of heparosan titer obtained in this work with published literature

Host/organism	Heparosan synthase source	Fermentation mode	Titer	Reference
E. coli BL21	*E. coli* K5 *kfiCADB*	Batch	652 mg/L	[133]
		Fed-batch	1.88 g/L	
E. coli BL21	*E. coli* K5 *kfiCADB*	Fed-batch	480 mg/L	[100]
E. coli BL21	*E. coli* K5 *kfiCADB*	Fed-batch	1.5 g/L	[60]
E. coli K12	*E. coli* K5 *kfiCADB*	Fed-batch	0.32 g/L	[8]
S. elongatus PCC 7942	*P. multocida pmHS2*	Photoautotropi mode	2.8 μg/L	[103]
B. subtilis 168	*E. coli* K5 *kfiCA*	Batch	2.65 g/L	[47]
		Fed-batch	5.82 g/L	
B. subtilis 168	*P. multocida pmHS1*	Shake flask	237.6 mg/L	[22]
B. megaterium MS941	*P. multocida pmHS2*	Shake flask	250 mg/L	[127]
		Fed-batch	2.74 g/L	
B. megaterium DSM319	*E. coli* K5 *kfiCA*	Batch	911 mg/L	This work
		Fed-batch	1.96 mg/L	

CHAPTER 6

CONCLUSIONS AND FUTURE DIRECTIONS

This thesis successfully addressed a safe and alternative approach to synthesize heparosan in *B. megaterium* employing *E. coli* K5 glycosyltransferases. Heterologous expression of *E. coli kfiC* and *kfiA* enabled the heparosan synthesis pathway in *B. megaterium*. Overexpression of UDP-GlcA and UDP-GlcNAc synthesis pathway genes (*tuaD*, *gtaB*, *gcaD* and *glmM*) enhanced the heparosan production, suggesting that UDP-GlcA and UDP-GlcNAc concentration were limiting the heparosan production in *B. megaterium*. Batch fermentation of UDP-GlcA synthesis pathway overexpressed *B. megaterium* strain (CA-DB) produced the maximum heparosan concentration of 394 mg/L in batch fermentation. Heparosan was purified and the structure was determined using NMR analysis. Polycistronic expression of *kfiC* and *kfiA* under xylose-inducible promoter suggested the imbalanced expression of KfiC and KfiA proteins. Dual promoter plasmid system expressing *kfiC* and *kfiA* was constructed to overcome the bottlenecks associated with expression of KfiC and KfiA proteins. Dual promoter expression system enhanced the heparosan production (627 mg/L) compared to polycistronic expression system. Concerted endeavors for optimizing the KfiC and KfiA expression, redirecting the carbon flux towards UDP-precursor synthesis pathway and optimizing the medium and fermentation strategies would further enhance the heparosan production. Briefly, codon optimization of *E. coli* K5 *kfiC* and *kfiA* for the expression in *B. megaterium*, down-regulation of key glycolysis pathway genes could divert the carbon flux towards heparosan synthesis pathway. The development of an optimal fermentation medium using design of experiments

and efficient bioprocess strategies such as repeated batch and fed-batch fermentation could improve the heparosan production. Further, kinetic modeling of *B. megaterium* fermentation on single substrate and multi-substrate clearly explained the relationship between the principal state variables and kinetic parameters. Lastly, the knowledge from kinetic parameters would aid in developing optimal feeding strategy for high cell density cultivation and also to develop soft sensor based real-time monitoring and control of heparosan production using recombinant *B. megaterium*.

BIBLIOGRAPHY

[1] S. Aiba, M. Shoda, and M. Nagatani. Kinetics of product inhibition in alcohol fermentation. Reprinted from Biotechnology and Bioengineering, Vol. X, Issue 6, Pages 845-864 (1968). *Biotechnology and bioengineering*, 67:671–90, Mar 2000.

[2] J. Almquist, M. Cvijovic, V. Hatzimanikatis, J. Nielsen, and M. Jirstrand. Kinetic models in industrial biotechnology - Improving cell factory performance. *Metabolic engineering*, 24:38–60, Jul 2014.

[3] J. F. Andrews. A mathematical model for the continuous culture of microorganisms utilizing inhibitory substrates. *Biotechnology and Bioengineering*, 10(6):707–723, 1968.

[4] C. Arrecubieta, T. C. Hammarton, B. Barrett, S. Chareonsudjai, N. Hodson, D. Rainey, and I. S. Roberts. The transport of group 2 capsular polysaccharides across the periplasmic space in *Escherichia coli*. roles for the KpsE and KpsD proteins. *The Journal of biological chemistry*, 276:4245–50, Feb 2001.

[5] C. Ash, J. Farrow, S. Wallbanks, and M. Collins. Phylogenetic heterogeneity of the genus *Bacillus* revealed by comparative analysis of small-subunit-ribosomal RNA sequences. *Letters in Applied Microbiology*, 13:202–206, 1991.

[6] A. Badri, A. Williams, R. J. Linhardt, and M. A. Koffas. The road to animal-free glycosaminoglycan production: current efforts and bottlenecks. *Current opinion in biotechnology*, 53:85–92, Oct 2018.

[7] P. M. Bapat, S. Bhartiya, K. V. Venkatesh, and P. P. Wangikar. Structured kinetic model to represent the utilization of multiple substrates in complex media during rifamycin B fermentation. *Biotechnology and bioengineering*, 93:779–90, Mar 2006.

[8] H. Barreteau, E. Richard, S. Drouillard, E. Samain, and B. Priem. Production of intracellular heparosan and derived oligosaccharides by lyase expression in metabolically engineered *E. coli* K-12. *Carbohydrate research*, 360:19–24, Oct 2012.

[9] O. Benkortbi, S. Hanini, and F. Bentahar. Batch kinetics and modelling of Pleuromutilin production by *Pleurotus mutilis*. *Biochemical Engineering Journal*, 36(1): 14–18, 2007.

[10] A. Berlec, K. Škrlec, J. Kocjan, M. Olenic, and B. Štrukelj. Single plasmid systems for inducible dual protein expression and for CRISPR-Cas9/CRISPRi gene regulation in lactic acid bacterium *Lactococcus lactis*. *Scientific reports*, 8:1009, Jan 2018.

[11] H. Beyenal, S. N. Chen, and Z. Lewandowski. The double substrate growth kinetics of *Pseudomonas aeruginosa*. *Enzyme and Microbial Technology*, 32(1):92–98, 2003.

[12] R. Biedendieck, M. Gamer, L. Jaensch, S. Meyer, M. Rohde, W.-D. Deckwer, and D. Jahn. A sucrose-inducible promoter system for the intra- and extracellular protein production in *Bacillus megaterium*. *Journal of biotechnology*, 132:426–30, Dec 2007.

[13] R. Biedendieck, M. Malten, H. Barg, B. Bunk, J.-H. Martens, E. Deery, H. Leech, M. J. Warren, and D. Jahn. Metabolic engineering of cobalamin (vitamin B12) production in *Bacillus megaterium*. *Microbial biotechnology*, 3:24–37, Jan 2010.

[14] T. Bitter and H. M. Muir. A modified uronic acid carbazole reaction. *Analytical biochemistry*, 4:330–4, Oct 1962.

[15] S. Burger, H. Tatge, F. Hofmann, H. Genth, I. Just, and R. Gerhard. Expression of recombinant *Clostridium difficile* toxin A using the *Bacillus megaterium* system. *Biochemical and biophysical research communications*, 307:584–8, Aug 2003.

[16] C.-H. Chang, L. S. Lico, T.-Y. Huang, S.-Y. Lin, C.-L. Chang, S. D. Arco, and S.-C. Hung. Synthesis of the heparin-based anticoagulant drug fondaparinux. *Angewandte Chemie (International ed. in English)*, 53:9876–9, Sep 2014.

[17] D. Charalampopoulos, J. A. Vázquez, and S. S. Pandiella. Modelling and validation of *Lactobacillus plantarum* fermentations in cereal-based media with different sugar concentrations and buffering capacities. *Biochemical Engineering Journal*, 44(2):96–105, 2009.

[18] A. A. E. Chavaroche, J. Springer, F. Kooy, C. Boeriu, and G. Eggink. In vitro synthesis of heparosan using recombinant *Pasteurella multocida* heparosan synthase PmHS2. *Applied microbiology and biotechnology*, 85:1881–91, Feb 2010.

[19] A. A. E. Chavaroche, L. A. M. van den Broek, C. Boeriu, and G. Eggink. Synthesis of heparosan oligosaccharides by *Pasteurella multocida* PmHS2 single-action transferases. *Applied microbiology and biotechnology*, 95:1199–210, Sep 2012.

[20] A. A. E. Chavaroche, L. A. M. van den Broek, and G. Eggink. Production methods for heparosan, a precursor of heparin and heparan sulfate. *Carbohydrate polymers*, 93:38–47, Mar 2013.

[21] J.-X. Chen, W. Liu, M. Zhang, and J.-H. Chen. Heparosan based negatively charged nanocarrier for rapid intracellular drug delivery. *International journal of pharmaceutics*, 473:493–500, Oct 2014.

[22] X. Chen, R. Chen, X. Yu, D. Tang, W. Yao, and X. Gao. Metabolic engineering of *Bacillus subtilis* for biosynthesis of heparosan using heparosan synthase from *Pasteurella multocida*, PmHS1. *Bioprocess and biosystems engineering*, 40:675–681, May 2017.

[23] B. Conrad, R. S. Savchenko, R. Breves, and J. Hofemeister. A T7 promoter-specific, inducible protein expression system for *Bacillus subtilis*. *Molecular & general genetics : MGG*, 250:230–6, Feb 1996.

[24] B. F. Cress, J. A. Englaender, W. He, D. Kasper, R. J. Linhardt, and M. A. G. Koffas. Masquerading microbial pathogens: capsular polysaccharides mimic host-tissue molecules. *FEMS microbiology reviews*, 38:660–97, Jul 2014.

[25] A. De Bary. *Vergleichende morphologie und biologie der pilze, mycetozoen und bacterien*. Engelmann, 1884.

[26] P. L. DeAngelis. Heparosan, a promising 'naturally good' polymeric conjugating vehicle for delivery of injectable therapeutics. In *Expert opinion on drug delivery*, volume 12, pages 349–52, Mar 2015.

[27] P. L. DeAngelis and C. L. White. Identification and molecular cloning of a heparosan synthase from *Pasteurella multocida* type D. *The Journal of biological chemistry*, 277:7209–13, Mar 2002.

[28] P. L. Deangelis and C. L. White. Identification of a distinct, cryptic heparosan synthase from *Pasteurella multocida* types A, D, and F. *Journal of bacteriology*, 186:8529–32, Dec 2004.

[29] M. M. Don and N. F. Shoparwe. Kinetics of hyaluronic acid production by *Streptococcus zooepidemicus* considering the effect of glucose. *Biochemical Engineering Journal*, 49(1):95–103, 2010.

[30] M. Eppinger, B. Bunk, M. A. Johns, J. N. Edirisinghe, K. K. Kutumbaka, S. S. K. Koenig, H. H. Creasy, M. J. Rosovitz, D. R. Riley, S. Daugherty, M. Martin, L. D. H. Elbourne, I. Paulsen, R. Biedendieck, C. Braun, S. Grayburn, S. Dhingra, V. Lukyanchuk, B. Ball, R. Ul-Qamar, J. Seibel, E. Bremer, D. Jahn, J. Ravel, and

P. S. Vary. Genome sequences of the biotechnologically important *Bacillus megaterium* strains QM B1551 and DSM319. *Journal of bacteriology*, 193:4199–213, Aug 2011.

[31] C. J. Gadgil and K. V. Venkatesh. Structured model for batch culture growth of *Lactobacillus bulgaricus*. *Journal of Chemical Technology & Biotechnology*, 68(1): 89–93, 1997.

[32] M. Gamer, D. Fröde, R. Biedendieck, S. Stammen, and D. Jahn. A T7 RNA polymerase-dependent gene expression system for *Bacillus megaterium*. *Applied microbiology and biotechnology*, 82:1195–203, Apr 2009.

[33] D. G. Gibson, L. Young, R.-Y. Chuang, J. C. Venter, C. A. r. Hutchison, and H. O. Smith. Enzymatic assembly of DNA molecules up to several hundred kilobases. *Nature methods*, 6:343–5, May 2009.

[34] R. Glaser and J. Venus. Model-based characterisation of growth performance and l-lactic acid production with high optical purity by thermophilic *Bacillus coagulans* in a lignin-supplemented mixed substrate medium. *New biotechnology*, 37:180–193, Jul 2017.

[35] K. Grage, P. McDermott, and B. H. A. Rehm. Engineering *Bacillus megaterium* for production of functional intracellular materials. *Microbial cell factories*, 16:211, Nov 2017.

[36] G. Griffiths, B. Barrett, N. Cook, and I. S. Roberts. Biosynthesis of the *Escherichia coli* K5 capsular polysaccharide. *Biochemical Society transactions*, 27:507–12, Aug 1999.

[37] M. Guerrini, D. Beccati, Z. Shriver, A. Naggi, K. Viswanathan, A. Bisio, I. Capila, J. C. Lansing, S. Guglieri, B. Fraser, A. Al-Hakim, N. S. Gunay, Z. Zhang, L. Robinson, L. Buhse, M. Nasr, J. Woodcock, R. Langer, G. Venkataraman, R. J. Linhardt, B. Casu, G. Torri, and R. Sasisekharan. Oversulfated chondroitin sulfate is a contaminant in heparin associated with adverse clinical events. *Nature biotechnology*, 26:669–75, Jun 2008.

[38] D. Gärtner, M. Geissendörfer, and W. Hillen. Expression of the *Bacillus subtilis* xyl operon is repressed at the level of transcription and is induced by xylose. *Journal of bacteriology*, 170:3102–9, Jul 1988.

[39] J. S. He and A. J. Fulco. A barbiturate-regulated protein binding to a common sequence in the cytochrome P450 genes of rodents and bacteria. *The Journal of biological chemistry*, 266:7864–9, Apr 1991.

[40] W. He, L. Fu, G. Li, J. Andrew Jones, R. J. Linhardt, and M. Koffas. Production of chondroitin in metabolically engineered *E. coli*. *Metabolic engineering*, 27:92–100, Jan 2015.

[41] A. M. Hickey, U. Bhaskar, R. J. Linhardt, and J. S. Dordick. Effect of eliminase gene (*elmA*) deletion on heparosan production and shedding in *Escherichia coli* K5. *Journal of biotechnology*, 165:175–7, Jun 2013.

[42] N. Hodson, G. Griffiths, N. Cook, M. Pourhossein, E. Gottfridson, T. Lind, K. Lidholt, and I. S. Roberts. Identification that KfiA, a protein essential for the biosynthesis of the *Escherichia coli* K5 capsular polysaccharide, is an alpha -UDP-GlcNAc glycosyltransferase. the formation of a membrane-associated K5 biosynthetic complex requires KfiA, KfiB, and KfiC. *The Journal of biological chemistry*, 275: 27311–5, Sep 2000.

[43] H. Huang, X. Liu, S. Lv, W. Zhong, F. Zhang, and R. J. Linhardt. Recombinant *Escherichia coli* K5 strain with the deletion of waaR gene decreases the molecular weight of the heparosan capsular polysaccharide. *Applied microbiology and biotechnology*, 100:7877–85, Sep 2016.

[44] T. Izumikawa, N. Egusa, F. Taniguchi, K. Sugahara, and H. Kitagawa. Heparan sulfate polymerization in Drosophila. *The Journal of biological chemistry*, 281: 1929–34, Jan 2006.

[45] S. Jagannath and K. Ramachandran. Influence of competing metabolic processes on the molecular weight of hyaluronic acid synthesized by *Streptococcus zooepidemicus*. *Biochemical Engineering Journal*, 48(2):148–158, 2010.

[46] P. Jin, Z. Kang, P. Yuan, G. Du, and J. Chen. Production of specific-molecular-weight hyaluronan by metabolically engineered *Bacillus subtilis* 168. *Metabolic engineering*, 35:21–30, May 2016.

[47] P. Jin, L. Zhang, P. Yuan, Z. Kang, G. Du, and J. Chen. Efficient biosynthesis of polysaccharides chondroitin and heparosan by metabolically engineered *Bacillus subtilis*. *Carbohydrate polymers*, 140:424–32, Apr 2016.

[48] W. Jing, J. W. Roberts, D. E. Green, A. Almond, and P. L. DeAngelis. Synthesis and characterization of heparosan-granulocyte-colony stimulating factor conjugates: a natural sugar-based drug delivery system to treat neutropenia. *Glycobiology*, 27: 1052–1061, Nov 2017.

[49] E. Jordan, L. Al-Halabi, T. Schirrmann, M. Hust, and S. Dübel. Production of single chain Fab (scFab) fragments in *Bacillus megaterium*. *Microbial cell factories*, 6:38,

Nov 2007.

[50] E. Jordan, M. Hust, A. Roth, R. Biedendieck, T. Schirrmann, D. Jahn, and S. Dübel. Production of recombinant antibody fragments in *Bacillus megaterium*. *Microbial cell factories*, 6:2, Jan 2007.

[51] P. Kanjanachumpol, S. Kulpreecha, V. Tolieng, and N. Thongchul. Enhancing polyhydroxybutyrate production from high cell density fed-batch fermentation of *Bacillus megaterium* BA-019. *Bioprocess and biosystems engineering*, 36:1463–74, Oct 2013.

[52] G. Kedia, J. A. Vázquez, and S. S. Pandiella. Evaluation of the fermentability of oat fractions obtained by debranning using lactic acid bacteria. *Journal of applied microbiology*, 105:1227–37, Oct 2008.

[53] K.-J. Kim, H.-E. Kim, K.-H. Lee, W. Han, M.-J. Yi, J. Jeong, and B.-H. Oh. Two-promoter vector is highly efficient for overproduction of protein complexes. *Protein science : a publication of the Protein Society*, 13:1698–703, Jun 2004.

[54] C. Korneli, R. Biedendieck, F. David, D. Jahn, and C. Wittmann. High yield production of extracellular recombinant levansucrase by *Bacillus megaterium*. *Applied microbiology and biotechnology*, 97:3343–53, Apr 2013.

[55] B. Kuberan, M. Z. Lech, D. L. Beeler, Z. L. Wu, and R. D. Rosenberg. Enzymatic synthesis of antithrombin III-binding heparan sulfate pentasaccharide. *Nature biotechnology*, 21:1343–6, Nov 2003.

[56] S. Kulpreecha, A. Boonruangthavorn, B. Meksiriporn, and N. Thongchul. Inexpensive fed-batch cultivation for high poly(3-hydroxybutyrate) production by a new isolate of *Bacillus megaterium*. *Journal of bioscience and bioengineering*, 107: 240–5, Mar 2009.

[57] S. Kühn and P. Fortnagel. Molecular cloning and nucleotide sequence of the gene encoding a calcium-dependent exoproteinase from *Bacillus megaterium* ATCC 14581. *Journal of general microbiology*, 139:39–47, Jan 1993.

[58] R. S. Lane, F. M. Haller, A. A. E. Chavaroche, A. Almond, and P. L. DeAngelis. Heparosan-coated liposomes for drug delivery. *Glycobiology*, 27:1062–1074, Nov 2017.

[59] R. Legoux, P. Lelong, C. Jourde, C. Feuillerat, J. Capdevielle, V. Sure, E. Ferran, M. Kaghad, B. Delpech, D. Shire, P. Ferrara, G. Loison, and M. Salome. N-acetylheparosan lyase of *Escherichia coli* K5: gene cloning and expression. *Journal of bacteriology*, 178:7260–4, Dec 1996.

[60] M. Leroux and B. Priem. Chaperone-assisted expression of KfiC glucuronyltransferase from *Escherichia coli* K5 leads to heparosan production in *Escherichia coli* BL21 in absence of the stabilisator KfiB. *Applied microbiology and biotechnology*, 100:10355–10361, Dec 2016.

[61] K. Lidholt, J. Riesenfeld, K. G. Jacobsson, D. S. Feingold, and U. Lindahl. Biosynthesis of heparin. Modulation of polysaccharide chain length in a cell-free system. *The Biochemical journal*, 254:571–8, Sep 1988.

[62] R. J. Linhardt. 2003 Claude S. Hudson Award address in carbohydrate chemistry. Heparin: structure and activity. *Journal of medicinal chemistry*, 46:2551–64, Jun 2003.

[63] H. Liu, Z. Zhang, and R. J. Linhardt. Lessons learned from the contamination of heparin. *Natural product reports*, 26:313–21, Mar 2009.

[64] Y. Liu, L. Liu, J. Chen, J. Li, G. Du, and J. Chen. Effects of carbon sources and feeding strategies on heparosan production by *Escherichia coli* K5. *Bioprocess and biosystems engineering*, 35:1209–18, Sep 2012.

[65] H. M. Lo, T. A. Kurniawan, M. E. T. Sillanpää, T. Y. Pai, C. F. Chiang, K. P. Chao, M. H. Liu, S. H. Chuang, C. J. Banks, S. C. Wang, K. C. Lin, C. Y. Lin, W. F. Liu, P. H. Cheng, C. K. Chen, H. Y. Chiu, and H. Y. Wu. Modeling biogas production from organic fraction of MSW co-digested with MSWI ashes in anaerobic bioreactors. *Bioresource technology*, 101:6329–35, Aug 2010.

[66] R. Luedeking and E. L. Piret. A kinetic study of the lactic acid fermentation. Batch process at controlled pH. Reprinted from Journal of Biochemical and Microbiological Technology Engineering Vol. I, No. 4. Pages 393-412 (1959). *Biotechnology and bioengineering*, 67:636–44, Mar 2000.

[67] M. Ly, Z. Wang, T. N. Laremore, F. Zhang, W. Zhong, D. Pu, D. V. Zagorevski, J. S. Dordick, and R. J. Linhardt. Analysis of *E. coli* K5 capsular polysaccharide heparosan. *Analytical and bioanalytical chemistry*, 399:737–45, Jan 2011.

[68] M. Malten, R. Hollmann, W.-D. Deckwer, and D. Jahn. Production and secretion of recombinant *Leuconostoc mesenteroides* dextransucrase DsrS in *Bacillus megaterium*. *Biotechnology and bioengineering*, 89:206–18, Jan 2005.

[69] M. Manzoni, S. Bergomi, and V. Cavazzoni. Production of K5 polysaccharides of different molecular weight by *Escherichia coli*. *Journal of bioactive and compatible polymers*, 11(4):301–311, 1996.

[70] M. Manzoni, S. Bergomi, and M. Rollini. Influence of the culture conditions on

extracellular lyase activity related to K5 polysaccharide. *Biotechnology letters*, 22 (1):81–85, 2000.

[71] L. Martín, M. A. Prieto, E. Cortés, and J. L. García. Cloning and sequencing of the *pac* gene encoding the penicillin G acylase of *Bacillus megaterium* ATCC 14945. *FEMS microbiology letters*, 125:287–92, Jan 1995.

[72] G. J. McCool and M. C. Cannon. PhaC and PhaR are required for polyhydroxyalkanoic acid synthase activity in *Bacillus megaterium*. *Journal of bacteriology*, 183: 4235–43, Jul 2001.

[73] F. Meinhardt, U. Stahl, and W. Ebeling. Highly efficient expression of homologous and heterologous genes in *Bacillus megaterium*. *Applied microbiology and biotechnology*, 30(4):343–350, 1989.

[74] F. Meinhardt, M. Busskamp, and K. D. Wittchen. Cloning and sequencing of the leuC and nprM genes and a putative spoIV gene from *Bacillus megaterium* DSM319. *Applied microbiology and biotechnology*, 41:344–51, May 1994.

[75] R. J. Metz, L. N. Allen, T. M. Cao, and N. W. Zeman. Nucleotide sequence of an amylase gene from *Bacillus megaterium*. *Nucleic acids research*, 16:5203, Jun 1988.

[76] N. Mohan, S. R. R. Tadi, S. S. Pavan, and S. Sivaprakasam. Deciphering the role of dissolved oxygen and N-acetyl glucosamine in governing higher molecular weight hyaluronic acid synthesis in *Streptococcus zooepidemicus* cell factory. *Applied microbiology and biotechnology*, 104:3349–3365, Apr 2020.

[77] M. Morita, K. Tomita, M. Ishizawa, K. Takagi, F. Kawamura, H. Takahashi, and T. Morino. Cloning of oxetanocin A biosynthetic and resistance genes that reside on a plasmid of *Bacillus megaterium* strain NK84-0128. *Bioscience, biotechnology, and biochemistry*, 63:563–6, Mar 1999.

[78] L. Na, H. Yu, J. B. McArthur, T. Ghosh, T. Asbell, and X. Chen. Engineer *P. multocida* heparosan synthase 2 (PmHS2) for size-controlled synthesis of longer heparosan oligosaccharides. *ACS catalysis*, 10(11):6113–6118, 2020.

[79] T. Nagao, T. Mitamura, X. H. Wang, S. Negoro, T. Yomo, I. Urabe, and H. Okada. Cloning, nucleotide sequences, and enzymatic properties of glucose dehydrogenase isozymes from *Bacillus megaterium* IAM1030. *Journal of bacteriology*, 174:5013–20, Aug 1992.

[80] G. Nehru, S. R. R. Tadi, A. M. Limaye, and S. Sivaprakasam. Production and characterization of low molecular weight heparosan in *Bacillus megaterium* us-

ing *Escherichia coli* K5 glycosyltransferases. *International journal of biological macromolecules*, 160:69–76, Oct 2020.

[81] G. Nehru, S. R. R. Tadi, and S. Sivaprakasam. Application of dual promoter expression system for the enhanced heparosan production in *Bacillus megaterium*. *Applied biochemistry and biotechnology*, Mar 2021.

[82] J. Nielsen and J. Villadsen. Modelling of microbial kinetics. *Chemical Engineering Science*, 47(17):4225–4270, 1992.

[83] J. Nielsen, J. Villadsen, and G. Lidén. *Modeling of Growth Kinetics*, pages 235–314. Springer US, Boston, MA, 2003.

[84] W. Panbangred, K. Weeradechapon, S. Udomvaraphant, K. Fujiyama, and V. Meevootisom. High expression of the penicillin G acylase gene (pac) from *Bacillus megaterium* UN1 in its own pac minus mutant. *Journal of applied microbiology*, 89:152–7, Jul 2000.

[85] K. K. Pandit and J. E. Smith. Capsular hyaluronic acid in *Pasteurella multocida* type A and its counterpart in type D. *Research in veterinary science*, 54:20–4, Jan 1993.

[86] A. Pelletier and J. Sygusch. Purification and characterization of three chitosanase activities from *Bacillus megaterium* P1. *Applied and environmental microbiology*, 56:844–8, Apr 1990.

[87] C. Petit, G. P. Rigg, C. Pazzani, A. Smith, V. Sieberth, M. Stevens, G. Boulnois, K. Jann, and I. S. Roberts. Region 2 of the *Escherichia coli* K5 capsule gene cluster encoding proteins for the biosynthesis of the K5 polysaccharide. *Molecular microbiology*, 17:611–20, Aug 1995.

[88] S. B. Prasad, G. Jayaraman, and K. B. Ramachandran. Hyaluronic acid production is enhanced by the additional co-expression of UDP-glucose pyrophosphorylase in *Lactococcus lactis*. *Applied microbiology and biotechnology*, 86:273–83, Mar 2010.

[89] S. Radha and P. Gunasekaran. Cloning and expression of keratinase gene in *Bacillus megaterium* and optimization of fermentation conditions for the production of keratinase by recombinant strain. *Journal of applied microbiology*, 103:1301–10, Oct 2007.

[90] S. Radha and P. Gunasekaran. Sustained expression of keratinase gene under PxylA and PamyL promoters in the recombinant *Bacillus megaterium* MS941. *Bioresource technology*, 99:5528–37, Sep 2008.

[91] S. Rami Reddy Tadi, S. Dutt Ravindran, R. Balakrishnan, and S. Sivaprakasam.

Recombinant production of poly-(3-hydroxybutyrate) by *Bacillus megaterium* utilizing millet bran and rapeseed meal hydrolysates. *Bioresource technology*, 326: 124800, Apr 2021.

[92] E. Raux, A. Lanois, M. J. Warren, A. Rambach, and C. Thermes. Cobalamin (vitamin B12) biosynthesis: identification and characterization of a *Bacillus megaterium cobI* operon. *The Biochemical journal*, 335 (Pt 1):159–66, Oct 1998.

[93] G. P. Rigg, B. Barrett, and I. S. Roberts. The localization of KpsC, S and T, and KfiA, C and D proteins involved in the biosynthesis of the *Escherichia coli* K5 capsular polysaccharide: evidence for a membrane-bound complex. *Microbiology (Reading, England)*, 144:2905–14, Oct 1998.

[94] R. B. Rimler. Presumptive identification of *Pasteurella multocida* serogroups A, D and F by capsule depolymerisation with mucopolysaccharidases. *The Veterinary record*, 134:191–2, Feb 1994.

[95] M. Rippe, T. F. Stefanello, V. Kaplum, E. A. Britta, F. P. Garcia, R. Poirot, M. V. P. Companhoni, C. V. Nakamura, A. Szarpak-Jankowska, and R. Auzely-Velty. Heparosan as a potential alternative to hyaluronic acid for the design of biopolymer-based nanovectors for anticancer therapy. *Biomaterials science*, 7:2850–2860, Jul 2019.

[96] S. G. Rohit, P. K. Jyoti, R. R. T. Subbi, M. Naresh, and S. Senthilkumar. Kinetic modeling of hyaluronic acid production in palmyra palm (*Borassus flabellifer*) based medium by *Streptococcus zooepidemicus* MTCC 3523. *Biochemical Engineering Journal*, 137:284–293, 2018.

[97] E. Roman, I. Roberts, K. Lidholt, and M. Kusche-Gullberg. Overexpression of UDP-glucose dehydrogenase in *Escherichia coli* results in decreased biosynthesis of K5 polysaccharide. *The Biochemical journal*, 374:767–72, Sep 2003.

[98] C. Rosenow, F. Esumeh, I. S. Roberts, and K. Jann. Characterization and localization of the KpsE protein of *Escherichia coli* K5, which is involved in polysaccharide export. *Journal of bacteriology*, 177:1137–43, Mar 1995.

[99] C. Rosenow, I. S. Roberts, and K. Jann. Isolation from recombinant *Escherichia coli* and characterization of CMP-kdo synthetase, involved in the expression of the capsular K5 polysaccharide (K-CKS). *FEMS microbiology letters*, 125:159–64, Jan 1995.

[100] A. Roy, Y. Miyai, A. Rossi, K. Paraswar, U. R. Desai, Y. Saijoh, and B. Kuberan. Metabolic engineering of non-pathogenic *Escherichia coli* strains for the controlled

production of low molecular weight heparosan and size-specific heparosan oligosaccharides. *Biochimica et biophysica acta. General subjects*, 1865:129765, Jan 2021.

[101] T. Rygus and W. Hillen. Inducible high-level expression of heterologous genes in *Bacillus megaterium* using the regulatory elements of the xylose-utilization operon. *Applied microbiology and biotechnology*, 35:594–9, Aug 1991.

[102] T. Rygus, A. Scheler, R. Allmansberger, and W. Hillen. Molecular cloning, structure, promoters and regulatory elements for transcription of the *Bacillus megaterium* encoded regulon for xylose utilization. *Archives of microbiology*, 155:535–42, 1991.

[103] A. Sarnaik, M. H. Abernathy, X. Han, Y. Ouyang, K. Xia, Y. Chen, B. Cress, F. Zhang, A. Lali, R. Pandit, et al. Metabolic engineering of cyanobacteria for photoautotrophic production of heparosan, a pharmaceutical precursor of heparin. *Algal Research*, 37:57–63, 2019.

[104] C. Senay, T. Lind, K. Muguruma, Y. Tone, H. Kitagawa, K. Sugahara, K. Lidholt, U. Lindahl, and M. Kusche-Gullberg. The EXT1/EXT2 tumor suppressors: catalytic activities and role in heparan sulfate biosynthesis. *EMBO reports*, 1:282–6, Sep 2000.

[105] V. Sieberth, G. P. Rigg, I. S. Roberts, and K. Jann. Expression and characterization of UDPGlc dehydrogenase (KfiD), which is encoded in the type-specific region 2 of the *Escherichia coli* K5 capsule genes. *Journal of bacteriology*, 177:4562–5, Aug 1995.

[106] A. E. Sismey-Ragatz, D. E. Green, N. J. Otto, M. Rejzek, R. A. Field, and P. L. DeAngelis. Chemoenzymatic synthesis with distinct *Pasteurella* heparosan synthases: monodisperse polymers and unnatural structures. *The Journal of biological chemistry*, 282:28321–7, Sep 2007.

[107] A. P. Spicer, L. A. Kaback, T. J. Smith, and M. F. Seldin. Molecular cloning and characterization of the human and mouse UDP-glucose dehydrogenase genes. *The Journal of biological chemistry*, 273:25117–24, Sep 1998.

[108] N. Sugiura, Y. Baba, Y. Kawaguchi, T. Iwatani, K. Suzuki, T. Kusakabe, K. Yamagishi, K. Kimata, Y. Kakuta, and H. Watanabe. Glucuronyltransferase activity of KfiC from *Escherichia coli* strain K5 requires association of KfiA: KfiC and KfiA are essential enzymes for production of K5 polysaccharide, N-acetylheparosan. *The Journal of biological chemistry*, 285:1597–606, Jan 2010.

[109] S. Tabor and C. C. Richardson. A bacteriophage T7 RNA polymerase/promoter system for controlled exclusive expression of specific genes. *Proceedings of the*

National Academy of Sciences of the United States of America, 82:1074–8, Feb 1985.

[110] Y. Takasaki. Novel maltose-producing amylase from *Bacillus megaterium* G-2. *Agricultural and biological chemistry*, 53(2):341–347, 1989.

[111] C. M. Taylor, M. Goldrick, L. Lord, and I. S. Roberts. Mutations in the waaR gene of *Escherichia coli* which disrupt lipopolysaccharide outer core biosynthesis affect cell surface retention of group 2 capsular polysaccharides. *Journal of bacteriology*, 188:1165–8, Feb 2006.

[112] C. K. Tseng, V. E. Marquez, G. W. Milne, R. J. J. Wysocki, H. Mitsuya, T. Shirasaki, and J. S. Driscoll. A ring-enlarged oxetanocin A analogue as an inhibitor of HIV infectivity. *Journal of medicinal chemistry*, 34:343–9, Jan 1991.

[113] J.-Y. van der Meer, E. Kellenbach, and L. J. van den Bos. From Farm to Pharma: An overview of industrial heparin manufacturing methods. *Molecules (Basel, Switzerland)*, 22, Jun 2017.

[114] W. F. Vann, M. A. Schmidt, B. Jann, and K. Jann. The structure of the capsular polysaccharide (K5 antigen) of urinary-tract-infective *Escherichia coli* O10:K5:H4. A polymer similar to desulfo-heparin. *European journal of biochemistry*, 116: 359–64, May 1981.

[115] C. A. Varela, M. E. Baez, and E. Agosin. Osmotic stress response: quantification of cell maintenance and metabolic fluxes in a lysine-overproducing strain of *Corynebacterium glutamicum*. *Applied and environmental microbiology*, 70: 4222–9, Jul 2004.

[116] P. S. Vary, R. Biedendieck, T. Fuerch, F. Meinhardt, M. Rohde, W.-D. Deckwer, and D. Jahn. *Bacillus megaterium*–from simple soil bacterium to industrial protein production host. *Applied microbiology and biotechnology*, 76:957–67, Oct 2007.

[117] M. A. Von Tersch and B. C. Carlton. Megacinogenic plasmids of *Bacillus megaterium*. *Journal of bacteriology*, 155:872–7, Aug 1983.

[118] M. A. Von Tersch and H. L. Robbins. Efficient cloning in *Bacillus megaterium*: comparison to *Bacillus subtilis* and *Escherichia coli* cloning hosts. *FEMS microbiology letters*, 58:305–9, Aug 1990.

[119] J. A. Vázquez and M. A. Murado. Unstructured mathematical model for biomass, lactic acid and bacteriocin production by lactic acid bacteria in batch fermentation. *Journal of Chemical Technology & Biotechnology*, 83(1):91–96, 2008.

[120] J. A. Vázquez, M. I. Montemayor, J. Fraguas, and M. A. Murado. Hyaluronic

acid production by *Streptococcus zooepidemicus* in marine by-products media from mussel processing wastewaters and tuna peptone viscera. *Microbial cell factories*, 9:46, Jun 2010.

[121] J. A. Vázquez, J. M. Lorenzo, P. Fuciños, and D. Franco. Evaluation of non-linear equations to model different animal growths with mono and bisigmoid profiles. *Journal of theoretical biology*, 314:95–105, Dec 2012.

[122] J. A. Vázquez, L. Pastrana, C. Piñeiro, J. A. Teixeira, R. I. Pérez-Martín, and I. R. Amado. Production of hyaluronic acid by *Streptococcus zooepidemicus* on protein substrates obtained from *Scyliorhinus canicula* discards. *Marine drugs*, 13:6537–49, Oct 2015.

[123] Z. Wang, M. Ly, F. Zhang, W. Zhong, A. Suen, A. M. Hickey, J. S. Dordick, and R. J. Linhardt. *E. coli* K5 fermentation and the preparation of heparosan, a bioengineered heparin precursor. *Biotechnology and bioengineering*, 107:964–73, Dec 2010.

[124] Z. Wang, J. S. Dordick, and R. J. Linhardt. *Escherichia coli* K5 heparosan fermentation and improvement by genetic engineering. *Bioengineered bugs*, 2:63–7, Jan-Feb 2011.

[125] Y. Wegrowski, C. Perreau, Y. Bontemps, and F. X. Maquart. Uridine diphosphoglucose dehydrogenase regulates proteoglycan expression: cDNA cloning and antisense study. *Biochemical and biophysical research communications*, 250:206–11, Sep 1998.

[126] B. Widner, R. Behr, S. Von Dollen, M. Tang, T. Heu, A. Sloma, D. Sternberg, P. L. Deangelis, P. H. Weigel, and S. Brown. Hyaluronic acid production in *Bacillus subtilis*. *Applied and environmental microbiology*, 71:3747–52, Jul 2005.

[127] A. Williams, K. S. Gedeon, D. Vaidyanathan, Y. Yu, C. H. Collins, J. S. Dordick, R. J. Linhardt, and M. A. G. Koffas. Metabolic engineering of *Bacillus megaterium* for heparosan biosynthesis using *Pasteurella multocida* heparosan synthase, PmHS2. *Microbial cell factories*, 18:132, Aug 2019.

[128] L. M. Willis and C. Whitfield. KpsC and KpsS are retaining 3-deoxy-D-manno-oct-2-ulosonic acid (Kdo) transferases involved in synthesis of bacterial capsules. *Proceedings of the National Academy of Sciences of the United States of America*, 110:20753–8, Dec 2013.

[129] J.-R. Wu, P.-Y. Chen, J.-H. Shien, C.-L. Shyu, H. K. Shieh, F. Chang, and P.-C. Chang. Analysis of the biosynthesis genes and chemical components of the capsule

of *Avibacterium paragallinarum*. *Veterinary microbiology*, 145:90–9, Sep 2010.

[130] Y. Xu, S. Masuko, M. Takieddin, H. Xu, R. Liu, J. Jing, S. A. Mousa, R. J. Linhardt, and J. Liu. Chemoenzymatic synthesis of homogeneous ultralow molecular weight heparins. *Science (New York, N.Y.)*, 334:498–501, Oct 2011.

[131] G. Yang, B. Zhou, J. Wang, X. He, X. Sun, W. Nie, S. Tzipori, and H. Feng. Expression of recombinant *Clostridium difficile* toxin A and B in *Bacillus megaterium*. *BMC microbiology*, 8:192, Nov 2008.

[132] Y. Yang, R. Biedendieck, W. Wang, M. Gamer, M. Malten, D. Jahn, and W.-D. Deckwer. High yield recombinant penicillin G amidase production and export into the growth medium using *Bacillus megaterium*. *Microbial cell factories*, 5:36, Nov 2006.

[133] C. Zhang, L. Liu, L. Teng, J. Chen, J. Liu, J. Li, G. Du, and J. Chen. Metabolic engineering of *Escherichia coli* BL21 for biosynthesis of heparosan, a bioengineered heparin precursor. *Metabolic engineering*, 14:521–7, Sep 2012.

[134] S. Ÿztürk, P. Ÿalık, and T. H. Ÿzdamar. Fed-batch biomolecule production by *Bacillus subtilis*: A state of the art review. *Trends in biotechnology*, 34:329–345, Apr 2016.

APPENDIX A

PUBLICATIONS

Patents

1. **Ganesh Nehru**, Subbi Rami Reddy Tadi, Senthilkumar Sivaprakasam, 2017, Recombinant *Bacillus megaterium* for production of Heparin precursors. Indian patent application 201831017897 [Published]

2. Subbi Rami Reddy Tadi, **Ganesh Nehru**, Senthilkumar Sivaprakasam, 2018, Methods for the increased production of D (-) Pantothenate in *Bacillus megaterium*. Indian patent application 201831039883 [Published]

Research Publications

1. **Nehru, G.**, Tadi, S. R. R., Limaye, A. M., & Sivaprakasam, S. (2020). Production and characterization of low molecular weight heparosan in *Bacillus megaterium* using *Escherichia coli* K5 glycosyltransferases. *International Journal of Biological Macromolecules*, 160, 69-76. DOI: 10.1016/j.ijbiomac.2020.05.159

2. **Nehru, G.**, Tadi, S. R. R., & Sivaprakasam, S. (2021). Application of Dual Promoter Expression System for the Enhanced Heparosan Production in *Bacillus megaterium*. *Applied Biochemistry and Biotechnology*, 1-14. DOI: 10.1007/s12010-021-03541-9

3. **Nehru, G.**, Tadi, S. R. R., Nivedhitha, S., Pavan, S. S., & Sivaprakasam, S. Influence of sucrose concentration and N-acetylglucosamine supplementation on heparosan biosynthesis in *B. megaterium* [Submitted to *Biochemical Engineering Journal*]

4. Tadi, S. R. R., **Nehru, G.**, Limaye, A. M., & Sivaprakasam, S. (2021). High-level expression and optimization of pantoate-β-alanine ligase in *Bacillus megaterium* for the enhanced biocatalytic production of D-pantothenic acid, *Journal of Food Science and Technology* [Accepted article]

Conferences/Schools/Workshops attended

1. **Ganesh Nehru**, Subbi Rami Reddy Tadi, Senthilkumar Sivaprakasam, Biosynthesis of Heparosan, a bioengineered heparin precursor in recombinant *Bacillus megaterium*, Biological engineering society conference (BESCON 2019), October 18-19, 2019, IIT Madras, India.

2. **Ganesh Nehru**, Subbi Rami Reddy Tadi, Senthilkumar Sivaprakasam, Biosynthesis of heparosan, a precursor for heparin polysaccharide in recombinant *Bacillus sp.*, International Symposium on Sustainable Polymers & Launch of SPSI-North East Chapter, August 23-25, 2019, IIT Guwahati, India.

3. **Ganesh Nehru**, Subbi Rami Reddy Tadi, Senthilkumar Sivaprakasam, Development of a dual promoter expression system for production of heparosan in recombinant *Bacillus sp.*, Bioprocessing INDIA 2018: Recent Advancements & Applications in Bioprocessing for Healthcare, Bioenergy and Environment, December 16-18, 2018, IIT Delhi, India

4. Subbi Rami Reddy Tadi, **Ganesh Nehru**, Senthilkumar Sivaprakasam, Metabolic engineering of *Bacillus megaterium* for the enhanced β-alanine production, EMBO Symposium Engineering meets evolution: Designing biological systems, January 30- February 1, 2020, IIT Madras, India

5. Subbi Rami Reddy Tadi, **Ganesh Nehru**, Senthilkumar Sivaprakasam, Production of 3-aminopropionic acid using metabolically engineered *Bacillus megaterium* whole-cell biocatalysis, Recent Advancements in Biochemical Engineering and Biotechnology (RABEB -2019), March 15-16, 2019, IIT BHU, India

6. Subbi Rami Reddy Tadi, **Ganesh Nehru**, Senthilkumar Sivaprakasam, Metabolic engineering of *Bacillus spp.* for the production of β-alanine , a vitamin B_5 precursor, 59^{th} International Annual Conference of The Association of Microbiologists of India (AMI- 2018), December, 9-12, 2018, University of Hyderabad, India

7. Subbi Rami Reddy Tadi, **Ganesh Nehru**, Senthilkumar Sivaprakasam. Over expression of L-aspartate α–decarboxylase enhances the 3-aminopropionic acid production in *Bacillus spp.* Bioprocessing INDIA 2018: Recent Advancements & Applications in Bioprocessing for Healthcare, Bioenergy and Environment, December 16-18, 2018, IIT Delhi, India